Stochastic Optimization for Integrated Energy System with Reliability Improvement Using Decomposition Algorithm

Yuping Huang
University of Central Florida

Showcase of Text, Archives, Research & Scholarship

STOCHASTIC OPTIMIZATION FOR INTEGRATED ENERGY SYSTEM WITH
RELIABILITY IMPROVEMENT USING DECOMPOSITION ALGORITHM

by

YUPING HUANG
M.S. West Virginia University, 2011

A dissertation submitted in partial fulfilment of the requirements
for the degree of Doctor of Philosophy
in the Department of Industrial Engineering and Management Systems
in the College of Engineering and Computer Science
at the University of Central Florida
Orlando, Florida

Fall Term
2014

Major Professor: Qipeng Phil Zheng

ABSTRACT

As energy demands increase and energy resources change, the traditional energy system has been upgraded and reconstructed for human society development and sustainability. Considerable studies have been conducted in energy expansion planning and electricity generation operations by mainly considering the integration of traditional fossil fuel generation with renewable generation. Because the energy market is full of uncertainty, we realize that these uncertainties have continuously challenged market design and operations, even a national energy policy. In fact, only a few considerations were given to the optimization of energy expansion and generation taking into account the variability and the uncertainty of energy supply and demand in energy markets. This usually causes an energy system unreliable to cope with unexpected changes, such as a surge in fuel price, a sudden drop of demand, or a large renewable supply fluctuation. Thus, for an overall energy system, optimizing a long-term expansion planning and market operations in a stochastic environment are crucial to improve the system's reliability and robustness.

As little consideration was paid to imposing risk measure on the power management system, this dissertation discusses applying risk-constrained stochastic programming to improve the efficiency, reliability and economics of energy expansion and electric power generation, respectively. Considering the supply-demand uncertainties affecting the energy system stability, three different optimization strategies are proposed to enhance the overall reliability and sustainability of an energy system. The first strategy is to optimize the regional energy expansion planning which focuses on capacity expansion of natural gas system, power generation system and renewable energy system, in addition to transmission network. With strong support of NG and electric facilities, the second strategy provides an optimal day-ahead scheduling for electric power generation system incorporating with non-generation resources, i.e. demand response and energy storage. Because of risk aversion, this generation scheduling enables a power system qualified with higher reliability and

promotes non-generation resources in smart grid. To take advantage of power generation sources, the third strategy strengthens the change of the traditional energy reserve requirements to risk constraints but ensuring the same level of systems reliability. In this way we can maximize the use of existing resources to accommodate internal or/and external changes in power system.

All problems are formulated by stochastic mixed integer programming, particularly considering the uncertainties from fuel price, renewable energy output and electricity demand over time. Taking the benefit of models structure, new decomposition strategies are proposed to decompose the stochastic unit commitment problems which are then solved by an enhanced Benders Decomposition algorithm. Compared to the classic Benders Decomposition, this proposed solution approach is able to increase convergence speed and thus reduce 25% of computation times on the same cases.

ACKNOWLEDGMENTS

I would like to express the greatest appreciation to my committee chair Professor Qipeng P. Zheng. This dissertation would not have been finished without the tremendous help and encouragement from him. He offered me many opportunities to explore different research directions. His insightful guidance and continuous supports in the past four years make me a qualified researcher and inspires me go further in academic career.

I would like to thank my committee members: Professor Andrew L. Liu, Professor Jennifer A. Pazour and Professor Petros Xanthopoulos, for their great efforts and help in my dissertation and defense.

I also sincerely acknowledge Professor Robert C. Creese, Professor Majid Jaridi, Professor Feng Yang, Professor Alan R. McKendall and Professor Wafik Iskander in West Virginia University. Their excellent teaching helps me lay down the foundation of dissertation and open the door for my research career.

Additionally, I am highly grateful to Professor Panos M. Pardalos, Dr. Jianhui Wang, Professor Steffen Rebennack and Professor Neng Fan for their support and productive collaboration. Besides, another thankful note goes to my other collaborators and appreciates their advices and suggestions.

Moreover, to my family, your unconditional love and support have been of immeasurable wealth to me. Specially thank to my dearest parents, Chuqiang Huang and Jianlan Deng, who encouraged me to pursue a doctorate and taught me self-belief, tenacity, kindness and dedication. Finally, I would like to thank all my friends during my PhD study in Orlando, Florida.

TABLE OF CONTENTS

LIST OF FIGURES

LIST OF TABLES

CHAPTER 1: INTRODUCTION

Electric power system is of utmost importance to generate electricity, move electricity and distribute electricity around the country so as to satisfy demands for electricity. Thousands of power generators are operated daily and most of them are controlled and managed by Independent System Operators (ISOs) and Regional Transmission Organization (RTOs) in United States. As three major components of electric power system, i.e. generation, transmission and distribution, they forms a multi-level network to connect original energy supplies to ultimate consumers for daily usage.

Power generation system is the main source of power supplies including fossil fuel resources and renewable resources for electricity generation. Fossil fuels plays an important role in energy sources, while renewable energy sources keeps fast growing because of their cost-effective as well as no/low greenhouse gas emissions. According to the statistics from EIA reports in 2012 [17], the current power systems remain fossil-fuel based systems along with emissions and other environmental issues.
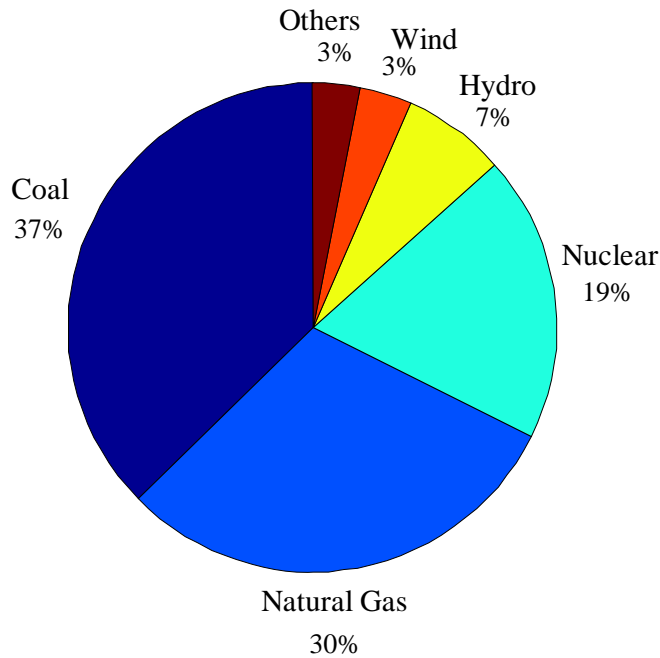
* Others represents the sources from petroleum, other gas, solar, wood, geothermal, biomass and other energy sources.

Figure 1.1: Total electric power net generation, 2012 (Thousand Megawatthours) [17]

As shown in Figure 1.1, the fossil fuel share of total energy sources still maintains above 68% in 2012 and The renewable share of total energy sources (including biofuels) grows up to 12%. Particularly, the wind and solar thermal and photovoltaic energy have respective 17% and 138% of growth rates on the contribution to energy generation, compared to their historical data in 2011. There is a clear trend appearing in Figure 1.2, where it can be expected that the mix of power generation will be dominated by coal, natural gas, renewable energy and nuclear. Thanks to effective energy policies and environmental policies, the coal share continues to be reduced significantly while the renewable share of total generation will increase at least to 15% in 2025.
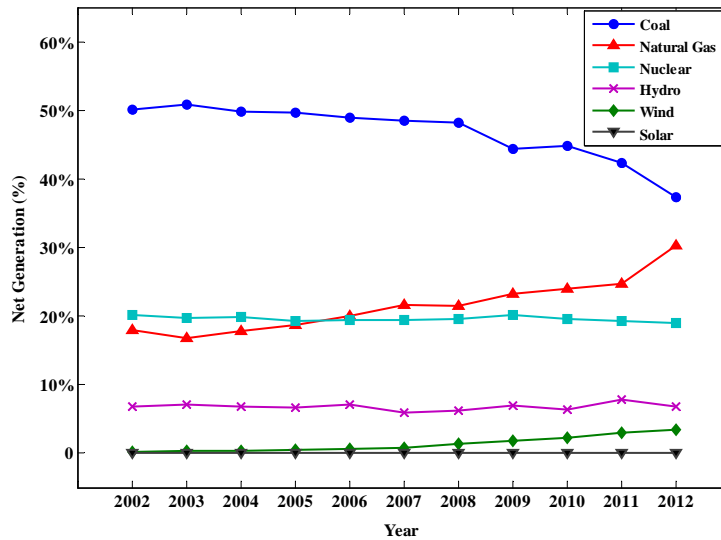
Figure 1.2: Statistics for power net generation, 2002-2012 (Thousand Megawatthours) [17]

Since electricity power is primarily contributed by fossil fuel sources, in which coal is a particularly significant contributor, greenhouse gas emissions from the electric power sector have contributed to global warming for a long time. The majority component of greenhouse gas is Carbon Dioxide (CO_2) and the minority component of greenhouse gas is made up of methane (CH_4) and Sulfur Dioxide (SO_2). During year 2012, the U.S. power industry produced $2,156,875$ thousand metric tons of CO_2 which, although reduced by 11% of emissions compared to year 2002, remain the largest source of GHG emissions. In order to mitigate climate change, the Environmental Protection Agency (EPA) takes many actions to reduce GHG emissions in the ways of increasing energy efficiency on power plants and end-use, fuel switching, renewable energy as well as the deployment of carbon capture and storage (CCS) [27, 94, 74]. Among of them, CCS is the final step to prevent CO_2 emitted to the atmosphere and further explored by optimizing operations scheduling so as to sequestrate CO_2 to underground storage areas with more energy benefits [28, 26].

The impacts of renewable energy on power generation systems

More general, renewable energy is defined as the energy offered by naturally and continually replenished resources, such as hydropower, wind power, solar power, biomass power, geothermal power. Renewable energy is very attractive and sustainable due to "no" costs or no pollutant emissions, which well fits the current and future needs of new energy systems. Due to the intermittent and uncertain nature of renewable energy, we realize that a fast growing penetration of renewable energy to current power grids brings a lot of challenges to power system management.

The current renewable generation is able to produce electricity in full conjunction with traditional thermal power generation. As its portion grows, power systems are required to be more flexible to accommodate the variability and uncertainty of renewable energy outputs. Considering one of main renewable energy resources, e.g. wind power, it's really hard to predict exact wind energy output based on the wind pattern and historical data. The deviations from the forecasted wind outputs due to dramatic decline/increase on wind speed will push conventional power plants ramp up/down their generations to maintain power balance. As this situation occurs frequently, the variability and unpredictability of generation systems are increased resulting in further intensify plant cycling and increase additional operation costs.

Compared to major continuous uncertainty caused by renewable energy and demand, the unplanned outages of generators or transmission elements are low-probability events and occur in much low frequency. This type of unexpected uncertainties like power blackout is covered by contingency control planning as well as taken into account through robust optimization approaches. In most instances, the power system is not able to avoid any uncertainties, but the operators are able to seek many effective solution methods to reduce the impacts from all these uncertainties.

The generation scheduling on power generation systems

Throughout power generation systems in practice, the minority of systems operate isolated from power grids, while the majority of systems participate in energy market and connect their resources to the ISO grids. Based on forecasted loads and available energy resources, ISOs perform generation scheduling and determine hourly market clearing prices for day-ahead market; besides, they perform energy procurement and congestion management in real-time market. The power generation scheduling, also namely unit commitment, is very essential for the whole power system operations from day-ahead schedule to real-time economic dispatch, even extended to contingency management. Unit commitment is also developed with solution methods capable of balancing energy supply and demand in day-ahead or hour-ahead markets, which has been widely used by ISOs in deregulated electricity market.
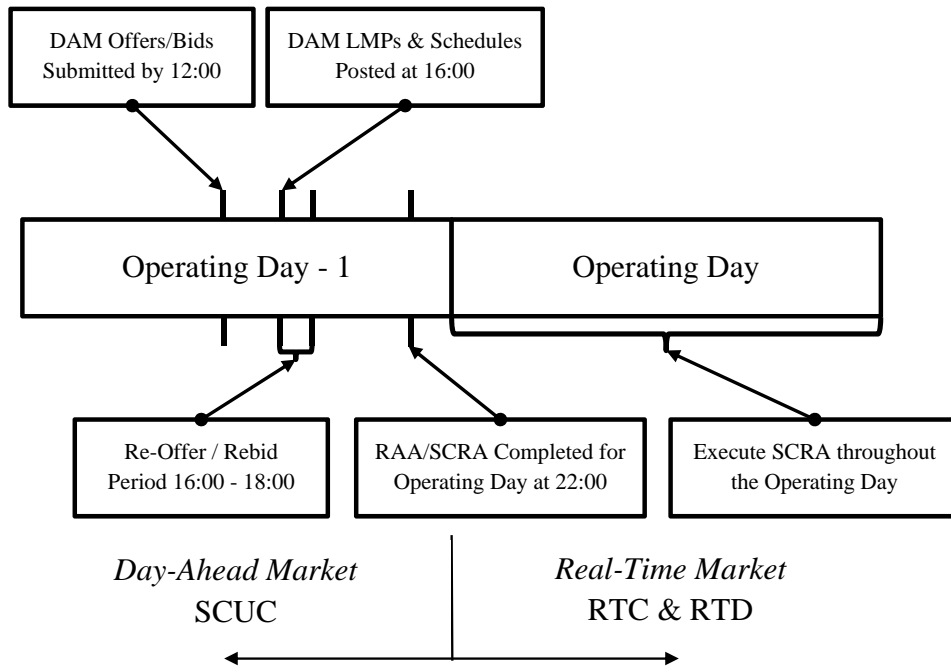
- DAM: Day-Ahead Market

- RTM: Real-Time Market

- RTC: Real-Time Commitment

- RTD: Real-Time Dispatch

- LMP: Locational Marginal Price

- RAA: Reserve Adequacy Assessment

- SCRA: Security-Constrained Reliability Assessment

- SCUC: Security-Constrained Unit Commitment

Figure 1.3: Day-Ahead market and real-time market timeline [31, 30]

The classic unit commitment problem is the security-constrained unit commitment (SCUC), in which system reliability is maintained by checking reliability at a certain operation level [60]. Since there are thousands of generation units and transmission lines in power systems, the unit commitment problem can become a very computationally challenging problem due to the large number of integer variables and constraints. From existing literature, many studies proposed some techniques and constraints to handle the reliability issues, such as transmission constraints [20, 21], "N-1" criteria [24], stochastic demands [79], etc. Many optimization-based techniques have been used to solve the problem [25, 60]. Among them, Benders' Decomposition and Lagrangian Relaxation techniques are two major techniques used to improve the computation performance in the way that the master unit commitment problem is separated from the reliability assessment subproblems [20, 21]. Benders cuts would be generated from the reliability assessment or contingency simulation subproblems and then added to the master unit commitment problem when any violation occurs [12, 21].

Unit commitment under uncertainty

As energy demands keep changing, the conventional unit commitment faces a lot of restrictions and challenges from current changes of energy market and ancillary market. Seeking higher reliability of power systems, ISOs plan to carry out market process and scheduling improvements using state-of-the-art unit commitment models which are based on operations management and optimization methods. What's more, because of a fast growing of renewable energy integrated into existing systems, this increases the intermittence and the variability of energy supplies in unit commitment problems. Here summarizes three main practical methods to manage the supply-demand uncertainties in UC:

- Implementing reserve requirements and providing related reserve services,

7

- Adopting non-generation resources, and

- Applying advanced solution methods, such as stochastic optimization and robust optimization.

Operating reserve is a widely used approach in power industry to deal with uncertainties on power systems. Generally, a part of generating resources will be retained in order to handle unexpected surges or contingency events. The current operating reserve is comprised of spinning reserve and non-spinning reserve, in addition to regulating reserve and contingency reserve. The timeline of four different reserves to provide services after an unexpected disruption is described in Figure 1.4, where they are provided or procured according to generator's characteristics or commitment from different energy sources. The regulating reserve consisting of regulation up and regulation down can give out the automatic response regarding the generation output frequency. The spinning reserve and non-spinning reserve are used in common and supported from internal or external systems. While the contingency reserve may overlap with non-spinning reserve with the aim of restoring operating reserve. Since above reserves don't require specific new technology or operating requirements, they have been successfully implemented in generating operations to manage uncertainty for a long time.
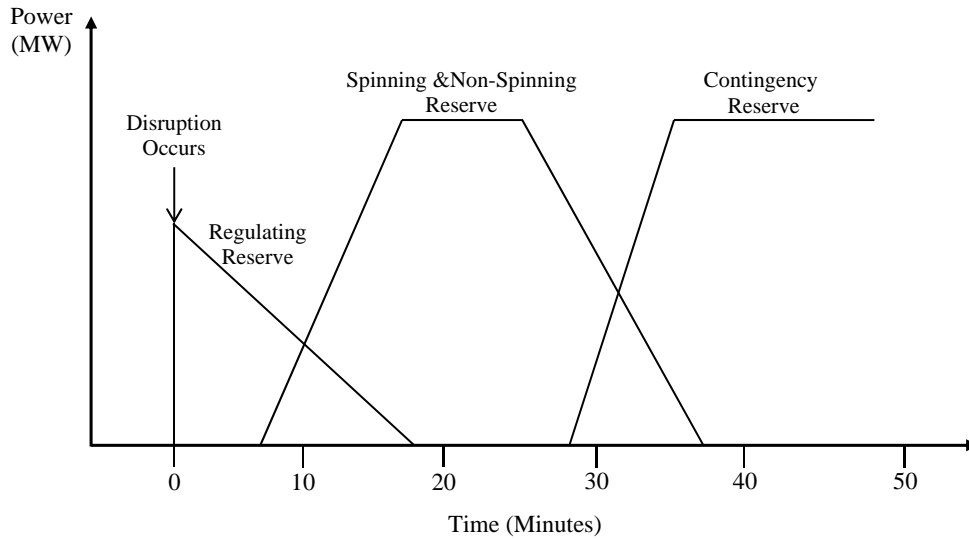
Figure 1.4: The general timeline of operating reserve

Non-Generation resource is viewed as non-conventional sources of energy and has been proposed to diversify power market services and further improve the stability, flexibility and reliability of energy supply. In the view of ISOs, non-generation resources consist of demand response resources, energy storage resources and other non-generation dispatchable resources to support power balance. Despite their advances and advantages known for several years, there are some technical and operational issues to resolve until ISOs allow for a wide range of implementation. As ISO wholesale market redesign running, CAISO attempts to allow non-generation resources to participate the ISO regulation markets and provide regulation services [8, 2].

On one side, non-generation techniques and programs, i.e. energy storage and demand response, have been well developed and helped expanding the usage of renewable energy as well as improving its cost-effectiveness. On the other side, management techniques for energy systems have been successfully applied to ensure the integration of existing power plants with renewable ener-

gy sources and Simultaneously, these techniques are able to optimize the power system operation scheduling and use of resources while meeting reliability needs.

In the past several years, more advanced power system operations methods have been proposed to address the variability and uncertainty brought by uncertain demand and increasing penetration of renewable energy sources. Stochastic unit commitment (SUC) has emerged as one of the most promising tools [5, 55, 72, 76]. The key idea of stochastic unit commitment is to capture the uncertainty and variability of the underlying factors by simulating a certain number of scenarios. Each scenario is expressed as a possible realization of the uncertain source, e.g. wind output, demand, or fuel price. By simulating the scenarios, the uncertainty can be represented to a large extent. However, due to the large number of scenarios, the computational requirement also increases dramatically. More advanced optimization techniques were proposed to solve for these cases. One of SUC examples is from [79]. The unit commitment problem with uncertain wind power was modeled as a two-stage problem where the master problem determines the unit commitment and the second stage simulates the possible wind power output scenarios. By Benders decomposition, the problem can be solved in an efficient manner because of the small size of the master and subproblems. These improvement efforts from recent studies demonstrated that mathematic optimization methods and techniques are the powerful tools to not only co-optimize generation dispatch, but also improve operational performance in subsequent research.

Outline of this dissertation

When ISOs schedule a day-ahead unit commitment, the uncertainties of renewable energy input and demand, the utilization of non-generation resources, operating reserve and risk control are involved and fully considered in the decision process. Nevertheless, they face a lot of challenges on dispatch planning, solution implementation, resource efficiency, system reliability, and so on. One can make the most conservative decision according the worst instance, however, it is unavoidably

accompanied by high operation costs, ultra-low resource utilization, less flexibility to respond to net load changes.

The dissertation is motivated by real world problems arising in current power system management. It aims to solve the capacity expansion planning problem and the unit commitment problem associated with the participation of non-generation resources, ancillary service and risk management through a stochastic optimization approach. Next, in order to improve computation performance, a modified Benders Decomposition algorithm is developed and applied to solve relatively large-scale SUC problems. This dissertation is divided into three parts of studies.

1. The first part is to develop a capacity expansion planning model for integrated energy system which is highly impacted from various uncertainties. This study proposes the gas-power system cooptimization concept to jointly improve expansion planning and long-term operation scheduling. The strengthens of the proposed model are demonstrated in a case study. The effects of increasing renewable integration on other facilities' expansion planning are discussed and further reveal the necessity of the gas-power system cooptimization.

2. The second part is to investigate the unit commitment scheduling cooperated with non-generation resources and risk control, which offers an initial protection of system reliability. The operations of individual resources (UC-DR and UC-ES) and the combined resource (integrated UC-DR-ES) are formulated in stochastic integer programs. Their unit commitment solutions are compared with the basic UC solutions, and a series of sensitivity analysis and gradient analysis are performed [29].

3. The third part is to solve the UC and reserve scheduling problem so as to meet the reliability standards more efficiently. To fulfill mandatory reliability requirements, the stochastic UC problem with fixed regulation reserve is modeled and its results are compared to those of stochastic UC model with CVaR measure. Moreover, the joint effects of reserve requirement

11

and risk-aversion measure are discussed in details.

The rest of dissertation is organized as follows. Chapter 2 provides a literature review of uncertainty management used in energy system, including applicable resources, operation requirements and solution techniques. Chapter 3 discusses a stochastic expansion planning model for a combined natural gas system and electric power system, in which energy allocation including gas and electricity is optimized so as to satisfy increasing energy demands and environment protections. Chapter 4 presents a stochastic unit commitment model incorporated with non-generation resources to optimize operation scheduling of power generation system. A enhanced decomposition approach is applied to solve large-scale power system and improve computation performance. Chapter 5 focuses on the improvement of power system's reliability in the way that both energy reserve and risk-aversion measure are adopted to SUC model to improve generation resource efficiency with minimum operational costs. Chapter 6 concludes the dissertation. Appendix A and B provide the nomenclature and the approach to generate renewable energy scenarios.

CHAPTER 2: LITERATURE REVIEW

Chapter 1 has introduced the major challenges that current energy and electricity power systems are facing. As supply/demand uncertainties always affecting power system, maintaining a high level of system's reliability has the same importance of a least-cost power generation. These observations have led to many studies on such areas: non-generation resources on energy service and operating reserve on ancillary service. Meanwhile, although many operation management problems are formulated by mathematical programming, a few advanced solution approaches are developed and applied to solve large-scale stochastic expansion planning problems and unit commitment problems. Particularly, solving UC problems efficiently is another key component for operation scheduling in ISOs. Thus literature reviews summarize the studies and findings regarding non-generation resources, operating reserve and proposing solution approaches on exact optimization, respectively.

2.1 Non-Generation Resources on Energy Service

Taking the advantages of non-generation resources, energy supply is not constrained by traditional thermal power generation and further supported by advanced devices as well as management techniques. The literature on power generation operation and planning integrated with individual resource, e.g. energy storage (ES) or demand response (DR), has a growing development as well.

On one hand, energy storage is one of typical non-generation resources and a feasible solution to facilitate the integration of wind power generation. The main advantage is that it is able to provide electricity supply when the peak demands occur to be greater than generation capacities in a power system, or the generation costs are extremely high. Since the storage devices can

store or release energy based on operations and demands, the incorporation of ES can increase the flexibility of power supply systems and decrease total costs at the same time. Some literature has discussed the economic value of ES investments, system-economic evaluations [14], optimal size and capacity for ES systems [11, 86], and stochastic operation management with ES on micro grid [41]. Recently, there are three main large-scale energy storage technologies, including pumped hydro accumulation storage (PAC), underground PAC and compressed air energy storage (CAES). Most studies of energy storage focus on CAES in the areas of economic value of investments, system-economic perspectives, technical challenges to the integration of wind power with power systems, and production planning [54, 32]. In most of the optimization models, energy storage is introduced as time-dependent multi-period storage constraints. Senjyu et al. [58] discuss the thermal UC problem consisting of generalized energy storage systems (ESS) and solve the model by extended priority list. Daneshi and Srivastva [14] develop enhanced security-constrained UC with wind generation and CAES, and conduct the comprehensive analysis of CAES on economics, peak-load shaving and wind curtailment. Except to the function of peak shaving provided by ESS, the primary reserve requirements and their combined provision are investigated via economic assessment [67].

On the other hand, demand response mechanisms have been proposed and praticed for several years to encourage consumers to reduce power consumption during on-peak hours and increase uses at off-peak hours or the times of high production. Since there exist unavoidable forecast errors for day-ahead wind resource, this increases re-dispatch costs and loss of load events. Sioshansi [68] discusses the introduction of demand response by real-time pricing in order to mitigate these wind integration costs. Zhao and Zeng [91] also proposed a two-stage robust optimization model for UC with DR in the integration of wind energy and solved the problem by a novel cutting plane algorithm. On one hand, the effect of demand response in an isolated system with wind integration has been studied in [16]. DR-based reserve capacity has also been proved to be an effective

mechanism to accommodate the uncertainty of wind generation, which has been studied by the extension of security-constrained unit commitment model with DR and performing simulation tests [34]. On the other hand, deterministic and stochastic security approaches were compared for energy and spinning reserve scheduling in presence of DR, where stochastic approach was shown to achieve a lower system cost and load shedding [48]. Later, Madaeni and Sioshansi [37] examined the effectiveness of stochastic programming and demand response on the reductions of wind uncertainty costs. Their empirical studies showed a stochastic program with DR brings more benefits significantly. Of the many modeling approaches of demand response, the method based on price elasticity matrix (PEM) will be utilized in our study. Although there are possibly some forecast errors existing in PEM, it is relatively easy to forecast loads which follow a specific end-user type. It is a good approximation for demand response and has been studied in [77]. The other benefit of this method offers easy incorporation with optimization models and produces sufficient results as well.

2.2 Operating Reserve on Ancillary Service

For all ancillary services, they primarily focus on the secondary frequency control and the tertiary frequency control through the automatic generation control of power system to adjust the operating levels [18]. In most circumstances, they are able to provide the unloaded generation which is synchronized to the grid and prepare to serve additional demand. According to operating characteristics and technical requirements, ancillary service is separated to three main products, including regulation, spinning reserve and non-spinning reserve. In fact that their durations of response are different, they require little specific generation technology on normal operations.

To optimize power system operations, neither energy nor ancillary service can be taken into account individually. Given available generation capacities, any reserve from ancillary service will

15

hold a portion of unloaded generation capacity, and therefore impact the regular operating levels. Recently, the co-optimization of energy and ancillary services has been verified as a practicable approach to resolve electric energy generation and energy reserve scheduling simultaneously. The deterministic joint energy/reserve market models were initially proposed to solve for market-clearing issues [3] and unit commitment problem [71] based on demand-side reserve. Zheng and Litvinov [97] proposed a nested zonal reserve model for the optimal allocation of energy and reserve, aiming to improve the reserve deliverability. With the consideration of wind energy integration, the operating reserve requirements are further explored by implementing a stochastic programming approach [47, 46]. Matos and Bessa [39] presented a management tool to determines the reserve needs in the aspects of risk evaluation. The operating reserve assessment was also discussed based on the Value-at-Risk (VaR) measure. In addition, Wang et.al. [80] proposed a model regarding contingency-constrained joint energy and ancillary services auction to calculate the procured reserve level based on contingency analyses. Regarding the joint energy and reserves auction, the opportunity cost payments for reserves was explicitly studied in [44].

Operating reserve operation has been proposed for many years to ensure power system's security and reliability. With the existence of explicit reserve requirements, it produces highly reserve costs when the planned reserve is not fully used and the unplanned reserve costs when the real-time demand exceeds the expected generation capacity. If the planned reserve is not able to cover the dramatic changes of energy demand or supply, the load-shedding losses will occur so as to keep the power balance in the entire network.

Although energy and reserve come from the same physical resources, the same amount of electricity shows price differences between energy market and reserve market. The GENCOs expect to maximize generator's as-bid profit and load's as-bid benefit/utility simultaneously. At the same time, ISO expects to benefit from the co-optimization by the effective determination of market clearing prices, the enhancement of reserve shortage pricing, the identification of units for system

16

re-dispatch and proper compensation, etc. [96].

To achieve the optimization of energy and reserve, Ni et.al. [42] presented an optimization-based algorithm to look for efficient energy and reserve offering strategies. The influence of reserve market on generation offering strategies also is demonstrated, but only limited to a hydrothermal power system. The research conducted by Bouffard et.al. [7] includes a more comprehensive formulation of stochastic unit commitment problem in which reserve determination constraints containing upward/downward reserve are explicitly divided to three components: supply-side spinning reserve provided by generators, demand-side spinning reserve, and nonspinning reserve. Except the physical generation requirements, their model also considers pre- and post-contingency and corresponding load flows as well. While Wu's studies focus on the long-term SCUC by addressing the reliability cost analysis, and use the stochastic program as a decision tool to provide system's reliability evaluation [84].

Except to cover the regular continuous uncertainties from supply and demand,the function of operating reserve is also to handle the contingencies from facility failure and transmission line outage. Wang et.al. [76] address a SCUC model for energy and ancillary services auction where the contingency-constrained reserve requirements is strengthen and determined from contingency analyses, rather than the conventional pre-specified quantity. The purpose doing so is to avoid unnecessarily large amount of reserves for commitment. Vrakopoulou et.al. [75] proposed a probabilistic framework for secondary frequency control reserve scheduling according to the N-1 security criterion. Meanwhile, considering n-K contingencies, a new approach of the energy and reserve joint scheduling is presented by Pozo et.al. [49]. When K-worst contingencies happen in a same scheduling period, a power system keeping stable needs higher requirements compared to the common N-1 security criterion.

Since the operating reserve is scheduled as a portion of generating capacities over the forecasted

load, excessive reserves for commitment would undermine the GENCOs' benefits while insufficient reserves can not cover supply-and-demand imbalances and increase system's risks. Ruiz et.al. [55] compare the stochastic programming method and reserve requirements, and then utilize their benefits to find out an efficient management of uncertainty. The solutions they obtained show the system improvements from more flexible commitment and relatively lower optimal reserve requirements. In the detail-view of operating reserve, Meibom et.al. [40] take into account of regulation as individual operation from spinning reserve. This definition for reserve decision variables helps to clarify the actual function of reserve service and provide better implantations in practice.

In the last three years, Sandia National Laboratories investigate the regulation and spinning reserve markets to locate the issues that hinder the optimization of reserve markets and resource efficiency. The reserve markets from all ISO/RTO were investigated and assume ramp-rate constrained, rather than capacity constrained, to be resources bidding into the reserve markets. This way leads to neglect the advantage of fast response resources, and then often results in the higher amount of capacity required to meet the regulation requirements. The suggestions therefore are placed on the better use of reserve resources by decoupling ramp-rate and capacity requirements and finding optimal portfolios of resources after the concepts of frequency domain used [18].

2.3   Solution Techniques

In the past ten years, the solution techniques to solve unit commitment problems have significant changes which occurred due to the development of mathematical formulations, i.e. from dynamic program to stochastic mixed integer program. One of improvements is reducing the solution computation times greatly based on the same-case comparisons under one scenario. Another improvement is embodied in using stochastic program to involve possible instances and stress

18

the probability of uncertainties. The literature reviews regarding recent applications of stochastic integer programming in power systems and their associated solution techniques are addressed individually.

2.3.1 Stochastic Integer Programming

Stochastic unit commitment (SUC) is one of effective management techniques and it has been introduced as a promising tool to deal with power generation problems involving uncertainties [5, 55, 72, 76, 79, 94]. The idea of SUC is to utilize scenario-based uncertainty representation in unit commitment problems; that is, it captures the uncertainty and variability of the underlying factors by simulating a large number of scenarios. Many studies taking into account of unit commitment have proven that the stochastic optimization models have better performance and less-cost schedules than any deterministic optimization [72, 7].

Stochastic optimization approach is to apply stochastic programming to model decisions under uncertainties. Here, an important feature is that uncertainties are assumed to be known and then presented in a scenario tree. Theoretically, the more scenarios are involved in a scenario tree, the more comprehensive uncertainties are involved due to all possible uncertainties discretized on scenarios. The abstract form of stochastic unit commitment (SUC) problem can be expressed as follow.

$$[\mathbf{P}]: \quad \min \quad \mathbf{c_1^T x} + \mathbb{E}((\mathbf{c_2^T})^\xi \mathbf{y}^\xi) \tag{2.1}$$

$$\text{s.t.} \quad \mathbf{A_1 x} = \mathbf{b}_1 \tag{2.2}$$

$$\mathbf{A_2}^\xi \mathbf{x} + \mathbf{E}^\xi \mathbf{y}^\xi = \mathbf{b_2}^\xi, \quad \forall \xi \in \Xi \tag{2.3}$$

$$\mathbf{x} \in \{0,1\}^{n_1} \tag{2.4}$$

$$\mathbf{y}^\xi \in \mathbb{R}_+^{n_2}, \quad \forall \xi \in \Xi \tag{2.5}$$

19

where $\mathbf{c}_1 \in \mathbb{R}^{n_1}, \mathbf{c}_2 \in \mathbb{R}^{n_2}, \mathbf{b}_1 \in \mathbb{R}^{m_1}, \mathbf{b}_2 \in \mathbb{R}^{m_2}, \mathbf{A}_i \in \mathbb{R}^{n_1 \times m_i}(i = 1, 2), \mathbf{E} \in \mathbb{R}^{n_2 \times m_2}$, and m_1, m_2 are scalars. From the above SUC model, decision variables can be separated to here-and-now variables (i.e. first-stage variables) and wait-and-see variables (i.e. second-stage variables). On a day-ahead power market, the here-and-now decisions are made one day in advance before all uncertainties are revealed. These here-and-now decisions can directly or indirectly affect wait-and-see decisions, but should offer enough generation resources to deal with forecasted uncertainties on next day.

A stochastic UC model with one scenario can be considered as a deterministic model. In doing so, solving a stochastic UC model is equivalent to solving a large-scale deterministic UC model, while the computational performance becomes challengeable.

As we mention above, the common uncertainties expressed in discrete scenarios include

- forecasted demand $D_{it}^{\xi 0}$,

- renewable energy output R_{it}^{ξ},

- electricity price Q_{it}^{ξ},

- generating unit outage $\alpha_{it}^{\xi} P_{gt}$, and

- transmission element outage, e.g. $\alpha_{ijt}^{\xi} F_{ijt}$.

The first three uncertainty resources are mainly reflected in successive fluctuations, while the latter uncertainty resources are intermittent occurrences. In stochastic optimization, continuous uncertainties are simulated to be possible random discrete values, which form a finite set. All these possible values as parameters/inputs can be easily incorporated to SUC models.

In the perspective of power balance, any changes from uncertainty resources lead to corresponding changes on generation and transmission. The decisions related to above uncertainties are modeled

to be higher dimensional variables based on each scenario ξ. The main decisions are made in each scenario including but not limited to

- dispatch level, p_{gt}^ξ

- spinning reserve, s_{gt}^ξ

- power flow from bus i to bus j, f_{ijt}^ξ

- load-shedding loss, δ_{it}^ξ

- phase angle, β_{it}^ξ

- shifted demand, y_{it}^ξ

- energy storage level, r_{it}^ξ

- energy storage injection, v_{it}^ξ

- energy storage dispatch level, x_{it}^ξ.

As high penetration of renewable energy to current power system, it brings a lot of uncertainties on energy supply and transmission. Considering one of renewable energy resources like wind energy, the forecasting errors or intermittent energy supply in net load will cause conventional power plants ramp up/down frequently to ensure their energy output satisfy real-time demand level. Therefore, on one side, non-generation resources typically like demand response and energy storage, have been well developed and facilitate the expansion of renewable energy's usage. On the other side, management techniques for energy systems can be used effectively to ensure the smooth integration of existing power plants with renewable energy output [35] as well as power system reliability, no matter in the real-time operating and long-term planning. Recently, a couple of studies are extended to more realistic generation schedules, *i.e.* the stochastic unit commitment

modeled with sub-hourly dispatch constraints to capture the sub-hourly variability of wind energy output [81].

2.3.2 Chance-Constrained Programming

To minor the likelihood of load losses due to uncertainties, risk management is becoming a mandatory task and is implemented on power generation systems. Value-at-risk (VaR) and conditional value-at-risk (CVaR) are two popular risk measure tools, especially in financial risk management. Due to their different mathematical properties, the choices between VaR and CVaR usually affects the type of problems, so their strong and weak features are illustrated through several examples by Sarykalin et.al [57].

Ozturk et.al. [45] presented an earlier stochastic unit commitment model with a consideration of demand uncertainties. The demand satisfaction constraint is reformulated by chance constrained programming to maintain a guaranteed level for the loss of load probability index. Chance-constrained optimization is also gradually applied to the UC problems with uncertain wind power output [82] and transmission network expansion planning [87]. Vrakopoulou et.al. [75] formulated a stochastic optimization program with chance constraints, but the model is only solved by simulation method. In addition, CVaR chance constraint as reliability constraint is applied in the SUC problem with α-quantile n-K security criterion to obtain a joint robust energy and reserve dispatch.

In scenario-based stochastic programming models, the actual loss can be allowed depending on each scenario. Since a large number of simulated scenarios (e.g., renewable outputs, nodal demands, fuel prices) are usually included to the stochastic models, particularly to the extreme cases included. The optimal solutions therefore might be very overconservative with high total cost because feasible solutions need to compensate much for the extreme scenarios. On the other hand, it's

more reasonable to base on each scenario to maintain a certain level of system reliability. To balance between the total cost and system reliability, chance or risk constraints are usually introduced in the stochastic programming models for this tradeoff.

2.3.2.1 *Value at Risk*

Risks in stochastic unit commitment usually are linked with loss of load since a reliable system should be able to meet as much demand as it can. Hence loss of load probability (LOLP) is usually required to stay below an allowed level in many previous approaches [45, 83]. In the following we introduce the basic formulation for the chance of not meeting demands [49]. Considering a robust scheduling, it should have enough generation capacities to satisfy any load, shown as

$$\sum_{g \in G} p_{gt} - r_{gt}^d \leq D_{it} \leq \sum_{g \in G} p_{gt} + r_{gt}^u, \quad \forall i \in N.$$

Note that the forecasted demand can be replaced by the net load which is defined by $\Lambda_{it}^0 = D_{it}^0 - R_{it}^0$. If the demand and renewable output are described by normal distributions, the net load deviation is expressed by $\sigma_{it}^2 = (\sigma_{it}^D)^2 + (\sigma_{it}^R)^2$. Additionally, the generation capacities can be expended including operating reserve and non-generation resources.

As we known, there exists a possibility that the scheduled generation and reserves fail to satisfy any demand. In this case, ISOs adopt load shedding or renewable energy curtailment, especially for wind generation. These two operations happen in the two tails of normal distribution respectively and therefore are deployed on the basis of following net load situations.

- Case I: High demands and low renewable generation

After upward regulation and spinning reserve deployed to satisfy demand, the unserved energy is

expressed by a reliability distribution function Υ_{it}^{ξ}, given as

$$\Upsilon_{it}^{\xi} = D_{it}^{\xi} - \sum_{g \in G_i} p_{gt}^{\xi} + (r_{gt}^u)^{\xi}, \quad \forall i \in N, \ t \in T, \ \xi \in \Xi.$$

When $\Upsilon_{it}^{\xi} \leq 0$, the system has no risk for any scenario. When $\Upsilon_{it}^{\xi} > 0$, the load shedding is executed and the corresponding possibility of occurrence is defined as

$$LOLP_{it} = \text{Prob}\left\{\Upsilon_{it}^{\xi} > 0\right\}, \quad \forall i \in N, \ t \in T.$$

The expected unserved energy is defined as

$$EUE_{it} = \mathbb{E}\left[\Upsilon_{it} | \Upsilon_{it}^{\xi} > 0\right], \quad \forall i \in N, \ t \in T.$$

- Case 2: Low demands and high renewable generation

Similar to case I, the renewable energy curtailment (ie. wind curtailment) is deployed to avoid a serious variation on thermal energy generation. The reliability distribution function Ψ_{it}^{ξ} is given as

$$\Psi_{it}^{\xi} = D_{it}^{\xi} - \sum_{g \in G_i} p_{gt}^{\xi} - (r_{gt}^d)^{\xi}, \quad \forall i \in N, \ t \in T, \ \xi \in \Xi.$$

When $\Psi_{it}^{\xi} \geq 0$, the system is considered to be nonrisky for any scenario. When $\Psi_{it}^{\xi} < 0$, the curtailment is performed in addition to regulation down. The probability and expected wind curtailment are respectively defined as follow

$$LORP_{it} = \text{Prob}\left\{\Psi_{it}^{\xi} < 0\right\}, \quad \forall i \in N, \ t \in T,$$

24

and

$$ERC_{it} = -\mathbb{E}\left[\Psi_{it}|\Psi_{it}^{\xi} < 0\right], \quad \forall i \in N, \ t \in T.$$

Compared to renewable curtailment, the loss of load is more important in operation scheduling since unserved energy cost may be produced. Thus LOLP is directly modeled by chance constraints to control load-shedding risks, which is equivalent to bound a θ-level Value at Risk (VaR) of the loss of load, where θ is usually a value close to 1. To define the LOLP constraints, different policies regarding how to aggregate loss of load (e.g., total loss over all time periods v.s. loss of each time period) can be used [82]. Depending on the degree of risk control in UC problem, one can bound the risks associated with each individual time period or for all periods.

Let $L(x,Y)$, a random variable, be the loss function (e.g., total loss of all buses at a time period), where x are the aggregated decision vector and Y is the random vector (e.g., wind outputs). $\text{VaR}_{\theta}[L(x,Y)]$ represents the θ-level Value-at-Risk (VaR) of the loss of load function $L(x,Y)$. It is also the θ-level quantile of the random variable $L(x,Y)$, which can be defined as follows,

$$\text{VaR}_{\theta}[L(x,Y)] = \min_{l}\left\{l\middle|\ \text{Prob}\Big(L(x,Y) \leq l\Big) \geq \theta\right\}.$$

Chance constraints are equivalent to bound $\text{VaR}_{\theta}[L(x,Y)]$ above by $\bar{l}$, which is the maximum tolerable loss of load, usually set as 0. From the definition of VaR, $\text{VaR}_{\theta}[L(x,Y)]$ is generally nonconvex with respect to $L(x,Y)$; in other words, $\text{VaR}_{\theta}[L(x,Y)] \leq l$ and $\text{Prob}\{L(x,Y) \leq l\} \geq \theta$ may be nonconvex constraints. These VaR constraints involve binary variables and big M to select good/bad scenarios in SUC models, so it will increase computational difficulties when solving the chance-constrained programs particularly with large number of scenarios. Approximation algorithms such as Sample Average Approximation are used to solve chance-constrained stochastic unit commitment problems [82, 83].

2.3.2.2 Conditional Value at Risk

There is an alternative option to bound another risk of load loss, Conditional Value at Risk (CVaR), also named as Average Value at Risk (AVaR) or Expected Tail Loss (ETL). As a coherent risk measure, it is still a percentile measure of risk widely used in many areas, e.g., financial and risk management [1], natural gas system expansion planning [93], power trading in day-ahead energy market [15], stochastic network optimization [95], home energy management system [85].

By the definition in [57], the CVaR of $L(x,Y)$ with confidence level $\theta \in [0,1]$ CVaR constraints only involve continuous variables and linear constraints, and then are computationally friendly even with a large number of scenarios. In addition, the optimal solution of CVaR-based models also provide information of corresponding VaR measure because CVaR is the conditional expectation of the loss function given that the loss is beyond $\text{VaR}_\theta[L(x,Y)]$. Hence the CVaR constraints also include VaR definition shown as follows,

$$\min_l \left\{ l \,\middle|\, \text{Prob}\Big(L(x,Y) \leq l\Big) \geq \theta \right\} \;=\; \eta \tag{2.6a}$$

$$\mathbb{E}\left\{L(x,Y) \middle| L(x,Y) \geq \eta\right\} \;\leq\; \bar{\phi} \tag{2.6b}$$

where $\mathbb{E}$ refers to the expectation, and η is $\text{VaR}_\theta[L(x,Y)]$, and $\bar{\phi}$ is the maximum tolerable loss for CVaR. Note that this does not mean maximum tolerable loss for η is $\bar{\phi}$. In fact $\text{VaR}_\theta[L(x,Y)]$ is bounded by a loss smaller than $\bar{\phi}$. Figure 2.1 shows the relationship between VaR and CVaR on bounding losses. We refer the readers to [53, 57] for further details including the discussion between VaR and CVaR, and the constraints to represent them.
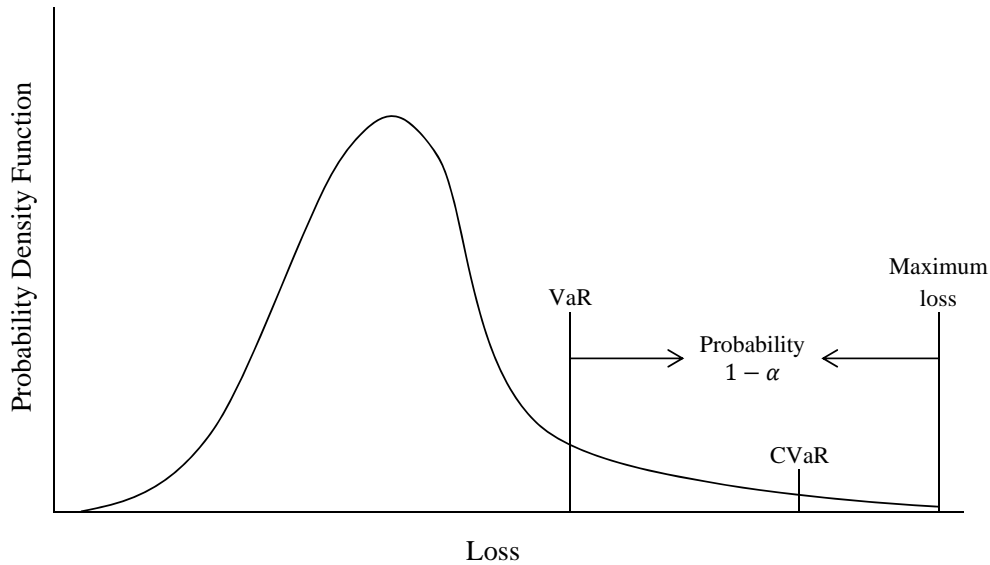
Figure 2.1: VaR and CVaR on loss [57]

2.3.3 Decomposition Algorithms

As a large number of scenarios are involved, the computational difficulties increases dramatically, reflected on the general computational complexity of NP-hard. Therefore more advanced discrete optimization techniques and solution algorithms need to be used to solve these cases, such as Bender's Decomposition [79, 92], column generation [65], Progressive Hedging [69], Lagrangian relaxation and Benders' Decomposition [70, 10]. From the literature, significant progress has been made on stochastic programming approaches to solve the cost minimization problems. These advanced techniques also can be extended and employed to the stochastic unit commitment problems.

The common use of Benders' decomposition is to decompose an original problem into a master problem (MP) and one/multiple subproblems (SP) by solving MP to get a lower bound, passing its current solutions to SP, solving SP to get a upper bound and then generating Bender's cuts

for MP until LB and UB are converged. Generally, the subproblem is a linear program (LP) or a convex nonlinear program [9], while the master problem include all discrete variables such as binary variables or integer variables. In some decomposition cases, one can also keep some of the continuous variables in the master problem according to the personal definition of SP.

Taking the benefits from decomposition methods, an original MILP model is decomposed into smaller subproblem(s) which can be solved by existing solution algorithms easily, so that computation performance is improved.

2.3.3.1 *Principles of Benders' Decomposition*

Here we take a generic MILP form of UC problem to illustrate the procedure of Benders' decomposition. For fixing values of $\mathbf{y}$, the original problem is given by

$$\min \{\mathbf{f}(\hat{\mathbf{x}}) + \mathbf{c_2^T y} \mid \mathbf{E y} \geq \mathbf{b_2} - \mathbf{A_2}\hat{\mathbf{x}}, \ \mathbf{y} \in \mathbb{R}_+, \ \mathbf{y} \geq 0\}. \tag{2.7}$$

Since the value of function $\mathbf{x}$ is fixed and moved out from the function $\mathbf{y}$, the problem (2.7) is rewritten as follow:

$$\mathbf{f}(\hat{\mathbf{x}}) + \min \{\mathbf{c_2^T y} \mid \mathbf{E y} \geq \mathbf{b_2} - \mathbf{A_2}\hat{\mathbf{x}}, \ \mathbf{y} \in \mathbb{R}_+, \ \mathbf{y} \geq 0\}. \tag{2.8}$$

So the inner minimization problem is called subproblem (SP).

Let μ denote dual variables (extreme points) associated with the constraint $\mathbf{E y} \geq \mathbf{b_2} - \mathbf{A_2}\hat{\mathbf{x}}$. If $\mathbf{y} \in \mathbb{Y}$ is a nonempty polytope, there exists an extreme point for optimal solution in SP. The dual

SP then is reformulated by

$$\min \{z \mid z \geq (\mathbf{b_2} - \mathbf{A_2}\hat{\mathbf{x}})^T \mu, \ \mathbf{E}^T \mu \leq \mathbf{c}_2, \ \mu \geq 0\}. \tag{2.9}$$

Solving the inner minimization problem means enumerating all extreme points of Y in the sub-problem. If there are partial k ($k < Q$) extreme points selected, the MP becomes a relaxed master problem (RMP) with less constraints given by

$$\min \{\mathbf{f}(\mathbf{x}) + z \mid \mathbf{x} \in \mathbb{X}, \ z \geq (\mathbf{b_2} - \mathbf{A_2}\mathbf{x})^T \hat{\mu}_j, \ \text{for } j = 1, 2, \ldots, k\}. \tag{2.10}$$

Let $(\bar{x}, \bar{z})$ denote an optimal solution to RMP. However, $(\bar{x}, \bar{z})$ is a feasible solution to the master problem ($k = Q$). In order to check this optimality condition, we equivalently check if the inequality (2.11) holds true.

$$\bar{z} \geq (\mathbf{b_2} - \mathbf{A_2}\bar{\mathbf{x}})^T \mu_j, \ \text{for } j = 1, 2, \ldots, Q \tag{2.11}$$

If the current solution of RMP, $(\bar{x}, \bar{z})$, violates one or partial constraints in SP, an *optimality cut* (2.12) will be imposed to RMP.

$$z \geq (\mathbf{b} - \mathbf{D}\mathbf{y})^T \hat{\mathbf{u}}_{k+1}. \tag{2.12}$$

If SP has infeasible solutions, a *feasibility cut* (2.13) will be added to RMP.

$$0 \geq (\mathbf{b} - \mathbf{D}\mathbf{y})^T \hat{\mathbf{u}}_{k+1}. \tag{2.13}$$

The solution types for MP and SP are summarized and shown in the Figure 2.2. After solving RMP, one can obtain a feasible solution which is passed to SP for the next-step solution or an infeasible

solution than indicates the original problem with infeasible solution. Then the suproblem is solved with three possible cases: feasible, infeasible and unbounded. Based on the solution type of SP, an optimality cut or a feasibility cut will be generated and then added to RMP for next iterations. If the SP has the unbounded case, it also means the original problem is unbounded.
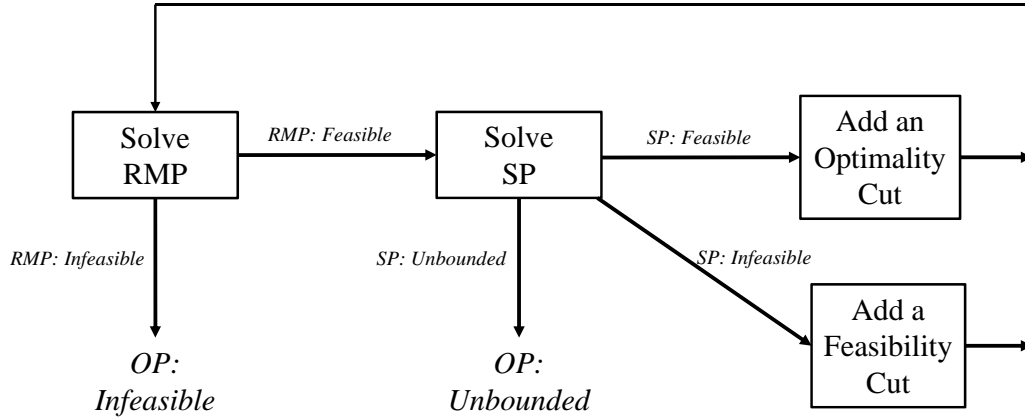
Figure 2.2: Solution types for master problem and subproblems in Benders' Decomposition

To solve a classical MILP problem with L-shaped structure, the traditional Benders' Decomposition algorithm is presented as follow:

▶ **Initialization**: Let $\hat{\mathbf{x}} :=$ initial feasible solution, only solve for the function of x to get the initial LB and then fix $\mathbf{x}$ to solve for UB.

▶ **Step 1**: Solve the RMP, $\min_x \{f(\mathbf{x}) + z | \mathbf{x} \in X, \text{cuts, } z \text{ unrestricted}\}$.
If RMP is feasible, get solutions $(\bar{\mu}, \bar{z})$ and $LB := f(\bar{\mathbf{x}}) + \bar{z}$; otherwise, the procedure is terminated.

▶ **Step 2**: Solve the SP, $\max_\mu \{\mathbf{f}(\hat{\mathbf{x}}) + (\mathbf{b_2} - \mathbf{A_2}\hat{\mathbf{x}})^T \mu | \mathbf{A}^T \mu \leq \mathbf{c}, \mu \geq 0\}$. If SP is feasible, get dual solutions $\hat{\mu}$ and $UB := \mathbf{f}(\hat{\mathbf{x}}) + (\mathbf{b_2} - \mathbf{A_2}\hat{\mathbf{x}})^T \hat{\mu}$.

30

Add optimality cut $z \geq (\mathbf{b_2} - \mathbf{A_2x})^T \hat{\mu}$ to RMP.

If SP is infeasible, add feasibility cut $0 \geq (\mathbf{b_2} - \mathbf{A_2x})^T \hat{\mu}$ to RMP.

► If $(UB - LB)/UB \leq \varepsilon$, the current solution is optimal and stop.

If $(UB - LB)/UB > \varepsilon$, perform next iteration and go to Step 1.

Since the basic Benders' decomposition method proposed by [6] is only suitable for specific structures of MILP and has many drawbacks when solving realistic cases, such as low quality of lower bound, redundant (useless) cuts. Therefore, the classical Bender's decomposition has been further developed and its extensions are not limited to generalized Bender's decomposition, logic-based Bender's decomposition, Bender's decomposition integrated with local branching [19, 50]. These enhanced Bender's decomposition approaches have specific schemes which are more suitable for different types of programs, like MILP, CP/MILP and MINLP.

2.3.3.2 *Application of Benders' Decomposition in UC problem*

Based on the above decomposition process, we can obtain the decomposed UC problems: an integer master problem (BD-MP) and a linear subproblem (BD-SP), which are given by

$$[\textbf{BD-MP}]: \quad LB = \min_{x,\pi} \quad \mathbf{c_1^T x} + \pi \tag{2.14a}$$

$$\text{s.t.} \quad \mathbf{A_1 x} = \mathbf{b}_1 \tag{2.14b}$$

$$\mathbf{x} \in \{0,1\}^{n_1} \tag{2.14c}$$

$$\pi \geq \mathscr{O}(\mathbf{x}) \tag{2.14d}$$

$$0 \geq \mathscr{F}(\mathbf{x}) \tag{2.14e}$$

$$[\textbf{BD-SP}]: \quad UB = \min_y \quad \mathbf{c_2^T y} \tag{2.15a}$$

$$\text{s.t.} \quad \mathbf{Ey} = \mathbf{b_2} - \mathbf{A_2}\hat{\mathbf{x}} \tag{2.15b}$$

$$\mathbf{y} \in \mathbb{R}_+^{n_2} \tag{2.15c}$$

where constraints (2.14d) and (2.14e) represents the optimality cut and feasibility cut, respectively.

The direct application of BD in UC problems is to decompose the original model depending on the variable types, as shown in (2.14) and (2.15).

- Solve the MP with unit commitment and generated cuts;

- Given the current solutions from MP, solve the SP associated with economic dispatch, operating reserve, emission, transmission, reactive power and unserved energy constraints. Generate Benders' cut(s) according to solution type of SP in current iteration.

Another common application of Benders' Decomposition is to solve general security-constrained unit commitment (SCUC) in two stages:

- Solve the MP with unit commitment, economic dispatch, operating reserve and emission constraints;

- Given the current solutions from MP, solve the SP only regarding to transmission, reactive power and unserved energy constraints. Check if any network violations occur and generate Benders' cuts.

In both decomposition schemes, the MP including new generated cuts and the SP are solved iteratively and checked for convergence. Using the second decomposition scheme, the MP become a mixed integer program while the SP is a simple linear program for meeting network constraint.

From the literature, the network security check is usually arranged in the SP. The DC network security check focuses on the power flow balance and flow limits on transmission lines. If the DC network constraint is replaced by more complicated AC network constraint, the scheme remains suitable for AC network security check. The DC network constraint only considers the power flow balance at a bus, ignoring bus voltage violations, feasible distribution of reactive power and interactions between real and reactive power conditions. When the AC network considers such requirements, it is more reasonable to handle them in SP as security check. The flow chart for a comprehensive network security check in subproblem is shown on Figure 2.3. This decomposition strategy is varied to effectively solve the deterministic large-scale UC problem, *i.e.* 118 bus system [20].
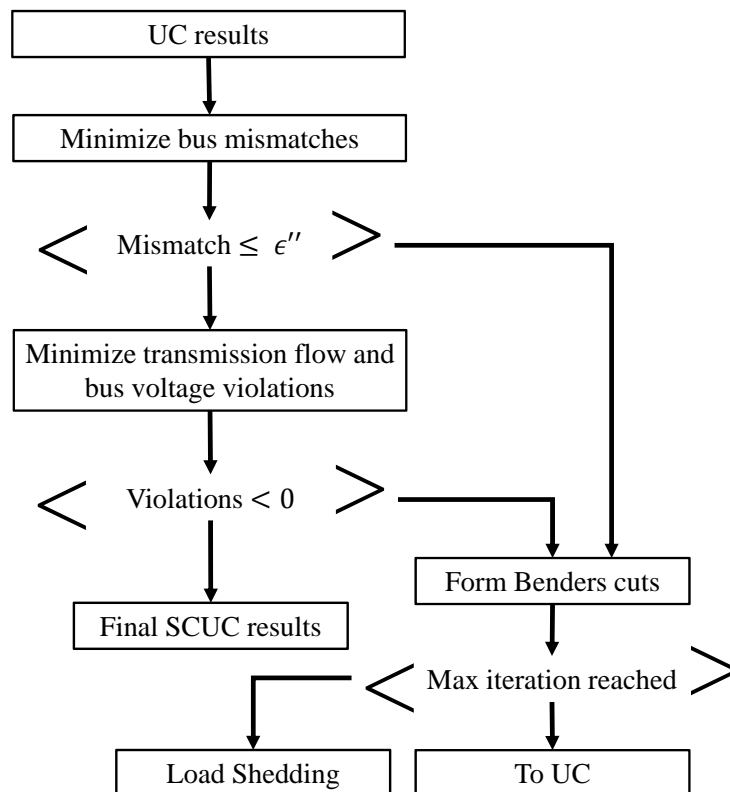
Figure 2.3: BD-SP: the flow chart of AC network security check [20]

2.3.3.3   Decomposition Algorithm with Strong Valid Cuts

The modification of Benders' Decomposition algorithm to solve special structure of MIP problems becomes a trend in the recent studies. Reformulation-Linearization Technique (RLT) and lift-and-project scheme are the key components of convexification procedure scheme. Sherali and Fraticelli [62] proposed to use an RLT or lift-and-project scheme to solve the subproblems of two-stage stochastic mixed integer programs which are incorporated with the classical Benders'Decomposition. The Benders' cuts are generated as functions of the first-stage variables and proven to be globally valid to improve lower bound. Also, Sherali and Zhu [64] proposed a decomposition-based branch-and-bound algorithm (DBAB) for solving SIP with mixed-integer variables in two stages. The DBAB is developed based on the process of hyperrectangle partitioning in the projected space of first-stage variables. Sherali and Smith [63] address how to use RLT to recast a class of two-stage stochastic hierarchical multiple risk problems and then apply Benders' partitioning approach. The two-stage SMIPs to be solved by the specialized Benders' Decomposition algorithm are targeted towards those programs having purely binary decision variables in first-stage and binary risk variables included in second-stage.

Another branch to implement the decomposition method for SMIP grows upon the foundation of disjunctive programming. In fact, a cutting plane decomposition method was developed to adopt the lift-and-project scheme and generate disjunctive cuts which are derived for one scenario but still valid for other scenarios [43]. By doing so, the solution time can be reduced potentially and the effectiveness of disjunctive cuts in solving large-scale SMIPs has been verified by stochastic supply chain management.

In addition, lifting techniques are applied to solve o-1 mixed integer programs. The typical application is to solve 0-1 knapsack problems which generate lifted cover inequalities and are solved by branch-and-cut algorithm [22, 23, 38]. The other successful applications include single node flow

model [36], MIP with variable upper bounds [61] and general mixed integer knapsack sets [4]. Lifting is the transformation process that a valid inequality from a restricted problem is converted to a valid inequality for the whole problem [51]. The basic concepts of lifting are based on valid inequalities and facets for related polyhedra. Richard et. al. [52] explored the lifting of continuous variables in a single knapsack constraint. The developed lifting theory focuses on the lifting of continuous variables fixed to 0 and 1 and the corresponding lifting algorithm.

However, the above studies only employ the single-dimensional lifting function and particularly most lifting functions are not superadditive. The interest thus is extended to build multidimensional superadditive lifting functions [88]. The framework of building high-dimensional superadditive lifting functions is proposed by Zeng and Richard [89] in view of the superadditive approximation of lower-dimensional lifting functions. In this way, strong inequalities can be more easily obtained and some stronger cutting planes can be generated not just from the knapsack or flow constraints. Meanwhile, the determination of lifting coefficients is a major part of lifting procedure, which is usually able to reduce finding extreme points of a small-dimensional polyhedron [51].

CHAPTER 3: STOCHASTIC EXPANSION PLANNING MODEL FOR COMBINED POWER AND NATURAL GAS SYSTEMS

3.1 Introduction

Capacity expansion planning problems have been widely discussed for natural gas production, transportation and storage as well as power generation, transmission and distribution. The objectives of this type of problems are to determine when, where, and which new facility should be constructed or existing facility should be expanded over a long-term planning hortation. When making a long-term expansion plan, decision makers have to take in account of a series of uncertainties, such as supply/demand uncertainties, economic and technical features of emerging generation techniques, construction durations, government regulations, and environmental policies. Any uncertain factors would more or less affect investment decisions or/and operational decisions in an overall planning project.

So far, more than two thirds of power generation are generated from fossil fuels resources along with a billion ton of GHG going into the atmosphere. The impacts of GHG have attracted people's attentions and adopted regional or national policies to combat climate changes. Thus more renewable energy generation resources are incorporated with traditional power generation systems and supplemented by gas-fired power generation. These two promising generation sources also encounter uncertainty issues, i.e. uncertain generation outputs and high volatile gas prices, separately, which further bring additional challenges to decision makers.

Making an individual expansion plan on either system simply neglects the dependence and correlations between both systems as well as the influence from the same uncertainty. This Chapter thus aims to provide another solution framework to solve the capacity expansion planning problem

for an integrated system including natural gas system, power generation system, renewable energy system and transmission network. Applying co-optimization on two main subsystems, i.e. gas system and power system, one can obtain comprehensively optimal solutions through considering relevant uncertainties in the following proposed model.

3.2   Problem Statement

Taking into account the dependance and correlation between natural gas system and electricity power system, the aim of the problem is to optimize the capacity expansion planning for an integrated energy system. In this integrated system, natural gas system and electricity power system are defined as two subsystems, where they share several common nodes e.g. Node 2 to Node 4 in the whole energy network, shown in Figure 3.1. These common nodes exist because NG power plants locate there and are connected with NG pipeline network as well as power transmission network. Thus, they make two individual systems as an integrated energy system.
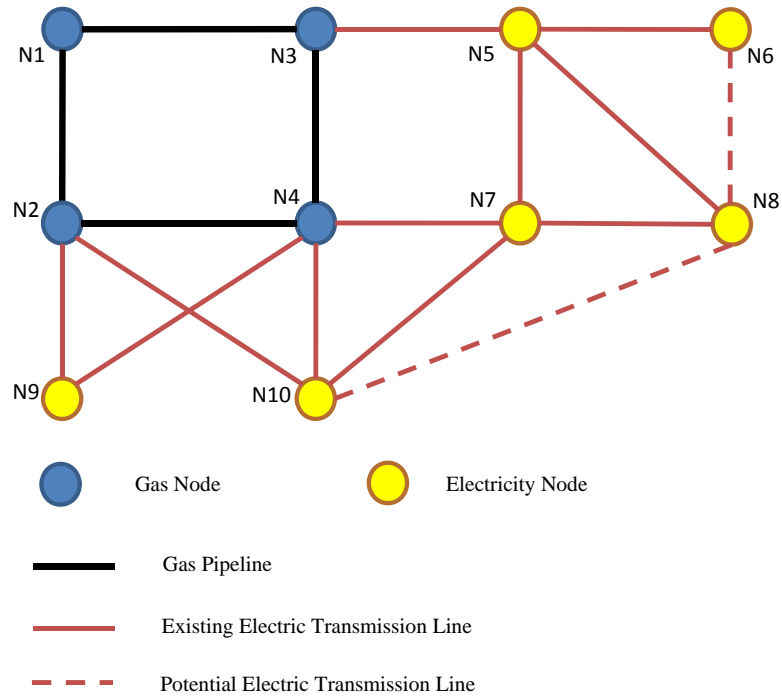
Figure 3.1: An integrated energy network

In NG system, an existing NG transmission network generally connect NG production wells, LNG ports and NG power plants, which can be improved by determining the expansion levels on LNG tanks and pipeline capacity. Imported LNG are delivered to specific LNG ports and reserved in LNG tanks for further pipeline transmission. In addition, local NG production may directly supply NG to power plants and other customers, or they are collected and delivered to assigned LNG tanks. Due to both NG supply and demand increase, NG pipeline transmission is considered to expand according to long-term NG import planning and forecasted NG demands including industrial uses and residential uses. The NG system optimization is decide which LNG ports are expanded to increase the tank capacities, which existing pipeline should be expand, or/and which potential pipeline can be built to satisfy NG demands. Meanwhile, the expansion levels for each port or arc are considered given to optional ranges and expansion economy.

In electric power system, NG power plants, coal-fired power plants and renewable energy farms, e.g. wind farms and solar farms, are classified as energy resources which able to provide electricity via electricity transmission network.

It's assumed that the facility expansion are discrete and instantaneous. For example, the diameters of gas pipeline are fixed and determined by their design or manufactures. The capacity expansion of a LNG port or a gas-fired power plant is given to other relevant proposed projects. All expansions for facilities and networks can be completed instantaneously without construction time.

3.3 Mathematical Formulation

3.3.1 Objective Function

The objective of expansion planning is to meet the NG demand and the electricity demand simultaneously and minimize the total expansion costs as well as the operation costs. The total expansion costs include any costs induced by LNG tank expansion, gas network expansion, gas-fired plant expansion, renewable energy farm expansion and power network expansion. We define a binary variable α_{ij}^k to denote whether a gas pipeline expansion GP_{ij}^k is made for gas arc (i, j), and another binary variable β_i^k to denote whether a LNG tank expansion NP_i^k is made in terminal i. Then the total cost of pipeline expansion cost is

$$\text{Cost}_{GL} = \sum_{(i,j)\in A_G} \sum_{k\in K} ECA_{ij}^k \alpha_{ij}^k.$$

So does the expansion cost for LNG tank in a gas terminal as follow,

$$\text{Cost}_{LNG} = \sum_{i\in N_{LNG}} \sum_{k\in K} ECL_i^k \beta_i^k.$$

39

In addition, we define other three binary variables for the expansion of electric power systems. A binary variable x_{ij}^k is denoted whether an electric transmission line expansion EF_{ij}^k is made for electricity line (i, j), a binary variable y_i^k to denote whether a gas-fired plant expansion EG_i^k is made at bus i, and a binary variable ϕ_i^k to denote whether a renewable generation expansion RP_i^k is made at bus i.

The total cost of transmission capacity expansion is

$$\text{Cost}_{EL} = \sum_{(i,j) \in A_E} \sum_{k \in K} ECE_{ij}^k x_{ij}^k.$$

Besides the total costs for possible gas-fired power plant expansion and renewable farm expansion are expressed as follow

$$\text{Cost}_{GGen} = \sum_{i \in N_{Gen}^G} \sum_{k \in K} ECP_i^k y_i^k$$

and

$$\text{Cost}_{Ren} = \sum_{i \in N_{REW}} \sum_{k \in K} ECN_i^k \phi_i^k.$$

The operation costs mainly cover gas transmission cost, gas holding cost in power plant and fuel cost for power generation. Particularly, power generation cost is time dependent and subject to the fuel price variation and uncertainty in practice. To incorporate price uncertainty into model, fuel price is considered as stochastic parameter and its possibilities can be presented by singly discrete scenarios. As the problem is formulated by stochastic programming, operational decisions are associated with a corresponding fuel price in each scenario and the total operational cost is

$$\text{Cost}_{OP} = \sum_{\xi \in \Xi} Prob(\xi) \sum_{t \in T} \left(\sum_{(i,j) \in A_G} TC_{ij} f_{ijt}^{G\xi} + \sum_{i \in N_{GEN}^G} \left(GP_{it}^\xi p_{it}^{G\xi} + GH_i r_{it}^\xi \right) \right) + \sum_{t \in T} \sum_{i \in N_{GEN}^C} CP_{it} p_{it}^C.$$

Thus the objective function is formulated in (3.1) to the facility expansion(s) which satisfies (satisfy) the NG demand and the electricity demand at minimum cost.

$$
\begin{aligned}
\text{Min} \quad & \sum_{(i,j)\in A_G}\sum_{k\in K} ECA_{ij}^k \alpha_{ij}^k + \sum_{i\in N_{LNG}}\sum_{k\in K} ECL_i^k \beta_i^k + \sum_{(i,j)\in A_{EL}}\sum_{k\in K} ECE_{ij} x_{ij}^k + \sum_{i\in N_{GEN}^G}\sum_{k\in K} ECP_i^k y_i^k \\
& + \sum_{i\in N_{REW}}\sum_{k\in K} ECN_i^k \phi_i^k + \sum_{\xi\in\Xi} Prob(\xi)\sum_{t\in T}\left(\sum_{(i,j)\in A_G} TC_{ij} f_{ijt}^{G\xi} + \sum_{i\in N_{GEN}^G}\left(FP_{it}^\xi p_{it}^{G\xi} + GH_i r_{it}^\xi \right) \right) \\
& + \sum_{t\in T}\sum_{i\in N_{GEN}^C} CP_{it} p_{it}^C
\end{aligned}
\tag{3.1}
$$

3.3.2 Natural Gas System Constraints

In this model, we interpret two interdependent networks for natural gas system and electric power system. As defining a set of nodes for an integrated system, each node can belong to one or more of sets, i.e. the set of nodes in gas network N_G, the set of LNG terminals N_{LNG}, the set of nodes in electricity network N_E, the set of renewable energy farms N_{REW}, the set of gas-fired power plants N_{GEN}^G, and the set of coal-fired power plants N_{GEN}^C. For example, as shown in Figure 3.3, Node 2 can be used for gas production, consumption and transportation through it ($i \in N_G$); meanwhile, it has electricity consumption ($i \in N_E$) and a gas-fired power plant ($i \in N_{GEN}^G$) connecting with electricity network. Note that for the LNG terminals we define a set N_{LNG}, which is a subset of N_G. For the gas-fired power plant, a set N_{GEN}^G is the subset of $N_G \cap N_E$. The similar concept applies to electric arc of the networks. A_G is the set of pipelines in the gas network and A_E is the set of electric transmission lines. All sets are summarized in Table A.7. The notations for parameters and decision variables are defined in Tables A.4 and A.3.

Constraint (3.2) defines the gas flow balance constraint, where the outgoing flow $\sum_{(i,j)\in A_{Gi}^+} f_{ijt}^{G\xi}$ minus the incoming flow multiplied by one minus loss rate $\sum_{(j,i)\in A_{Gi}^-}(1-TL_{ji}) f_{jit}^{G\xi}$ are equal to

41

the gas supply s_{it}^{ξ} minus the gas demand for industrial use $D_{it}^{0\xi}$ and for electric power generation $d_{it}^{P\xi}$ at that node if there is a gas-fired power plant there. The loss rate imposed by the fact that gas pumps consume consume gas in order to transport it over the network of pipelines. We assume that the existing pipeline network has an arborescence(tree) structure and consider the gas pipeline transportation with both directions. Constraints (3.3) and (3.4) defines outgoing pipeline capacity and incoming pipeline capacity, respectively.

Gas Transportation Constraints:

$$\sum_{(i,j)\in A_{Gi}^+} f_{ijt}^{G\xi} - \sum_{(j,i)\in A_{Gi}^-}(1-TL_{ji})f_{jit}^{G\xi} = s_{it}^{\xi} - D_{it}^{0\xi} - d_{it}^{P\xi}, \quad \forall\, i \in N_G,\, t \in T,\, \xi \in \Xi, \quad (3.2)$$

$$f_{ijt}^{G\xi} \leq \underline{U}_{ij} + \sum_{k\in K} GP_{ij}^k \alpha_{ij}^k, \quad \forall\, (i,j) \in A_G^+,\, t \in T,\, \xi \in \Xi, \tag{3.3}$$

$$f_{jit}^{G\xi} \leq \underline{U}_{ij} + \sum_{k\in K} GP_{ji}^k \alpha_{ji}^k, \quad \forall\, (j,i) \in A_G^-,\, t \in T,\, \xi \in \Xi, \tag{3.4}$$

$$f_{ijt}^{G\xi} \geq 0, \quad \forall\, (i,j) \in A_G,\, t \in T,\, \xi \in \Xi, \tag{3.5}$$

$$\alpha_{ij}^k \in \{0,1\}, \quad \forall\, k \in K,\, (i,j) \in A_G, \tag{3.6}$$

In addition, all LNG tanks in terminals are already connected to the gas network and continuously supplied with imported LNG. Constraint (3.7) limits the throughput capacity of LNG terminals to a gas node where LNG terminals expansion projects are considered to expand the storage size of LNG tank. Constraints (3.8) shows that LNG storage amount can not exceed its own LNG tank capacity. Assuming that NG produced from local gas wells does not go through LNG tank, constraint (3.9) indicates that NG supply to a gas network would be the total gas supply from LNG tank plus gas production at a common node. The gas supply process at one node is shown in Figure 3.2.
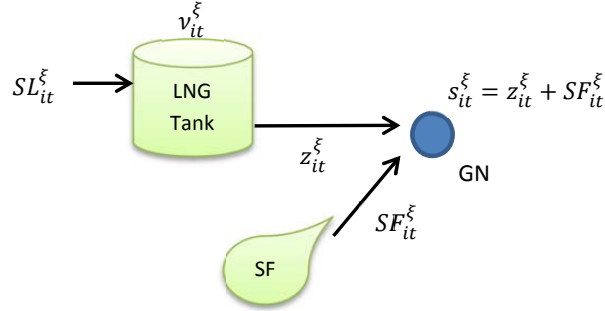
Figure 3.2: Natural gas supply at a node

LNG System Constraints:

$$z_{it}^{\xi} \leq \underline{V}_i + \sum_{k \in K} NP_i^k \beta_i^k, \quad \forall i \in N_{LNG}, t \in T, \xi \in \Xi, \tag{3.7}$$

$$SL_{it}^{\xi} - z_{it}^{\xi} + v_{it-1}^{\xi} \leq \underline{V}_i + \sum_{k \in K} NP_i^k \beta_i^k, \quad \forall i \in N_{LNG}, t \in T, \xi \in \Xi, \tag{3.8}$$

$$s_{it}^{\xi} = z_{it}^{\xi} + SF_{it}^{\xi}, \quad \forall i \in N_G, t \in T, \xi \in \Xi, \tag{3.9}$$

$$d_{it}^{P\xi}, s_{it}^{\xi}, z_{it}^{\xi}, v_{it-1}^{\xi} \geq 0, \quad \forall i \in N_G, t \in T, \xi \in \Xi, \tag{3.10}$$

$$\beta_i^k \in \{0, 1\}, \quad \forall k \in K, i \in N_{LNG}, \tag{3.11}$$

3.3.3 Electrical Power System Constraints

Electricity expansion and transmission constraints are imposed by equations (3.21) - (3.25). Since a gas-fired plant is equipped with one or more NG storage tanks to maintain normal operations. The NG holding constraints ensure that NG consumption for power generation $d_{it}^{P'\xi}$ can not exceed the current NG storage amount r_{it}^{ξ} in (3.13) and the NG storage amount r_{it}^{ξ} is limited by NG storage tank capacity in (3.14).

Constraint (3.15) represents the efficiency of a gas-fired power plant, which indicates the amount of NG used to generate a MW of electricity. According to U.S. EIA data, a MW of electricity generation consumes 7.86 MMcf of NG on average. Constraints (3.16) and (3.17) limit the output of a power plant to its physical capabilities which can be expanded in expansion projects. Due to environmental policies, coal-fired power plant is not considered to expand in this plan but it still operates to provide certain electricity to power system in (3.18). The total CO_2 emissions from both gas-fired and coal-fired power plants are constrained by emission allowance ψ_t, shown in constraint (3.19).

Electricity Generation Constraints:

NG holding (storage):

$$r_{it}^{\xi} = r_{it-1}^{\xi} + d_{it}^{P\xi} - d_{it-1}^{P'\xi}, \quad \forall\, i \in N_{GEN}^G, t \in T, \xi \in \Xi \tag{3.12}$$

$$0 \le d_{it}^{P'\xi} \le r_{it}^{\xi}, \quad \forall\, i \in N_{GEN}^G, t \in T, \xi \in \Xi \tag{3.13}$$

$$0 \le r_{it}^{\xi} \le D_i^{Cap}, \quad \forall\, i \in N_{GEN}^G, t \in T, \xi \in \Xi \tag{3.14}$$

Power generation: NG and Coal

$$p_{it}^{G\xi} = \mu_i d_{it}^{P'\xi}, \quad \forall\, i \in N_{GEN}^G, t \in T, \xi \in \Xi, \tag{3.15}$$

$$p_{it}^{G\xi} \le \underline{G}_i^{Gmax} + \sum_{k \in K} EG_i^k y_i^k, \quad \forall\, i \in N_{GEN}^G, t \in T, \xi \in \Xi, \tag{3.16}$$

$$p_{it}^{G\xi} \ge 0.4(\underline{G}_i^{Gmax} + \sum_{k \in K} EG_i^k y_i^k), \quad \forall\, i \in N_{GEN}^G, t \in T, \xi \in \Xi, \tag{3.17}$$

$$0 \le p_{it}^C \le \underline{G}_i^{Cmax}, \quad \forall\, i \in N_{GEN}^C, t \in T, \tag{3.18}$$

Emission limit:

$$\sum_{i \in N_{GEN}^G} EC_i^G p_{it}^{G\xi} + \sum_{i \in N_{GEN}^C} EC_i^C p_{it}^{C\xi} \le \psi_t, \quad \forall\, t \in T, \xi \in \Xi, \tag{3.19}$$

$$p_{it}^{C\xi}, p_{it}^{G\xi}, r_{it}^{\xi} \ge 0, \quad \forall\, i \in N_{GEN}, t \in T, \xi \in \Xi, \tag{3.20}$$

Renewable Resource Constraints:

$$\sum_{i \in N_{REW}} \sum_{k \in K} RP_i^k \phi_i^k \geq RL_t, \quad \forall\, t \in T \tag{3.21}$$

$$NRE_{it}^{\xi} \leq \sum_{k \in K} RP_i^k \phi_i^k, \quad \forall\, i \in N_{REW},\, t \in T,\, \xi \in \Xi \tag{3.22}$$

$$w_{it}^{\xi} = ORE_{it}^{\xi} + NRE_{it}^{\xi}, \quad \forall\, i \in N_{REW},\, t \in T,\, \xi \in \Xi \tag{3.23}$$

$$\phi_i^k \in \{0,1\}, \quad \forall\, i \in N_{REW},\, k \in K \tag{3.24}$$

$$w_{it}^{\xi} \geq 0, \quad \forall\, i \in N_{REW},\, t \in T,\, \xi \in \Xi \tag{3.25}$$

Power balance at each node is enforced by constraint (3.26), where power though existing electrical lines plus power through proposed lines plus electricity generation at that node are equal to electricity demand. Kirchhoff's laws are implemented in constraints (3.26) for existing and potential electrical lines. Constraints (3.27) impose the electric transmission capacity of existing and potential electric lines. If a potential electric line is proposed, the line only has corresponding expansion levels without current capacity. Voltage and voltage angle limits are not considered in a long-term expansion planning.

Electric Transmission Constraints:

$$\sum_{(i,j) \in A_{Ei}^+} f_{ijt}^{E\xi} - \sum_{(i,j) \in A_{Ei}^-} f_{ijt}^{E\xi} = p_{it}^{G\xi} + p_{it}^C + w_{it}^{\xi} - D_{it}^{E\xi}, \quad \forall\, i \in N_E,\, t \in T,\, \xi \in \Xi, \tag{3.26}$$

$$-F_{ij}^{E_{max}} - \sum_{k \in K} EF_{ij}^k x_{ij}^k \leq f_{ijt}^{E\xi} \leq F_{ij}^{E_{max}} + \sum_{k \in K} EF_{ij}^k x_{ij}^k, \quad \forall\, (i,j) \in A_E,\, t \in T,\, \xi \in \Xi, \tag{3.27}$$

$$x_{ij}^k \in \{0,1\}, \quad \forall\, (i,j) \in A_E, \tag{3.28}$$

$$f_{ijt}^{E\xi}, \quad \forall\, (i,j) \in A_E,\, t \in T,\, \xi \in \Xi, \tag{3.29}$$

The complete SEP-IES model is formulated by using stochastic mixed integer linear programming,

shown as follow.

$$[\textbf{SEP-IES}]: \min \quad Z_{(}\alpha, \beta, x, y, \phi, p^C, p^G, f^G, r)$$

$$\text{s.t.} \quad \text{Gas Pipeline Constraints (3.2)-(3.6)},$$

$$\text{LNG System Constraints (3.8)-(3.11)},$$

$$\text{Electricity Generation Constraints (3.12)-(3.19)},$$

$$\text{Renewable Resource Constraints (3.21)-(3.25)},$$

$$\text{Transmission Constraints (3.26)-(3.29)},$$

$$\text{A set of binary variable restrictions.}$$

3.4 Computational Results

This section is to test the validity of the proposed SEP model and discuss the advantages of SEP model for integrated energy system. A 7-node energy system is used as a test case and the solution comparisons focus on the expansion size and the total cost. The SEP model is coded in C++ while solved by CPLEX 12.5. All experiments are implemented on a PC Dell OPTIPLEX 980 with Intel Core i7 vPro at 2.80 GHz and 8 GB memory in a Windows 7 operating system.

3.4.1 Test Case and Input Data

This integrated system includes a 3-node NG network and a 6-node electricity network (see Figure 3.3). A LNG terminal is located at node 1 (N1) with a $10,000$ Mcf of tank capacity. A gas production exists at node 2 (N2) and continuously supplies NG to two gas-fired power plants at N2 and N3. These two power plants are equipped with small NG storage tanks. A coal-fired power plant is located at N3 and a wind farm is located at N7, which are connected to the electricity net-

work. Electric demands occur at N2 to N6 and show different consumption patterns in response to changes in electricity price over time. The energy system parameters and capacity expansion parameters are listed in Table 3.1 and 3.2, respectively. For system network, gas pipeline is presented by black solid line, existing electric transmission line is presented by red solid line, and potential electric transmission line is presented by red dash line. The gas pipeline parameters and electric transmission parameters are listed in Table 3.3 and 3.4.
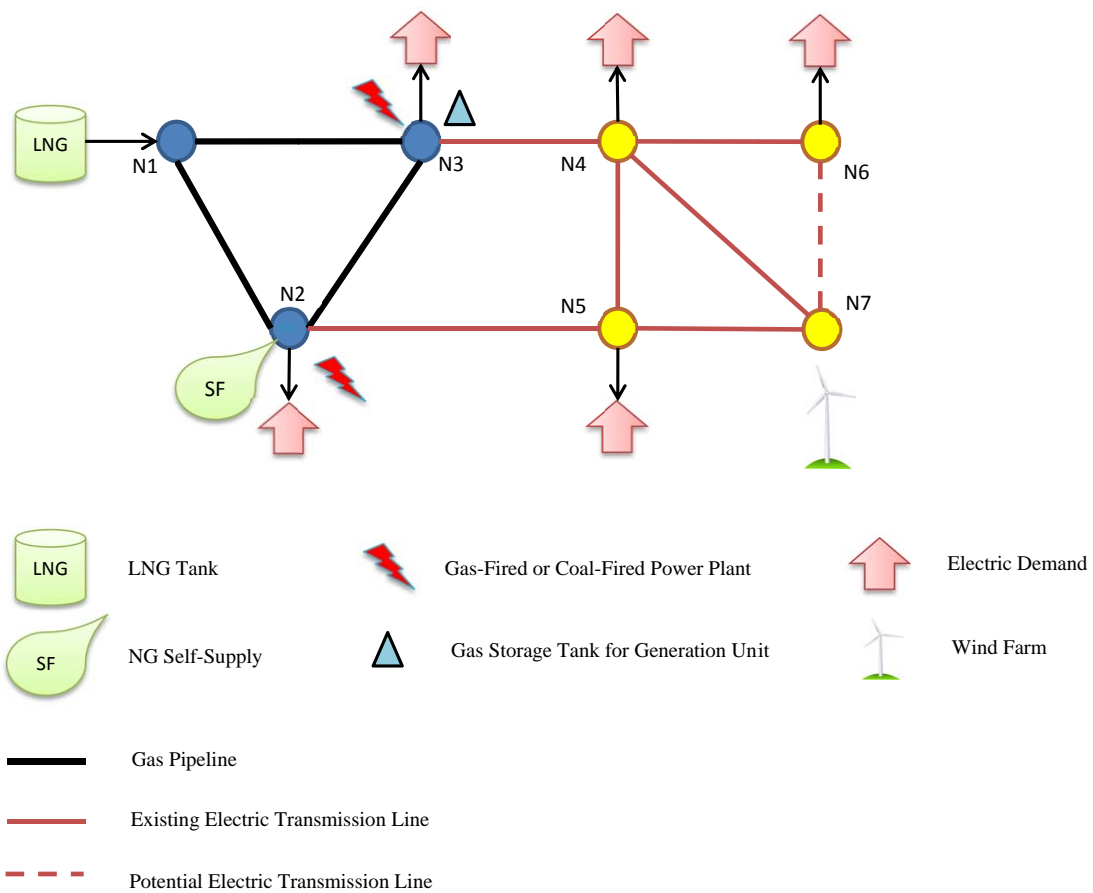
Figure 3.3: An integrated 7-node energy network

Table 3.1: Energy System Parameters

Natural Gas System

		N1	N2	N3
LNG Storage Capacity	V_i	10 MMcf	-	-
Avg. Gas Demand	D_{it}^0	-	2.5 MMcf	1.5 MMcf
Avg. LNG Supply	SL_{it}	35 MMcf	-	-
Avg. NG Production	SF_{it}	-	10 MMcf	-

Electric Power System

		N1	N2	N3
LNG Storage Capacity	D_i^{Cap}	-	120 Mcf	60 Mcf
Heat Rate	$1/\mu_i$	-	0.1277 MWh/Mcf	0.1277 MWh/Mcf
Gas-Fired Generation Capacity	G_i^{Gmax}	-	100 MWh	80 MWh
Coal-Fired Generation Capacity	G_i^{Cmax}	-	-	100 MWh

[a] The symbol, '-', represents no facility or demand available at this node

Table 3.2: Capacity Expansion Parameters

Expansion Level	ECL_1 ($/Mcf)	NP (Mcf)	ECP_2 ($/MWh)	EG_2 (MWh)	ECP_3 ($/MWh)	EG_3 (MWh)	ECN_7 ($/MWh)	RP_7 (MWh)
1	500	4000	500	50	600	40	800	50
2	500	6000	500	70	580	50	800	70
3	500	8000	500	90	550	60	800	90
4	500	10000	500	110	520	70	800	110

Table 3.3: Gas Pipeline Parameters

ID	From	To	Status	Flow Capacity(MMcf)	Transport Cost ($/MMcf)	Loss Rate
L1	N1	N2	E	16	2	0.005
L2	N1	N3	E	16	4	0.005
L3	N2	N3	E	16	2	0.005
L4	N2	N1	E	12	5	0.005
L5	N3	N1	E	12	5	0.005
L6	N3	N2	E	12	5	0.005

Table 3.4: Electric Transmission Parameters

ID	From	To	Status	Flow Capacity(MMcf)	Transport Cost ($/MMcf)
L1	N2	N3	E	120	11
L2	N2	N5	E	120	6
L3	N3	N4	E	120	14
L4	N4	N5	E	120	7
L5	N4	N6	E	120	7
L6	N4	N7	E	120	10
L7	N5	N7	E	120	14
L8	N6	N7	P	-	5

[a] The symbol, 'E', represents existing electric transmission line.

[b] The symbol, 'P', represents potential electric transmission line, which can be built during expansion.

In this case, the fuel price, the NG demand, the NG self-supply, the imported LNG, the electric demand and the renewable energy output are considered as stochastic inputs in the SEP models. According to their individual data patterns and distributions, stochastic inputs can be generated by selecting specific distribution generators. For example, the wind farm as renewable energy resource can provide electricity output within the range of [5,100] MW and the output is simulated by adding the random number generated from normal distribution generators in C++ to the base load. For the detailed number generation process, one can refer Appendix B.
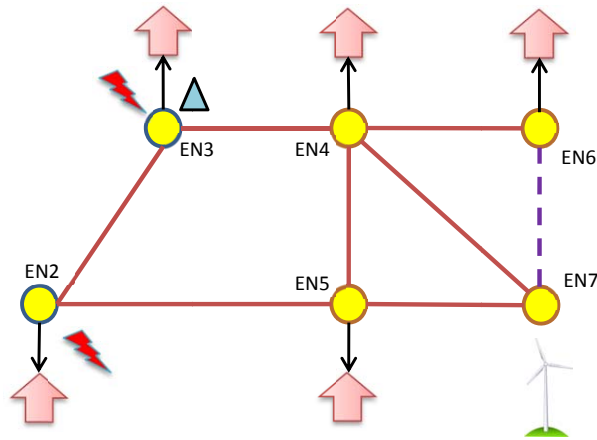
Figure 3.4: An separated electric transmission network
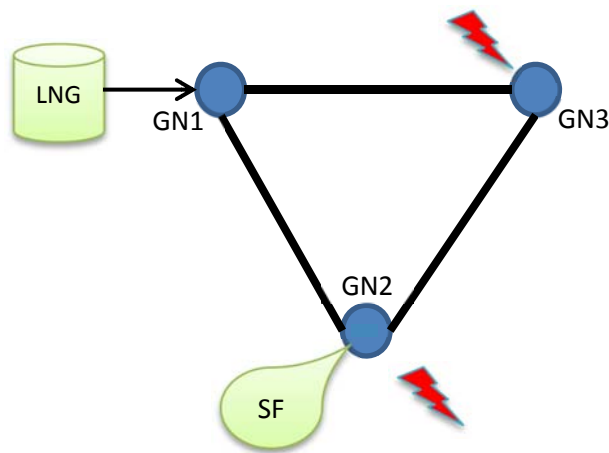
Figure 3.5: An separated gas transport network

50

3.4.2   Result Analysis

The computational experiments mainly focus on the test of SEP model validity, the effects of wind generation uncertainty on an integrated expansion planning, and the impacts of volatile natural gas price on both gas system expansion and power system expansion.

3.4.2.1   SEP model validity

Since existing literature manages the expansion of gas system and power system in isolation, this readily accumulates the forecasted errors from the other system and thus increase more deviations from real cases. This experiment therefore is carried to compare the individual-system optimization and the integrated system optimization on stochastic expansion planning. Two cases are proposed and use same instances to compute individual solutions.

- Case I: Solve for gas system and electric power system individually. Since electricity demands are viewed as final destinations, it's more reasonable to solve for isolated power system prior to isolated gas system. When the gas consumptions for power plant are obtained, they will be passed to the gas system model as parameter inputs where $d_{it}^{P\xi}$ becomes a constant given values from power system solutions. The gas system model then will be solved individually.

- Case II: Apply SEP model to solve for integrated energy system.

Table 3.5: SEP Case I: Capacity Expansion Results

Expn	β_1	y_1	y_2	ϕ_7	α_{01}	α_{02}	α_{12}
k=1	1	0	0	0	1	0	0
k=2	1	0	0	0	1	0	0
k=3	1	0	0	1	1	0	0
k=4	1	1	0	0	1	1	0
Total	28000	70	0	90	6000	2000	0

Table 3.6: SEP Case II: Capacity Expansion Results

Expn	β_1	y_1	y_2	ϕ_7	α_{01}	α_{02}	α_{12}
k=1	0	0	0	0	1	0	0
k=2	0	0	0	0	1	0	0
k=3	0	1	0	1	1	0	0
k=4	1	0	0	0	1	0	0
Total	17000	60	0	90	6000	0	0

In Case I, the objective value of gas system is $301,181$ and the objective value of power system is $162,868$, with $464,049$ of total costs. While the objective value of Case II is only $307,157$ and the costs can be reduced significantly by 51.08%. The detailed expansion levels on both cases are reported in Tables 3.5 and 3.6. Apparently, by considering two systems simultaneously, SEP model is able to reduce the expansion levels on LNG storage capacity, gas-fired power plant capacity and pipeline capacity effectively. More importantly, to satisfy the same level of electricity demands, decision makers can averse partial investment risks on gas system due to supply or demand forecast

errors, two-level system difference and time difference.

3.4.2.2 *The effects of wind generation uncertainty on energy system expansion*

Since each wind turbine has its own range of wind speeds and produces as its rated or maximum capacity. Assuming a 1.5 MW wind turbine with a 30% capacity factor, its daily wind generation is calculated as

$$1.5\text{MW} \times 24\text{hours} \times 30\% = 10.8MW.$$

The aim of this section is to investigate the effects of wind generation uncertainty on integrated energy system expansion, such as NG storage tanks, pipeline network, and gas-fired power generators. In order to present wind uncertainties, daily wind outputs are simulated with a normal distribution $\mathcal{N}(\mu, \sigma^2)$. Different from hourly wind outputs, the daily wind outputs are independent each other and based on the individual mean output of a wind farm. For example, the wind farm at node 7 has a random output NRE_t distributed normally with mean μ_t and variance σ_t^2, under scenario ξ.

Through increasing the variance of output at each time period, other two cases are used to show the effects of wind generation on capacity expansion.

- Case III: Low uncertainty with $\mu = 60$ MW and $\sigma = 8$ MW (Figure 3.6).

- Case IV: High uncertainty with $\mu = 60$ MW and $\sigma = 20$ MW (Figure 3.7).

The average wind outputs in Case III have less volatility between 40 MW and 80 MW than Case IV. While Case IV involves some extreme outputs in specific days resulting in large variations. Solving both cases via SEP model, the objective value and the expansion level of facility on each case are captured and compared in Tables 3.7 and 3.8.
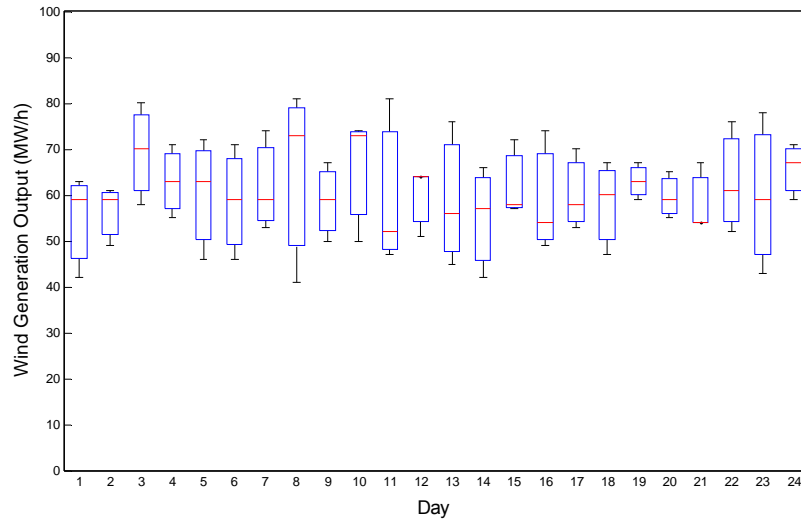
Figure 3.6: Daily wind outputs with low uncertainty
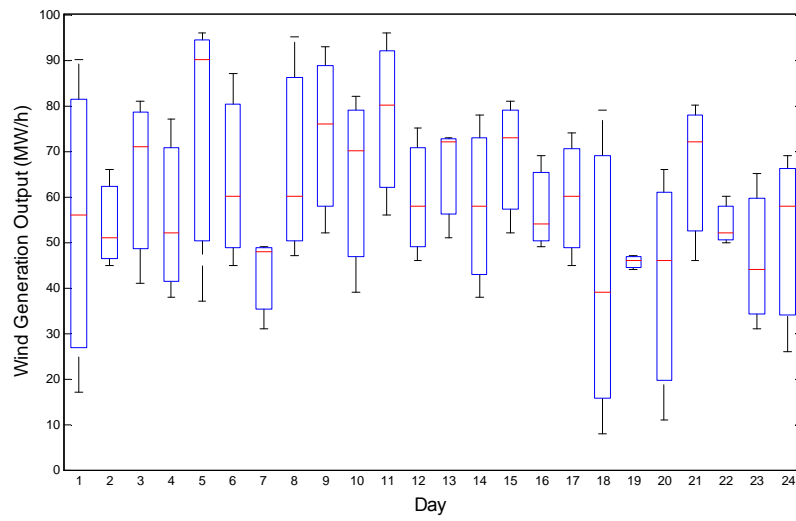
Figure 3.7: Daily wind outputs with high uncertainty

Table 3.7: SEP Case III: Capacity Expansion Results

Expansion	β_1	y_1	y_2	ϕ_7	α_{01}	α_{02}	α_{12}
k=1	0	0	0	0	1	0	0
k=2	1	0	0	0	1	0	0
k=3	1	0	0	0	1	0	0
k=4	1	1	0	1	1	0	0
Total	26000 Mcf	150 MW	0	80 MW	6000 Mcf	0	0

Table 3.8: SEP Case IV: Capacity Expansion Results

Expansion	β_1	y_1	y_2	ϕ_7	α_{01}	α_{02}	α_{12}
k=1	1	0	0	0	1	0	0
k=2	1	1	0	0	1	0	0
k=3	1	0	0	0	1	1	0
k=4	1	0	0	1	1	1	0
Total	30000 Mcf	50 MW	0	80 MW	6000 Mcf	3500 Mcf	0

The objective value of Case III is $1,560,770$ and the objective value of Case IV is $1,560,220$. It can be observed that both objective values are very close considering different wind scenarios. However, the expansion costs on each case are various since there appears the different expansion sizes on gas pipeline network and gas-fired power plants. In Case III, the power plant G2 is expanded by 180 MW and only gas pipeline $(0,1)$ gets enlarged with 6000 Mcf due to lower transportation unit cost on this arc. In Case IV, only 50 MW of generation capacity is added to G2 but the gas pipeline $(0,2)$ is expanded by 3500 Mcf in addition to full expansion on arc $(0,1)$.

55

The reason causes the different expansion levels is that the original pipeline capacity not satisfying gas consumptions. Highly variable wind outputs means highly variable gas consumptions at power plants, which usually triggers the low-generation power plant increases generation level frequently and thus largely increase corresponding pipeline capacity to accommodate generation changes. Although the pipeline transportation cost of arc $(0, 2)$ is higher than that of $(0, 1)$, this is not necessary to increase the long-term expected operational costs due to the wind variation range and the scenario probability. If wind output has lower uncertainty, the system tends to operate the low-generation-cost power plant at full generation level and use other power plants to accommodate extreme peak loads, when wind outputs happen to the low level. Therefore, by considering an integrated energy system, the system can obtain a more applicable expansion planning based on renewable generation characteristics, rather than simply expanding power plant capacities or transmission capacities.

3.4.2.3 *The effects of NG price variation on energy system expansion*

Based on historical LNG price pattern, it's generally divided into two various price patterns, low volatility and high volatility. Both patterns are easily found in LNG imports prices at U.S. EIA historical data. To increase the forecasted gas prices, the standard deviation in Case VI is increased by 1$/Mcf due to different regions and the individual boxplots regarding single-location forecasted gas prices are shown in Figure 3.8 and 3.9, respectively.

- Case V: Low volatility with $\mu = \$7/\text{Mcf}$ and $\sigma = \$2/\text{Mcf}$ (Figure 3.8).

- Case VI: High volatility with $\mu = \$7/\text{Mcf}$ and $\sigma = \$3/\text{Mcf}$ (Figure 3.9).
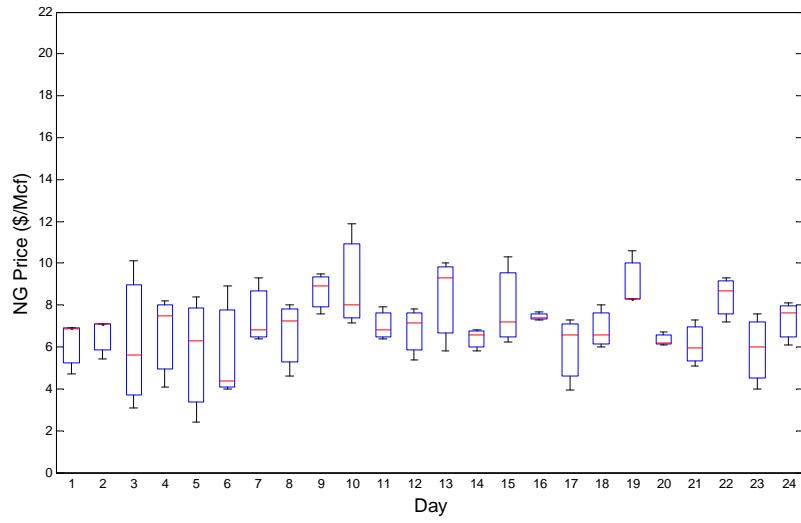
Figure 3.8: Daily NG prices with low volatility
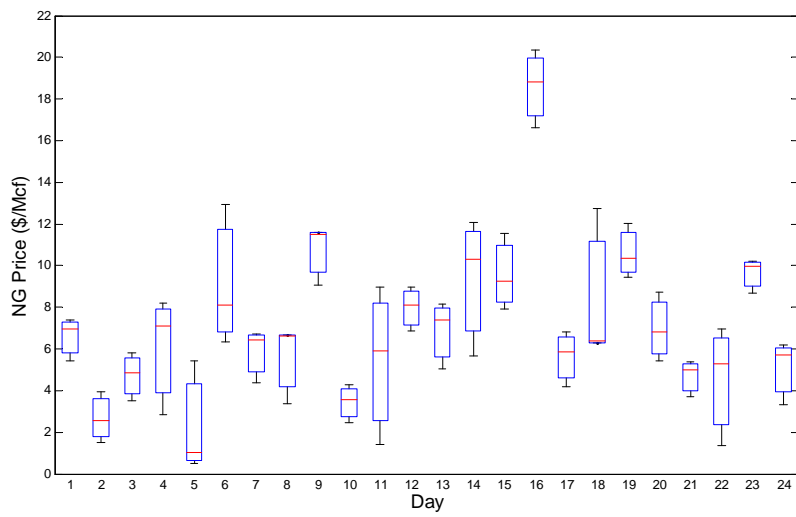
Figure 3.9: Daily NG prices with high volatility

Table 3.9: SEP Case V and Case VI: Capacity Expansion Results

Expansion	β_1	y_1	y_2	ϕ_7	α_{01}	α_{02}	α_{12}
k=1	1	0	0	0	1	0	0
k=2	1	1	0	0	1	0	0
k=3	1	0	0	0	1	1	0
k=4	1	0	0	1	1	1	0
Total	30000 Mcf	50 MW	0	80 MW	6000 Mcf	3500 Mcf	0

The objective value of Case V is $\$1,375,080$ and the objective value of Case VI is $\$1,393,440$. These two cases have 1.34% difference of total costs which comes from the expected operational costs. Table 3.9 lists the expansion levels on each facility for both cases. Since they share the same expansion planning in the same instances, NG prices directly affect the operational costs, particularly in power generation costs. However, based on this case, NG prices is not able to impact the gas consumption on power plants in the fact that gas consumption is highly dependent of electricity demands and renewable energy supply. In addition, this case assumes LNG imports are offered according to signed contracts, which means LNG supply is fixed over a long-time period. If considering LNG imports as variables, it leads to change the original gas system constraints and LNG storage strategy, which is left for future research.

CHAPTER 4: A SUC MODEL WITH NON-GENERATION RESOURCES USING RISK CONSTRAINTS

4.1 Introduction

Stochastic unit commitment (SUC) is an effective modeling technique and it has been introduced as a promising tool to deal with power generation problems involving uncertainties [5, 55, 72, 76, 79, 94]. SUC assumes scenario-based uncertainty in unit commitment problems, *i.e.* it captures the uncertainty and variability of the underlying factors by simulating a large number of scenarios. One of prominent factors is the high penetration of renewable energy to current power systems, which brings a lot of uncertainties on energy supply and transmission. Considering one of renewable energy resources like wind energy, the forecasting errors or intermittent energy supply in net load will cause conventional power plants to ramp up/down frequently to ensure their energy outputs satisfy real-time demand levels. Therefore, on one side, non-generation resources, *e.g.*, demand response (DR) and energy storage (ES), have been well developed and facilitate the expansion of renewable energy's usage. On the other side, management techniques for energy systems can be used effectively to ensure the smooth integration of existing power plants with renewable energy outputs [35] as well as power system reliability. This chapter aims to investigate the unit commitment scheduling cooperated with non-generation resources and risk control so as to improve power system reliability and reduce cost. The main uncertainties in consideration of this chapter include renewable energy output and demand response. This real-world problem is formulated through a two-stage stochastic mixed integer program.

To limit the likelihood of load losses due to uncertainties, risk management has been merging to daily operations of power generation. Chance-constrained optimization models have been devel-

oped to deal with uncertain wind power output [82], uncertain load [45] and transmission network expansion planning [87]. Chance constraints are equivalent to constraints that bound the risk measure Value-at-risk (VaR). Another tighter risk measure defined upon VaR is conditional value-at-risk (CVaR). As popular risk measures, VaR and CVaR have been widely used in financial risk management [53, 73, 57]. Compared to VaR based models, CVaR based models are less computationally demanding due to the fact that modeling CVaR only requires linear constraints and continuous variables. We thus introduce CVaR to our SUC model to maintain system reliability at various levels.

Compared to the recent works of stochastic programming approaches on unit commitment problems (e.g., [56, 13, 47, 37]), the main contributions of this study are summarized as follow:

1. A comprehensive two-stage stochastic mixed intger programming model for unit commitment with risk constraints based on CVaR is developed to control risk of loss of loads while including non-generation resources. The proposed optimization model helps to satisfy real-time demands and minimize the total operation costs with the support of non-generation resources. The model can help balance between expected cost and risks of load losses.

2. A modified Benders' Decomposition algorithm is applied to solve for this CVaR-based model and reduce computation times.

3. Numerical experiments are conducted to find out optimal unit commitment solutions and compare the effects of the risk resilience of non-generation resources on power generation. Sensitivity analyses are also carried out to evaluate reliability parameters on reducing the generation costs.

The remainder of this chapter is organized as follows. Section 5.2 discusses the mathematical formulations for risk-constrained unit commitment including demand response constraints, energy

storage constraints, the integrated model with CVaR risk measures and solution approach. Section 4.4 provides numerical examples for the 7-bus system and the 118-bus system, respectively, and discusses their computational results and sensitivity analyses.

4.2 Mathematical Formulation

In this paper, we formulate a two-stage stochastic programming model for the unit commitment problem under uncertainties. Commitment decisions (here-and-now) are assumed to be made a day ahead, which is considered as the first stage. These decisions need to be able to accommodate the real-time situations with uncertain demands and renewable energy outputs. In order to model uncertainties, we use discrete scenarios within the set Ξ. Simulation techniques are used to generate different scenarios in real time. The second stage is addressing the real-time decisions (dispatch, transmission, etc.) under all scenarios, which are captured by $|\Xi|$ sets of constraints and variables. In addition, the second stage is linked with day-ahead unit commitment decisions through dispatch constraints. The unit commitment decisions on the first stage only contain binary decision variables and are determined before the uncertain demands and renewable generation outputs realized. The second stage handles the issues regarding economic dispatch, power transmission, demand response and energy storage after the uncertainties unfold. To incorporate reliability explicitly using scenario information, we also introduce the risk constraints in the second stage. A comprehensive nomenclature of sets, parameters, and variables in this paper is attached after the last section.

The objective function (4.1) is composed of two parts. The first part is the total start-up and shut-down cost for day-ahead unit commitment decisions (in first stage) since we assume no reschedules of units in real time. The second part is the total cost associated with the second stage, which is the expected fuel cost. Because we are using discrete scenarios, it is a weighted average of the fuel costs of all scenarios. The objective function of this two-stage stochastic model is presented

61

as follows,

$$\sum_{g \in G} \sum_{t \in T} (SU_{gt} v_{gt} + SD_{gt} w_{gt}) + \sum_{\xi \in \Xi} Prob^{\xi} \sum_{g \in G} \sum_{t \in T} F_g(p_{gt}^{\xi}) \qquad (4.1)$$

Note the first part of the objective function is deterministic (determined by here-and-now decisions) while the second term is an expected cost for electricity dispatch. The fuel cost is actually a quadratic function of the dispatch/production level, p, *i.e.*, for generator g, $F_g(p) = a + bp + cp^2$, where a, b and c are usually positive coefficients. An example of these parameters can be found in Table 4.3. Because the fuel cost function is nonlinear (which can complicate the computation with the presence of binary decisions), a piecewise linear approximation is used to yield very close solutions instead of directly solving the mixed integer quadratic problem. In order to obtain the piecewise linear approximation of the fuel cost function, SOS techniques are used to replace the original function $F_g(p)$ by $\sum_{k=1}^{K} C_k \lambda_k$ with additional constraints, $\{p = \sum_{k=1}^{K} \Delta_k \lambda_k, \sum_{k=1}^{K} \lambda_k = u, \lambda_k \geq 0, k = 1, \ldots, K\}$, where u is the commitment status of generator g, and Δ_k and C_k are parameters used to approximate the quadratic curve. For more details please refer to [92]. Hence, with the piecewise linear approximation, we have a purely mixed integer program. In the following subsections, we will explain the different sets of constraints and variables for the two-stage stochastic mixed integer linear programming model.

4.2.1 Unit Commitment and Dispatch Formulation

As the here-and-now decision making part, unit commitment is to determine the operating status of generation units in a power system to meet the next day's demands. But the first stage mainly involves the constraints on the commitment status of generators at different times. The following constraints (5.2)-(5.5) represent the requirements for minimum up time, minimum down time,

startup action, and shutdown action of each unit at each time period, respectively.

$$u_{gt} - u_{g(t-1)} \le u_{g\tau} \qquad \forall\, g \in G,\, t \in T,$$
$$\tau = t, \dots, min\{t + L_g - 1, |T|\} \qquad (4.2)$$

$$u_{g(t-1)} - u_{gt} \le 1 - u_{g\tau} \qquad \forall\, g \in G,\, t \in T,$$
$$\tau = t, \dots, min\{t + l_g - 1, |T|\} \qquad (4.3)$$

$$v_{gt} \ge u_{gt} - u_{g(t-1)} \qquad \forall\, g \in G,\, t \in T \qquad (4.4)$$

$$w_{gt} \ge -u_{gt} + u_{g(t-1)} \qquad \forall\, g \in G,\, t \in T \qquad (4.5)$$

$$u_{gt},\, v_{gt},\, w_{gt} \in \{0,1\} \qquad \forall\, g \in G,\, t \in T \qquad (4.6)$$

where three binary variables, u_{gt}, v_{gt}, w_{gt}, are defined as commitment decision, startup action and shutdown action of unit g at period t respectively. L_g and l_g are minimum-on time and minimum-down time, respectively.

As the wait-and-see decision making part, economic dispatch is to fulfill system operations subject to available resources and then to achieve the optimal output for demand satisfactions. The dispatch or generation levels are treated as the wait-and-see decisions given the day-ahead unit commitment status. Their function is mainly reflected in the generation lower limit (5.10) and the upper limit constraint (4.8), and the ramping up and down limit constraint (4.9). In addition, there exist some possibilities at specific generators to increase power output by spinning reserve, which are shown in the constraints of satisfying system spinning reserve (4.10) and spinning reserve limit (4.11). The nonnegative restriction of generator dispatch is ensured by constraint (4.12). Note that there are $|\Xi|$ sets of these decision variables and constraints, with each set representing a scenario indexed by ξ. The constraints are shown as follows,

$$P_g^{min} u_{gt} \le p_{gt}^{\xi} \qquad \forall\, g \in G,\, t \in T,\, \xi \in \Xi \qquad (4.7)$$

$$p_{gt}^{\xi} + s_{gt}^{\xi} \leq P_g^{max} u_{gt} \qquad\qquad \forall\, g \in G, t \in T,\, \xi \in \Xi \qquad\qquad (4.8)$$

$$-RD_g \leq p_{gt}^{\xi} - p_{gt-1}^{\xi} \leq RU_g \qquad\qquad \forall\, g \in G, t \in T,\, \xi \in \Xi \qquad\qquad (4.9)$$

$$\sum_{g \in G_i} s_{gt}^{\xi} \geq RS_{it} \qquad\qquad \forall\, i \in N, t \in T,\, \xi \in \Xi \qquad\qquad (4.10)$$

$$0 \leq s_{gt}^{\xi} \leq S_g^{max} \qquad\qquad \forall\, g \in G, t \in T,\, \xi \in \Xi \qquad\qquad (4.11)$$

$$p_{gt}^{\xi} \geq 0 \qquad\qquad \forall\, g \in G, t \in T,\, \xi \in \Xi \qquad\qquad (4.12)$$

4.2.2 Demand Response Formulation

Demand side management or demand response (DR) can be an effective tool to mitigate the peak load or peak-to-average ratio. To avoid the extensive use of the expensive peak load plants, system operators take into account responsive demands to price signals. This fact can be approximated by a set of linear constraints using a price elasticity matrix when price variation is small as in [77]. In these linear constraints, the shifted demand at time t is an affine function of the price variations in all other time periods, where the constant term is the reference demand at time t. Actually, the major uncertainty on the demand sides is the responding behaviors of end consumers (modeled by the price elasticity matrix $\mathbf{E}_i^{\xi}$) on varying electricity prices. The real-time demand comprises the forecasted demand and the demand adjustment caused by changes of electricity prices from the benchmark price $\mathbf{Q}_i^{\xi}$ (by multiplying the price elasticity matrix $\mathbf{E}_i^{\xi}$ with the price variation vector $\mathbf{q}_i^{\xi} - \mathbf{Q}_i^{\xi}$). Although renewable energy is considered as another uncertainty source in our computational model, we assume that renewable energy output is independent of DR and electricity price over the planning horizon. Thus, the demand adjustment is only affected by the uncertain price elasticity matrix and varying electricity prices. Within a scenario, we also assume the total sum of demands at all time period at any location/bus is a constant. This is guaranteed by the loss price elasticity matrix $\mathbf{E}_i^{\xi}$ for each bus, in which the summation of each column equals to

zero [33, 78].

Constraint (4.13) demonstrates that the real-time demand is equal to the summation of forecasted benchmark demand and elastic demand based on the price elasticity matrix. Besides, the electricity price constraint (4.14) controls the real-time price fluctuation in a reasonable range. These two constraints are shown as follows,

$$\mathbf{y}_i^\xi = \mathbf{D}_i^0 + \mathbf{E}_i^\xi(\mathbf{q}_i^\xi - \mathbf{Q}_i^\xi) \quad \forall\, i \in N,\ \xi \in \Xi \tag{4.13}$$

$$\alpha\mathbf{Q}_i^\xi \le \mathbf{q}_i^\xi \le \gamma\mathbf{Q}_i^\xi \quad \forall\, i \in N,\ \xi \in \Xi \tag{4.14}$$

where $\mathbf{y}_i^\xi$ is the real-time demand vector at node i under scenario ξ; $\mathbf{D}_i^0$ is the hourly benchmark/reference demand vector forecasted in day ahead; $\mathbf{E}_i^\xi$ is the uncertain price elasticity matrix reflecting demand change rates due to varying electricity prices; $\mathbf{q}_i^\xi$ is the real-time electricity price vector; $\mathbf{Q}_i^\xi$ is the benchmark/reference electricity price vector at node i in scenario ξ. In the above linear constraints, $\mathbf{y}_i^\xi$ and $\mathbf{q}_i^\xi$ are the decision variables, and the others are given parameters. Each of the vectors are composed of the elements of different time periods, for example, $\mathbf{y}_i^\xi = [y_{it}^\xi,\ \forall t \in T]^T$. α and γ are coefficients used to bound the possible electricity prices, which is necessary to maintain the validity of the linear approximation of demand response [77].

4.2.3 Energy Storage Formulation

In the current electrical power systems, electricity has to be used immediately according to the physical law on power circuits. This fact leads to many issues concerning the power systems, *e.g.*, high redundancy, supply and demand imbalance, *etc*. Meanwhile, the renewable energy penetration continues growing and greatly increases the difficulty of power system operations. With the advancement of energy storage devices, these issues can be mitigated using these devices in the

65

power systems. We formulate a set of energy storage (ES) constraints to address the accumulators status, power saving and dispatch at each period of a scenario. Constraint (4.15) indicates energy balance for each accumulator; the other constraints (4.16) and (4.17) indicate the available dispatch level and power storage capacity, respectively.

$$r_{it}^{\xi} = r_{it-1}^{\xi} + v_{it-1}^{\xi} - x_{it-1}^{\xi} \qquad \forall\, i \in N,\, t \in T,\, \xi \in \Xi \qquad (4.15)$$

$$0 \le x_{it}^{\xi} \le r_{it}^{\xi} \qquad \forall\, i \in N,\, t \in T,\, \xi \in \Xi \qquad (4.16)$$

$$0 \le r_{it}^{\xi} \le \kappa_i \qquad \forall\, i \in N,\, t \in T,\, \xi \in \Xi \qquad (4.17)$$

$$v_{it}^{\xi} \ge 0 \qquad \forall\, i \in N,\, t \in T,\, \xi \in \Xi \qquad (4.18)$$

where r_{it}^{ξ} is the total remaining power in storage facilities of unit i at time t, v_{it-1}^{ξ} is the power storage at node i in period t of scenario ξ, x_{it-1}^{ξ} is the renewable energy dispatch amount at node i in period t of scenario ξ and κ_i is the maximum storage capacity at node i under scenario ξ. Note that N can be replaced by a subset $N' \subset N$, because ES devices are not necessarily at every bus.

4.2.4 Transmission Formulation

In our application, we formulate the power transmission using an approximation of power flows. Generally, Kirchhoff's current and voltage laws apply to interconnected electrical network (e.g., a electrical power grid), and are used to find out electricity characteristics of transmission and distribution systems. To consider possible loss from load-shedding, the traditional DC approximation of Kirchhoff's current law (KCL) constraints are modified to involve the loss that occurs at location i at time t under scenario ξ, l_{it}^{ξ}, shown in constraint (5.17). In many cases, we can restrict l_{it}^{ξ} to zero.

66

And a DC approximation of Kirchhoff's voltage law is expressed in constraint (5.18).

$$\sum_{(i,j)\in A_i^+} f_{ijt}^{\xi} - \sum_{(j,i)\in A_i^-} f_{jit}^{\xi} = \sum_{g\in G_i} p_{gt}^{\xi} + R_{it}^{\xi} - D_{it}^0 + l_{it}^{\xi}, \quad \forall\, i \in N, t \in T, \xi \in \Xi \tag{4.19}$$

$$(f_{ijt}^{\xi} - f_{jit}^{\xi}) - B_{ijt}^{\xi}(\beta_{it}^{\xi} - \beta_{jt}^{\xi}) = 0, \qquad\qquad \forall\, (i,j) \in A, t \in T, \xi \in \Xi \tag{4.20}$$

$$f_{ijt}^{\xi}, l_{it}^{\xi} \geq 0, \qquad\qquad \forall\, (i,j) \in A, i \in N, t \in T, \xi \in \Xi \tag{4.21}$$

where f_{ijt}^{ξ} is an unrestricted variable representing a bi-direction flow between bus i and bus j; A_i^+ and A_i^- denote the set of flow starting at bus i and the set of flow ending at bus i, respectively. As the absence of demand response program, the real-time demand is equivalent to the benchmark demand $D_{it}^{\xi 0}$.

When ES devices are connected to the grid at some nodes and DR programs are implemented, the transmission constraints are also revised to adopt the process of energy storage and dispatch. In fact, the operation of energy storage can be considered as power consumption from the bus and the operation of dispatch can be considered as power supply to the electric grid, the amounts of which are represented by v and x, respectively. The implementation strategy of UC combined with DR and ES is able to affect the total expected generation cost under their joint actions. Therefore, the KCL constraint is modified as follows,

$$\sum_{(i,j)\in A_i^+} f_{ijt}^{\xi} - \sum_{(j,i)\in A_i^-} f_{jit}^{\xi} = \sum_{g\in G_i} p_{gt}^{\xi} + \rho_i x_{it}^{\xi} + R_{it}^{\xi} + l_{it}^{\xi} - v_{it}^{\xi} - y_{it}^{\xi},$$

$$\forall\, i \in N, t \in T, \xi \in \Xi \tag{4.22}$$

where ρ_i addresses the ES efficiency which is determined by device properties and y_{it}^{ξ} is the real-time demand influenced by DR.

67

4.2.5 Risk Constraints

In scenario-based two-stage stochastic programming models, usually a large number of simulated scenarios (e.g., wind outputs, nodal demands) are used. Since the stochastic programming formulation includes all scenarios, the optimal solutions might be very overconservative with high total cost because feasible solutions need to compensate much for the extreme scenarios. On the other hand, we also need to maintain a certain level of system reliability. Hence we need to balance between the total cost and system reliability. To this end, chance or risk constraints are usually introduced in the stochastic programming models for this tradeoff.

Risks in stochastic unit commitment usually are linked with loss of load since a reliable system should be able to meet as much demand as it can. Hence loss of load probability (LOLP) is usually required to stay below an allowed level in many previous approaches [45, 83]. LOLP can be directly modeled by chance constraints, which is equivalent to bound a θ-level Value at Risk (VaR) of the loss of load, where θ is usually a value close to 1. Different policies regarding how to aggregate loss of load (e.g., total loss over all time periods v.s. loss of each time period) can be used to define the LOLP constraints [82]. In this paper, we are trying to bound the risks associated with each individual time period. Let $L(x,Y)$, a random variable, be the loss function (e.g., total loss of all buses at a time period), where x are the aggregated decision vector and Y is the random vector (e.g., wind outputs). $\text{VaR}_\theta[L(x,Y)]$ is the θ-level Value-at-Risk (VaR) of the loss of load function $L(x,Y)$. It is also the θ-level quantile of the random variable $L(x,Y)$, which can be defined as follows,

$$\text{VaR}_\theta[L(x,Y)] = \min_l \left\{ l \,\middle|\, \text{Prob}\left(L(x,Y) \le l\right) \ge \theta \right\}.$$

Chance constraints are equivalent to bound $\text{VaR}_\theta[L(x,Y)]$ above by $\bar{l}$, which is the maximum tolerable loss of load, usually set as 0. Since VaR constraints involve binary variables and big M to select good/bad scenarios, it will cause many computational difficulties when solving the chance-

constrained programs especially with large number of scenarios. Approximation algorithms such as Sample Average Approximation are used to solve chance-constrained stochastic unit commitment problems [82, 83].

Here we choose to bound another risk of load loss, Conditional Value at Risk (CVaR), also named as Average Value at Risk (AVaR) or Expected Tail Loss (ETL). It is a coherent risk measure widely used in many areas, e.g., financial and risk management [1], natural gas system expansion planning [93], stochastic network optimization [?]. CVaR constraints only involve continuous variables and linear constraints, and then are computationally friendly even with a large number of scenarios. In addition, the optimal solution of CVaR-based models also provide information of corresponding VaR measure because CVaR is the conditional expectation of the loss function given that the loss is beyond $\text{VaR}_\theta[L(x,Y)]$. Hence the CVaR constraints also include VaR definition shown as follows,

$$\min_l \left\{ l \,\middle|\, \text{Prob}\Big(L(x,Y) \le l\Big) \ge \theta \right\} \;=\; \eta \tag{4.23a}$$

$$\mathbb{E}\left\{ L(x,Y) \middle| L(x,Y) \ge \eta \right\} \;\le\; \bar{\phi} \tag{4.23b}$$

where $\mathbb{E}$ refers to the expectation, and η is $\text{VaR}_\theta[L(x,Y)]$, and $\bar{\phi}$ is the maximum tolerable loss for CVaR. Note that this does not mean maximum tolerable loss for η is $\bar{\phi}$. In fact $\text{VaR}_\theta[L(x,Y)]$ is bounded by a loss smaller than $\bar{\phi}$. We refer the readers to [53, 57] for further details including the discussion between VaR and CVaR, and the constraints to represent them.

For the stochastic unit commitment problem, we choose to bound the CVaR linked to the total load loss of all bus at each time period. Because we have to model the expectation beyond $\text{VaR}_\theta[L(x,Y)]$, we need to split the loss of time period t into two parts η_t and ζ_t^ξ as shown in (5.23). η_t represents the actual $\text{VaR}_\theta[L(x,Y)]$ at time t, and ζ_t^ξ represent the loss beyond the value at risk in scenario ξ because both of them only take nonnegative values. On the left hand side of constraint (5.24), these two are combined again to calculate the conditional expectation, which is

69

$CVaR_\theta[L(x, Y)]$. Then it is bounded above by $\bar{\phi}$, a loss allowance parameter. The risk constraints based on CVaR are shown as follows,

$$\sum_{i \in I} l_{it}^{\xi} \leq \eta_t + \zeta_t^{\xi}, \qquad\qquad \forall\, t \in T,\ \xi \in \Xi \qquad (4.24)$$

$$\eta_t + (1 - \theta)^{-1} \sum_{\xi \in \Xi} \mathrm{Prob}^{\xi} \zeta_t^{\xi} \leq \bar{\phi}, \qquad\qquad \forall\, t \in T \qquad (4.25)$$

$$\eta_t \geq 0,\ \zeta_t^{\xi} \geq 0, \qquad\qquad \forall\, t \in T,\ \xi \in \Xi \qquad (4.26)$$

Risk management on load-shedding losses is employed by introducing CVaR constraints to the traditional two-stage stochastic UC models. On one hand, this approach helps the ISOs control the risks resulting from the load-shedding losses under different instances. On the other hand, CVaR constraints can keep the stochastic MILP models favorable for computation.

4.2.6 SUCR-DR-ES Model

We then propose the following integrated model for the security-constrained unit commitment with risk control including DR and ES constraints at the same time, called **SUCR-DR-ES**. The integrated model includes UC constraints (5.2)-(4.12), DR constraints (4.13)-(4.14), ES constraints (4.15)-(4.18), transmission constraints (5.18)-(4.22), and risk constraints (5.23)-(5.25).

$$\textbf{[SUCR-DR-ES]:} \quad \min \quad \sum_{g \in G} \sum_{t \in T} (SU_{gt} v_{gt} + SD_{gt} w_{gt})$$

$$+ \sum_{\xi \in \Xi} Prob^{\xi} \sum_{g \in G} \sum_{t \in T} F_g(p_{gt}^{\xi})$$

$$\text{s.t.} \quad (5.2)\text{-}(4.12),\ (4.13)\text{-}(4.14),\ (4.15)\text{-}(4.18)$$

$$(5.18)\text{-}(4.22),\ (5.23)\text{-}(5.25)$$

4.3   Solution Approach

When a large number of scenarios are included in the stochastic models, Benders decomposition can be utilized to address the computational issues, especially for the special structures of mixed integer linear programs [59]. While applying Benders decomposition, the original **SUCR-DR-ES** problem is decomposed into a relaxed master problem and multiple subproblems based on each scenario. In the classical Benders decomposition algorithm, Benders' cuts are constructed using the optimal dual solutions of subproblem in each iteration. Then they are added to the relaxed master problem (**RMP**) for the next iteration, so as to improve the lower bound on the original problem.

In general cases, an original model is decomposed to an integer program of **RMP** and a linear program of subproblem. According to this decomposition strategy, **SUCR-DR-ES** is naturally decomposed into the **RMP** only with unit commitment constraints and the subproblem with the resting constraints. However, this decomposition can produce low-density cuts that only involve single decision variable **u** and practically cause a slow convergence. In addition, in the subproblem, all scenarios are coupled together by the CVaR constraints, which could potentially restrict the use of parallel computing resources. We then choose an alternative decomposition strategy to handle this issue, in the way of increasing the density of Benders cuts. In the fact that a coupling constraint (5.24) appears in the CVaR constraints, this coupling structure is not easy to handle on decomposition algorithms. Thus all CVaR constraints are placed on **RMP**, and only the incumbent solutions (**u**,**l**) will be passed to $\mathbf{SP}^{\xi}$. In doing so, multiple Benders cuts are generated including loss variable **l** and able to restrict equivalent or more solution space of **RMP** in one iteration. In addition, we have multiple uncoupled subproblems, which can take advantage of parallel computing resources to reduce computing times. Let π^{ξ} be an unrestricted variable to represent the minimum total fuel cost in a scenario. The relaxed master problem includes unit commitment and CVaR

71

constraints, shown as,

$$[\textbf{RMP}]: \quad \min \quad \sum_{g \in G}\sum_{t \in T}(SU_{gt}v_{gt}+SD_{gt}w_{gt}) + \sum_{\xi \in \Xi}\text{Prob}^{\xi}\pi^{\xi}$$

$$\text{s.t.} \quad (5.2)\text{-}(4.6),\ (5.23)\text{-}(5.25),$$

$$\mathbb{F}(u_{gt},l_{it}^{\xi},\pi^{\xi}) \geq 0,\ \forall\, \xi \in \Xi$$

where constraint $\mathbb{F}(u_{gt},l_{it}^{\xi},\pi^{\xi}) \geq 0$ stands for Benders' cuts associated with the commitment variable u_{gt} and loss variable l_{it}^{ξ}. These cuts are generated based on solutions from the subproblem based on one scenario.

To avoid the case of infeasible subproblems, the subproblem formulation of **SUCR-DR-ES** adopts the Big-M method, in which nonnegative artificial variables are introduced (with a big penalty in the objective function) to insure $\textbf{SP}^{\xi}$ maintain the feasibility given any first-stage decision. The artificial variable ω_{it} is introduced to the system spinning reserve constraint (4.10); the artificial variables o_{it}^{+}, and o_{it}^{-} are introduced to the KCL transmission constraint (4.22). If any of the artificial variables is not equal to zero, the objective function of $\textbf{SP}^{\xi}$ then will be penalized with a large number M associated with artificial variables. Given the incumbent solutions $(\textbf{u},\textbf{l})$, the subproblem (5.31) is to optimize the generation dispatch, subject to scenario-independent inequalities. The subproblems with Big-M method is shown as follows,

$$[\textbf{SP}^{\xi}]: \quad \min \quad \sum_{g \in G}\sum_{t \in T}F_g(p_{gt}^{\xi}) + M\sum_{t \in T}\sum_{i \in N}(\omega_{it}+o_{it}^{+}+o_{it}^{-})$$

$$\text{s.t.} \quad (4.9),\ (4.11)\text{-}(4.18),\ (5.18)\text{-}(5.19) \tag{4.27a}$$

$$p_{gt}^{\xi} \geq P_g^{min}\hat{u}_{gt},\ \forall\, g \in G,\ t \in T \tag{4.27b}$$

$$p_{gt}^{\xi}+s_{gt}^{\xi} \leq P_g^{max}\hat{u}_{gt},\ \forall\, g \in G, t \in T \tag{4.27c}$$

$$\sum_{g \in G_i}s_{gt}^{\xi}+\omega_{it} \geq RS_{it},\ \forall\, i \in N, t \in T \tag{4.27d}$$

$$\sum_{(i,j)\in A_i^+} f_{ijt}^{\xi} - \sum_{(j,i)\in A_i^-} f_{jit}^{\xi} + o_{it}^+ - o_{it}^-$$

$$= \sum_{g\in G_i} p_{gt}^{\xi} + \rho_i x_{it}^{\xi} + R_{it}^{\xi} - v_{it}^{\xi} - y_{it}^{\xi} + \hat{l}_{it}^{\xi}, \ \forall\, i \in N,\, t \in T \qquad (4.27e)$$

where only the second-stage constraints are included such as economic dispatch, non-generation resources and power transmissions.

We define a series of dual variables, *i.e.* ε_{gt}^{ξ}, ρ_{gt}^{ξ}, χ_{gt}^{ξ}, σ_{gt}^{ξ}, $\tau_{it}^{\xi}, \upsilon_{gt}^{\xi}$, λ_{it}^{ξ}, μ_{it}^{ξ}, v_{it}^{ξ}, ϑ_{it}^{ξ}, φ_{it}^{ξ}, corresponding to the constraints (5.31a), (5.31d), (4.9), (4.9), (4.27d), (4.11), (4.13), (4.14), (4.14), (4.17), (5.31g). For example, dual variables χ_{gt}^{ξ} and σ_{gt}^{ξ} correspond to the ramping up and ramping down in (4.9), respectively. After solving the **SP$^{\xi}$**, one can obtain the optimal dual values corresponding to the above constraints. These dual values for one scenario are then used to construct an optimality cut $\mathbb{F}(u_{gt}, l_{it}^{\xi}, \pi^{\xi})$, which is presented in (4.28).

$$\begin{aligned}
\pi^{\xi} \ \geq\ & \sum_{g\in G}\sum_{t\in T}\hat{\varepsilon}_{gt}^{\xi} P_g^{min} u_{gt} + \sum_{g\in G}\sum_{t\in T}\hat{\rho}_{gt}^{\xi} P_g^{max} u_{gt} + \sum_{g\in G}\sum_{t\in T}\hat{\chi}_{gt}^{\xi} RU_g \\
& + \sum_{g\in G}\sum_{t\in T}\hat{\sigma}_{gt}^{\xi} RD_g + \sum_{i\in N}\sum_{t\in T}\hat{\tau}_{it}^{\xi} RS_{it} + \sum_{g\in G}\sum_{t\in T}\hat{\upsilon}_{gt}^{\xi} S_g^{max} \\
& + \sum_{i\in N}\sum_{t\in T}\hat{\lambda}_{it}^{\xi}(D_{it}^0 - E_{it}^{\xi} Q_{it}^{\xi}) + \sum_{i\in N}\sum_{t\in T}\hat{\mu}_{it}^{\xi}\alpha Q_{it}^{\xi} + \sum_{i\in N}\sum_{t\in T}\hat{v}_{it}^{\xi}\gamma Q_{it}^{\xi} \\
& + \sum_{i\in N}\sum_{t\in T}\hat{\vartheta}_{it}^{\xi}\kappa_i + \sum_{i\in N}\sum_{t\in T}\hat{\varphi}_{it}^{\xi}(R_{it}^{\xi} + l_{it}^{\xi}) \qquad (4.28)
\end{aligned}$$

In the classic Benders' decomposition method, all Benders cuts generated from each iteration are appended to **RMP** directly and then **RMP** is solved for optimality again. This way of adding the cuts to **RMP** iteratively keeps increasing the size of active constraint set, but do not guarantee to provide stronger restriction of the solution space. It probably yields the considerable rework and leads to the slow convergence of the algorithm. In this paper, we implement Benders' Decom-

position using CALLBACK function in CPLEX. The solution flowchart (Figure 5.1) explicitly addresses Benders' decomposition used to solve **SUCR-DR-ES** model by implementing CALL-BACK function. The vector ς represents all continuous variables involved in the subproblems. Compared to the classical method, the Benders' decomposition with CALLBACK function has one of prominent advantages, where only violated cuts are chosen and added to **RMP** and other cuts are carried in a pool. In other words, this means is capable of maintaining the small size of **RMP** and applying a limited number of stronger or equivalent Benders's cuts.
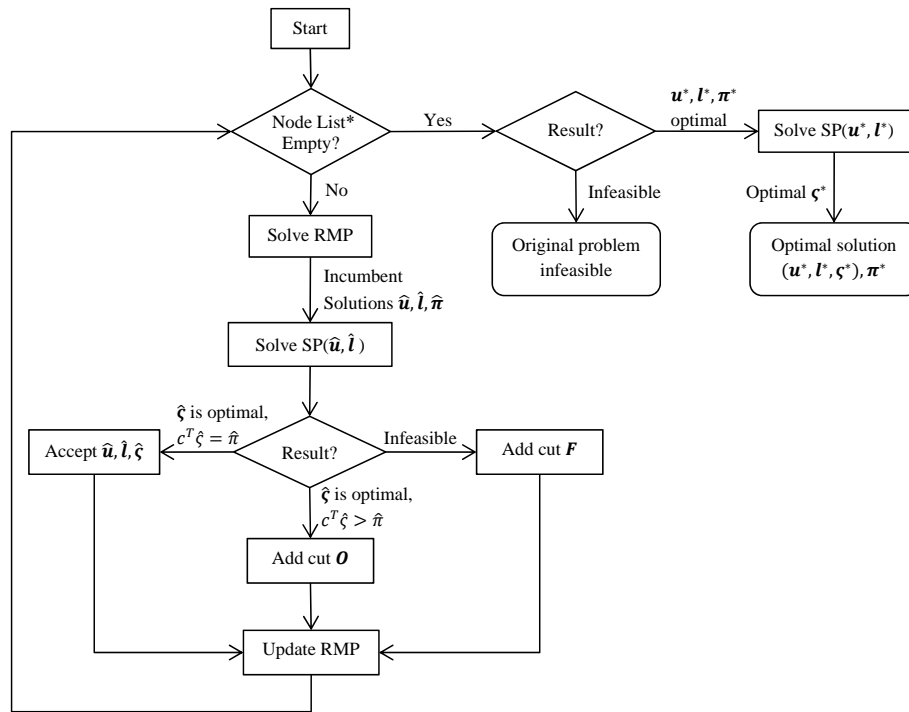
* Brand-and-Bound node list

Figure 4.1: The solution flowchart of Benders' Decomposition with CALLBACK function

The other advantage of implementing CALLBACK function is that **RMP** is solved only once. The whole process of solving **RMP** utilizes Branch-and-Bound-and-Cut algorithm. Meanwhile, Benders' cuts are generated at the branching nodes and added within the Branch-Bound-and-Cut

algorithm. Particularly, only the most violated Benders' cuts are involved. The lower bound is being updated along with the **RMP** solving procedure (the branch-and-bound tree) where the upper bound also is created at a branching node after solving the **SP**$^\xi$ for all scenarios. Until the **RMP** solving procedure is finished, the lower bound and upper bound are obtained and converged. Since the lower bound can be effectively improved with the help of Benders' cuts during a **RMP** solving procedure, it can avoid that the **RMP** is solved iteratively in the classical method, and thus the overall computation time is reduced.

4.4   Computational Results

To test the effects of reliability parameter variations, we perform the computational experiments to test the SUCR-DR-ES model described in section 5.2. In addition, we study the effects on risk resilience of using different non-generation resources. To this end, we also test another three models, namely, the SUCR model, SUCR-DR model and SUCR-ES model. They are all simplified versions of the SUCR-DR-ES model. For example, SUCR model does not include any DR and ES resources; SUCR-DR model only includes DR resources; SUCR-ES model only incorporates ES resources. Then their results are compared with the SUCR-DR-ES model based on the case studies with same inputs.

In the 7-bus system, four models are tested to compare the effects of their optimal schedules on the total thermal generation costs, based on a day ahead 100-scenario case. Additionally, we perform sensitivity analysis on reliability parameters, shadow price analysis and reliability parameter analysis to identify most affected range of cost increment as well as the relationship between objective value and the percentage change rate of cost increment. In the enhanced 118-bus system, we run each model at 10 different loss allowance cases with 7 different confidence levels to compare the strategies for using non-generation resources. It aims to verify the effectiveness of modified

75

Bender's decomposition approach on solving our proposed models and find out risk management settings to reduce total costs. Normal distribution is assumed to generate renewable energy and demand change scenarios. All models are coded in C++ while solved by CPLEX 12.5. All experiments are implemented on a PC Dell OPTIPLEX 980 with Intel Core i7 vPro at 2.80 GHz and 8 GB memory in a Windows 7 operating system.

4.4.1 Seven-Bus System

The 7-bus system includes one wind farm, four generators, five loads and ten transmission lines. The characteristics of buses, the wind farm, thermal units and transmission lines are shown in Table 5.1 - 4.4, respectively. The renewable energy resource is located at Bus 1 with a generating capacity of 100 MW. In many of the existing research efforts on stochastic UC with renewable energy resources, wind power output is assumed to be normally distributed (e.g., [66, 79, 82]). Following this stream, we also use normal distribution to generate the wind power output scenarios, although our models and algorithms can easily take on data generated from other distributions. The hourly renewable energy output falls in the range of $[5, 100]$ MW and is produced by adding the random number from normal distribution generators in C++ to the hourly base load. The piecewise linear fuel cost function is used in the objective function. The estimated benchmark electricity prices are generated based on the pattern of hourly real-time locational marginal prices (LMP). The demand elasticity matrix includes the random load increase during 1 a.m. to 5 a.m. and the load reduction between 12 p.m. and 7 p.m., within the range of variation ratio, $[-1, 1]$. The storage facilities are located at Bus 1, 2, 4 and 5 with corresponding storage capacities as shown in Table 5.1.

Table 4.1: Bus Parameters

ID	Type	Gen ID	Gen. Cap. (MW)	Strg. Cap. (MW)
B1	Renewable	R1	100	80
B2	Coal	G1	110	20
B3	Coal	G2	50	-
B4	Gas	G3	90	20
B5	-	-	-	10
B6	-	-	-	-
B7	Coal	G4	70	-

[a] The symbol, '-', represents no generation unit available at a corresponding bus

Table 4.2: Generator Parameters

	G1	G2	G3	G4
Min-ON (h)	2	1	2	4
Min-OFF (h)	2	2	2	1
Ramp-Up (MW/h)	60	30	60	60
Ramp-Down (MW/h)	60	30	60	60
Pmin (MW)	10	5	9	7
Pmax (MW)	110	50	90	70
Max-Spn (MW)	20	20	15	15
Required Spn (MW)	10	0	0	0

Table 4.3: Generation Cost Parameters

	G1	G2	G3	G4
Startup ($)	50	500	800	30
Shutdown ($)	50	500	800	20
Fuel Cost a ($)	6.78	6.78	31.67	10.15
Fuel Cost b ($/MWh$)	12.888	12.888	26.244	17.820
Fuel Cost c ($/MWh^2$)	0.0109	0.0109	0.0697	0.0128

Table 4.4: Transmission Line Parameters

ID	From	To	Flow Capacity(MW)	Voltage(V)
L1	B1	B2	50	500
L2	B1	B3	160	500
L3	B1	B4	80	500
L4	B2	B3	100	500
L5	B2	B5	50	500
L6	B3	B5	30	500
L7	B3	B6	100	500
L8	B4	B6	50	500
L9	B4	B7	60	500
L10	B6	B7	50	500

Firstly, we run all four models with 85% confidence level to show the effects of using different non-generation resources or their combination on unit commitment scheduling and its total cost.

The loss allowance from load-shedding, $\bar{\phi}$, is fixed to 5% of maximum hourly demand, whereas price velocity indicators (α, γ) are set to $(0.95, 1.05)$. From the unit commitment results shown in Table 4.5, it can be observed that all four models have G1 and G2 operate for the whole day and G3 off because it has very high fuel cost and startup/shutdown cost. The difference among power generation schedules occurs on G4. The SUCR model always requires G4 online to satisfy the demand and accommodate the volatility of renewable energy inputs. However, it is not necessary to keep G4 online at any period in a day when the DR program is implemented. In SUCR-DR results, G4 is off at 2 a.m. and 3 a.m. according to the known daily load shifting. The SUCR-ES model is more flexible as compared to SUCR-DR model, because it further reduces the G4's generation time, only from 8 a.m. to 9 p.m. As in the case of SUCR-DR-ES, the optimal schedule only requires G4 online for 12 hours between 8 a.m. to 8 p.m., and has the lowest total cost $50480.5. It is clear that the combined effects of DR and ES improve the generation schedule most significantly in terms of the total cost. The system benefits not only from load-shedding and load-shifting to lower the usage of generating equipments and fuel consumption, but also the increased flexibility and reliability of power supply.

Table 4.5: Optimal Unit Commitment For 7-Bus System

Model Type	Objective Value	Unit ID	Hour (1-24)
SUCR	$54917.9	G1	1 1 1 1 1 1 1 1 1 1 1 1 1 1 1 1 1 1 1 1 1 1 1 1
		G2	1 1 1 1 1 1 1 1 1 1 1 1 1 1 1 1 1 1 1 1 1 1 1 1
		G3	0 0 0 0 0 0 0 0 0 0 0 0 0 0 0 0 0 0 0 0 0 0 0 0
		G4	1 1 1 1 1 1 1 1 1 1 1 1 1 1 1 1 1 1 1 1 1 1 1 1
SUCR-DR	$52758.6	G1	1 1 1 1 1 1 1 1 1 1 1 1 1 1 1 1 1 1 1 1 1 1 1 1
		G2	1 1 1 1 1 1 1 1 1 1 1 1 1 1 1 1 1 1 1 1 1 1 1 1
		G3	0 0 0 0 0 0 0 0 0 0 0 0 0 0 0 0 0 0 0 0 0 0 0 0
		G4	1 0 0 1 1 1 1 1 1 1 1 1 1 1 1 1 1 1 1 1 1 1 1 1
SUCR-ES	$52594.6	G1	1 1 1 1 1 1 1 1 1 1 1 1 1 1 1 1 1 1 1 1 1 1 1 1
		G2	1 1 1 1 1 1 1 1 1 1 1 1 1 1 1 1 1 1 1 1 1 1 1 1
		G3	0 0 0 0 0 0 0 0 0 0 0 0 0 0 0 0 0 0 0 0 0 0 0 0
		G4	0 0 0 0 0 0 0 1 1 1 1 1 1 1 1 1 1 1 1 1 0 0 0 0
SUCR-DR-ES	$50480.5	G1	1 1 1 1 1 1 1 1 1 1 1 1 1 1 1 1 1 1 1 1 1 1 1 1
		G2	1 1 1 1 1 1 1 1 1 1 1 1 1 1 1 1 1 1 1 1 1 1 1 1
		G3	0 0 0 0 0 0 0 0 0 0 0 0 0 0 0 0 0 0 0 0 0 0 0 0
		G4	0 0 0 0 0 0 0 1 1 1 1 1 1 1 1 1 1 1 1 0 0 0 0 0

Secondly, we conduct another set of numerical tests regarding risk management settings in the risk-constrained stochastic unit commitment. Sensitivity analyses are performed with respect to the confidence level θ and the load-shedding loss allowance $\bar{\phi}$. The optimal cost variations are presented when we increase the confidence level θ from 60% to 99% and the percentage of load-shedding loss allowance $\bar{\phi}$ from 1% to 20% (defined as [*Loss Limit*/(*Max Total Demand*)] × 100%). The optimal objective values for all four models with different confidence levels and loss allowances

are shown in the three-dimensional diagram (Figure 4.2). One of horizontal axes represents the percentage of loss allowance, the other horizontal axis represents the confidence level, and the vertical axis represents the cost reduction percentage. In comparisons of the heights of each plane, the SUCR-DR-ES model can yield the smallest objective costs since it takes advantage of combined actions of DR and ES. When the reliability parameters (θ and $\bar{\phi}$) are altered, the SUCR-DR-ES model still yields the lowest expected generation costs compared to the other three models given the same risk/reliability parameters.

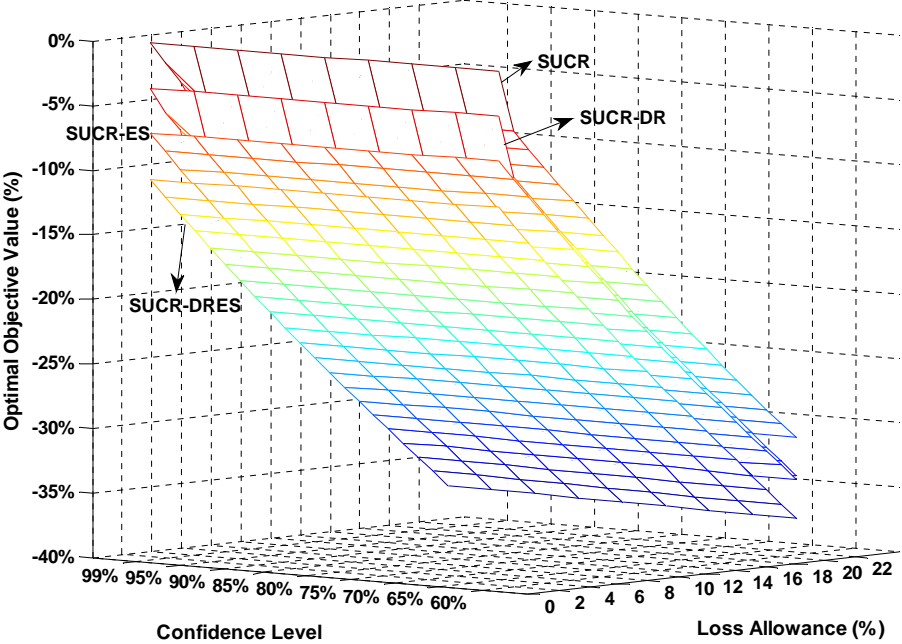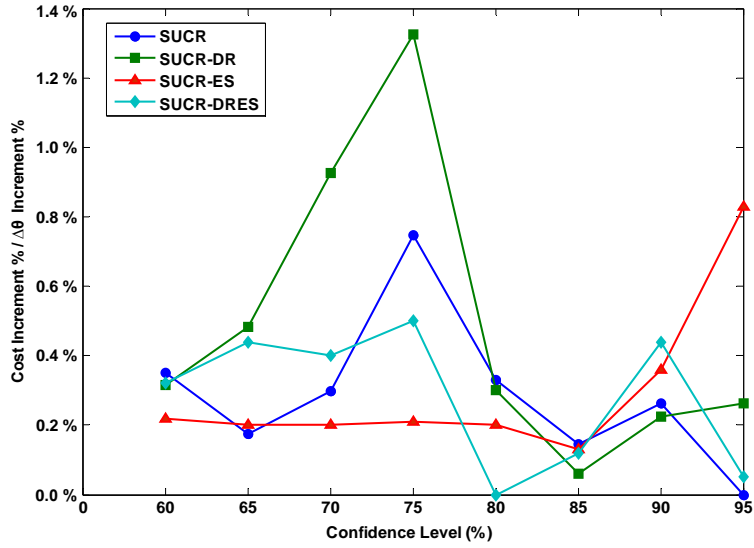Figure 4.2: Cost Saving Comparisons in Three-Dimension (7-Bus System)

Figure 4.3: The percentage change rates on confidence level at $\bar{\phi} = 10\%$
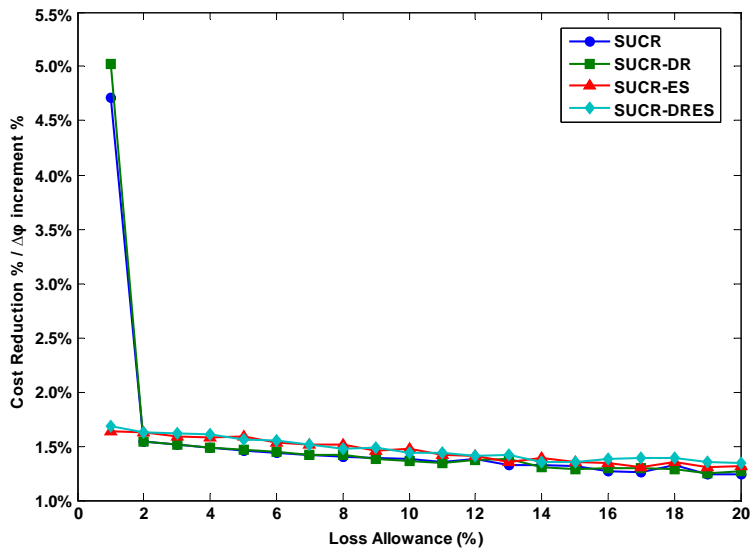

Figure 4.4: The percentage change rates on loss allowance at $\theta = 90\%$

Thirdly, we discuss the shadow price analysis on the reliability parameters, i.e., confidence level and loss allowance. Because all models are mixed integer linear programs, the dual information

(denoting the shadow prices) are not readily available. Instead, we use the approximated shadow price for loss allowance, defined as $\partial z^*/\partial\bar{\phi} \approx (z_N^* - z_{N-1}^*)/(\bar{\phi}_N - \bar{\phi}_{N-1})$, where z^* denotes the optimal total cost and N is the index. It means the unit total cost reduction per increment of loss allowance. In addition, holding loss allowance fixed, the approximated shadow price of confidence level is defined as $\partial z^*/\partial\theta \approx (z_N^* - z_{N-1}^*)/(\theta_N - \theta_{N-1})$. In this way, we can find out the change rate of optimal objective value with respect to the increment of decision parameter. It helps the decision makers (e.g., ISOs) clearly locate the levels of reliability parameters that can impact the optimal cost significantly, and therefore make the right choice of parameters.

Figure 4.3 and 4.4 show the percentage change rates comparisons for four models at different confidence levels and loss allowances, respectively. In Figure 4.3, the percentage change rate of total cost increment with respect to confidence level is calculated by the formula $[(z_\theta^* - z_{\theta-5\%}^*)/(z_{\theta=99\%}^* \times 5\%)] \times 100\%$. The percentage change rates of total cost increment for SUCR-DR form a sharp peak between 60% and 80% and flatten out from 85% confidence level. However, the SUCR-ES has an opposite trend where the percentage change rates hold steady until a big jump occurs after 85% confidence level. This observation demonstrates that the effective range of confidence levels works differently on different models. Generally, a higher confidence level used in models means that the generation system has higher reliability. Thus all models except SUCR-ES show an applicable advantage at the high confidence level ($\geq 85\%$) because they increase the optimal cost more slowly.

In the Figure 4.4, the comparisons of the percentage change rates of total cost reduction aim to identify the intensity response for each model while increasing the loss allowance. The percentage change rate of total cost reduction is defined as $[(z_{\bar{\phi}-1\%}^* - z_{\bar{\phi}}^*)/(z_{\bar{\phi}=0}^* \times 1\%)] \times 100\%$, which shows the relationships between the percentage change rate of total cost reduction and loss allowance by percentage. Since the total cost reduction percentage change rates are negative in our case studies, they are converted to positive values so that it's convenient for comparison and analysis. Both

SUCR and SUCR-DR have significantly higher percentage change rates than the other two models in the instance of 1% loss allowance. This indicates that the SUCR and SUCR-DR are affected by the change of loss allowance more significantly, especially on the range of low loss allowance. When the loss allowance is greater than the regular loss cap (3%), the models using DR, ES or both have similar percentage change rates of total cost reduction and begin a steady downward trend, slightly below 1.5%.
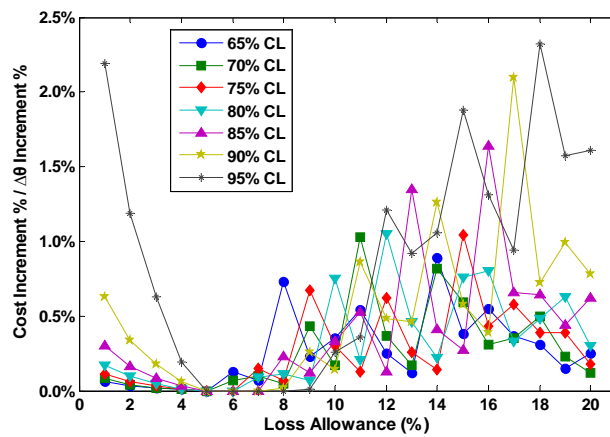
Figure 4.5: Reliability parameter analysis for SUCR Model
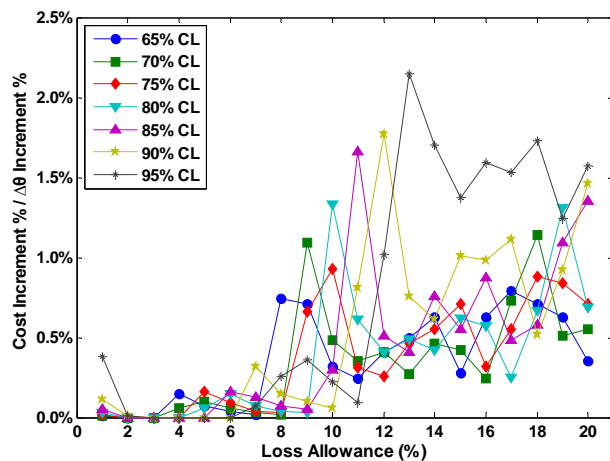
Figure 4.6: Reliability parameter analysis for SUCR-DR Model
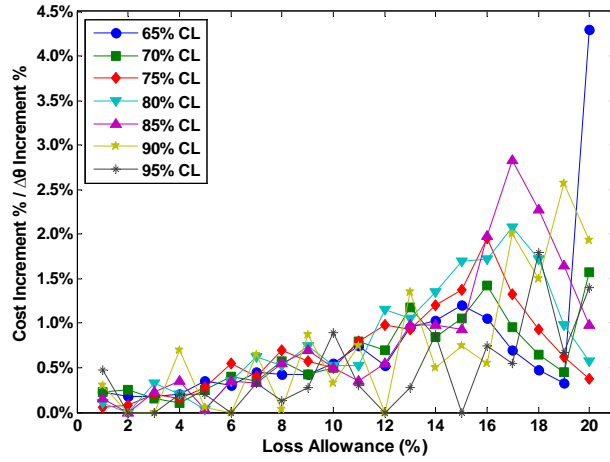
Figure 4.7: Reliability parameter analysis for SUCR-ES Model
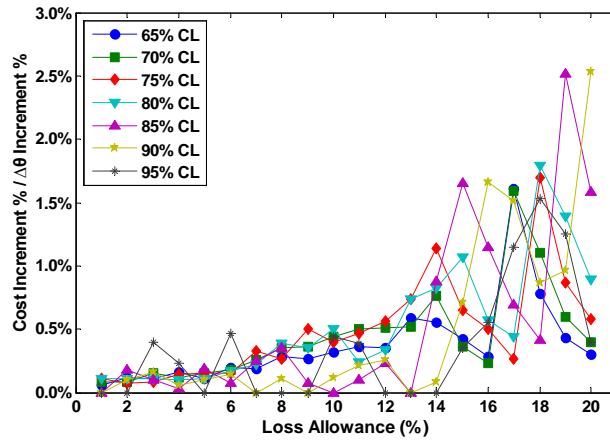
Figure 4.8: Reliability parameter analysis for SUCR-DR-ES Model

We continue to perform reliability parameter analysis based on each model so as to identify the specific range significantly affected by decision preferences, like confidence level and load-shedding loss allowance. Figures 4.5 to 4.8 show the percentage change rate of total cost increment as percentage loss allowance is increased (i.e., $\frac{\partial z^*}{\partial \theta}(\bar{\phi})$), where four models are displayed in the subgraphs individually. Each type of line with a specific marker represents a confidence level. Although

the different confidence levels show their own volatilities, the significant percentage change rates based on each model generally lie between specific loss allowance. While increasing the percentage loss allowance, the SUCR has a wide volatile range covering percentage loss allowance from 8% to 20%, where the confidence level makes a big difference among the lines. The SUCR-DR model has a similar volatile range. While the obvious volatile range for SUCR-ES stays below 10%, and the SUCR-DR-ES volatile range is between 14% and 20%. Therefore, these percentage change rate results demonstrate that different models have their own active cost increasing ranges, which are highly dependent on the chosen loss allowance and confidence level. Meanwhile, if the low-level loss allowance ($< 10\%$) is selected, any non-generation resources can keep the total generation cost increments at a lower level and maintain the relatively steady generation costs. In particular, the percentage change rate of SUCR-DR-ES for different confidence levels have less variations until the percentage loss allowance rises to 14%. It again confirms that it is capable of the least-cost generations given the same level of reliability.
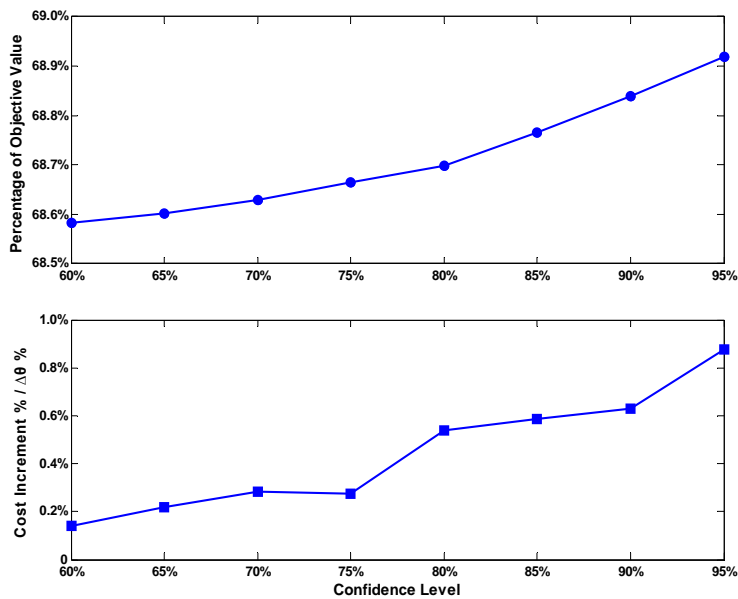
Figure 4.9: Comparisons of objective values and percentage change rates at confidence level: SUCR-DR Model
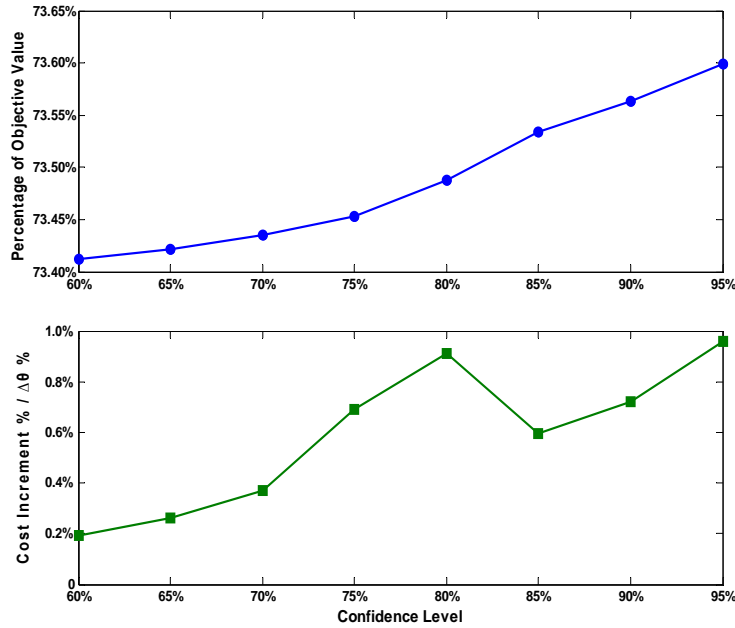
Figure 4.10: Comparisons of objective values and percentage change rates at confidence level: SUCR-ES Model

Figure 4.9 and 4.10 explicitly display the relationship between the optimal objective value and the percentage change rate of total cost increment. The percentage of objective value is used to represent the current level of an objective value given the specific reliability parameter, which is divided by the highest point of objective value at $\theta = 99\%$ and $\bar{\phi} = 0$. We here choose the SUCR-DR model and the SUCR-ES model to illustrate the effects of confidence level on the optimal objective value as well as the percentage change rate of total cost increment corresponding to individual non-generation resource. We observe that the 75% confidence level is likely a threshold since the objective values have explicit increases in both models and the the percentage change rates over 75% confidence level rise to relatively higher levels. If less than 75% confidence level is selected, these two resources are not able to reduce the generation costs significantly but sacrifice the system's reliability quite a lot. Therefore, it's more sensitive and reasonable to control the

load-shedding loss risks by selecting a much higher confidence level.

4.4.2   Enhanced 118-Bus System

The IEEE 118-bus system has been widely used to verify the adaptability and effectiveness of proposed models (e.g., [79, 91]) and further test the performance of proposed algorithms (e.g., the Sampling Average Approximation method [82] and Benders' Decomposition [90]). To adopt high renewable penetration and non-generation resources to current power networks, we added new features on the original IEEE 118-bus system, by including renewable energy resources, adjusting demand locations, setting energy storage locations and restricting transmission line capacities. An enhanced IEEE 118-bus system is used to test the proposed models for the comparisons of confidence level and loss allowance on generation cost. The system has 54 thermal units, 186 transmission lines and 103 demand sides. The total peak load from benchmark demand is 6961 MW and occurs at hour 19. The renewable energy resources are located at Bus 1, 9, 10 and 12; meanwhile, the renewable energy output at each bus is based on the same normal distribution with 7-Bus system but different data patterns. There are 100 scenarios generated for renewable energy supply, electricity price and price elasticity, respectively. Due to the physical memory limitation, Bender's decomposition is applied to solve SUCR-DR-ES model with larger numbers of scenarios. The computational time for the SUCR-DR-ES model with 100 scenarios generally is around 60 minutes on a 2.8 GHz PC with 8 GB memory, which verifies that the modified Bender's decomposition can effectively solve the 118-bus system within reasonable computation times.
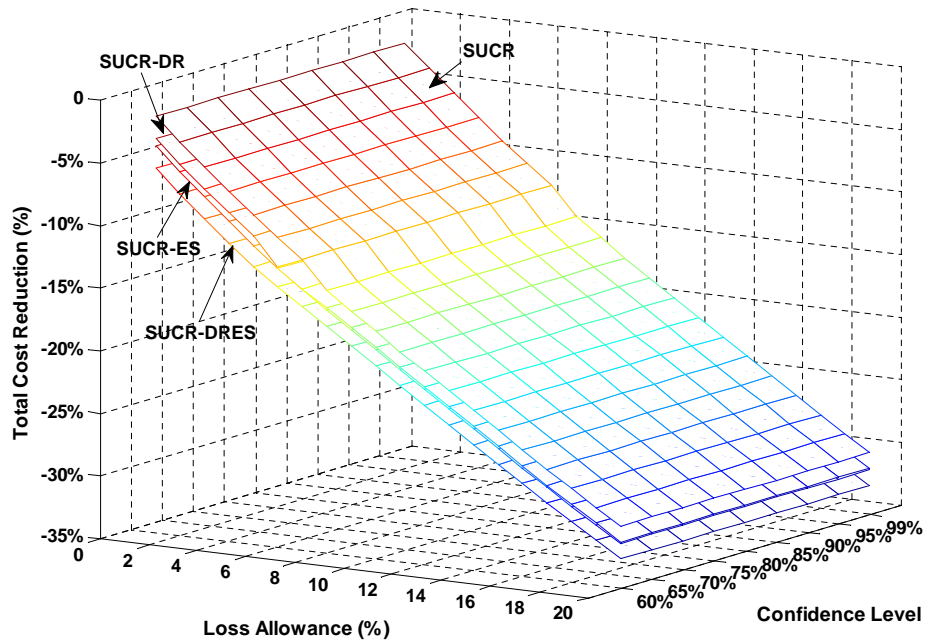
Figure 4.11: Cost saving comparisons in Three-Dimension (118-Bus System)
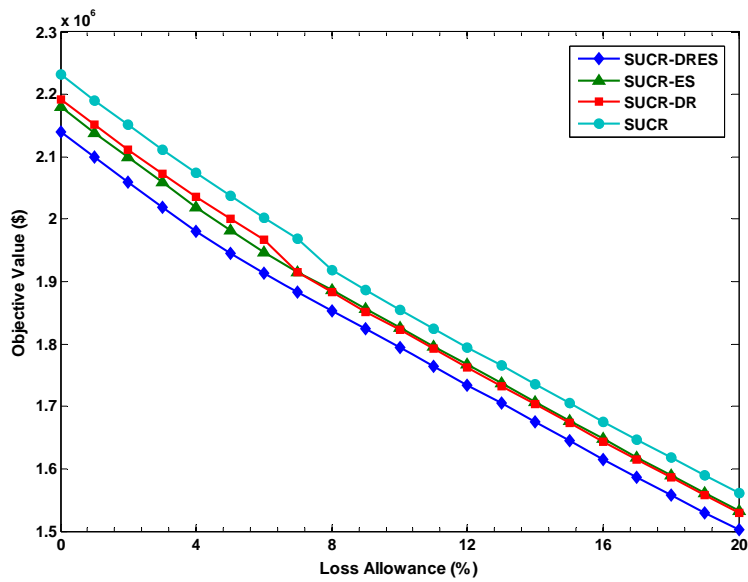
Figure 4.12: Objective value v.s. loss allowance (118-Bus System)

89

We run the four models by adjusting loss allowance $\bar{\phi}$ with 1% increment and then the percentages of cost reduction are plotted in Figure 4.11. While selecting the reliability requirements, the SUCR-DR-ES model can achieve the largest generating cost reduction, followed by SUCR-ES, SUCR-DR and SUCR. As the loss allowance increases, the abilities of cost reduction from SUCR-ES doesn't show an absolute advantage over SUCR-DR, shown in Figure 4.12. If the loss allowance is less than or equal to 6%, SUCR-ES is able to decrease total generation costs up to 1%; If the loss allowance rises over 7%, SUCR-DR appears to be slightly more cost-efficient than SUCR-ES, with the difference between them being no more than 0.3%. However, SUCR-DR-ES still provides the minimum objective costs in all instances. This observation again indicates that the ability of SUCR-DR-ES model to reduce generating costs is apparently superior to the other models. In other words, the operation including both DR and ES is more attractive and competitive in the short-term operation.

CHAPTER 5: SUC MODELS WITH EXPLICIT RELIABILITY REQUIREMENTS THROUGH CONDITIONAL VALUE-AT-RISK

5.1 Introduction

Currently renewable integration market is growing fast, reflecting the successful penetration of various renewable energy into the electric grid. With the increasing penetration of renewable energy, such as wind and solar, the power systems face an increasing number of operation uncertainties resulting from the renewable energy outputs. Demand fluctuations also require timely operational changes to secure power balance. Electric power markets thus offer various ancillary services to handle the uncertainties from demand-supply changes as well as facility outages.

Taking into account of reducing the unnecessary reserve cost and the risk from unserved energy, we therefore propose a stochastic co-optimization approach integrated with risk measures for scheduling energy and reserve services. Value-at-Risk (VaR) and Conditional Value-at-Risk (CVaR) are two popular risk measures widely used in financial risk management, but here we adopt CVaR to this co-optimization approach. Compared to VaR, CVaR is a more computationally attractive tool since it can be incorporated into optimization models with only linear constraints and continuous variables [53, 73, 57]. Additionally, VaR-based optimization was attempted to solve the stochastic UC problems due to uncertain wind power output [82] or uncertain load [45], and transmission network expansion planning [87].

This chapter is organized as follows. Section 5.2 presents two optimization models incorporating with explicit reserve requirements and CVaR measures, respectively. Section 5.4 provides illustrative examples and performs the comparisons between two operation strategies in a normal state and in an outage state, respectively. The sensitivity analyses are also presented regarding the reliability

91

parameters on the total generation cost.

5.2   Mathematical Formulation

The two-stage stochastic unit commitment models are developed to solve for the joint energy/reserve co-optimization under uncertainties. In the first stage, day-ahead reliability assessment commitment (RAC) is performed regarding unit commitment schedule and reserve commitment schedule; the second stage is to optimize real-time energy dispatch, reserve dispatch and power transmission based on all independent scenarios. Within the optimization procedure, the decisions of unit commitment and reserve commitment are applied to guide the next-day energy generation and operating reserve.

To strengthen the features of reserve requirements and CVaR measures, we assume that only regulation-up and regulation-down reserves are provided at a part of available generators. The reason we only handle one type of the reserve service is that we do not include sub-hourly modeling. Regulation services in general are more expensive to operate than spinning reserves (and of course much more expensive than non-spinning reserves). But regulation services can respond to system imbalances the quickest (within minutes). Since we don't have the time scale at minute level, if we have both regulation and spinning reserve resources in the model, the optimization will pick the cheaper reserve resources to use first (i.e., the spinning reserve), which would distort our modeling results then.

In a renewable integration market, the power system requires additional generation support to adopt changes caused by the variability and intermittency of renewable energy outputs. Thus, the uncertainties from actual wind output, load realization and generator outage are included to the models in presentence of discrete scenarios within the set Ξ. We then use some simulation

92

techniques to generate different scenarios in real time.

The following subsections discuss two stochastic unit commitment models considering system reliability. One model is developed for two-stage SCUC with fixed reserve requirements (Model I), and the other model is two-stage SCUC incorporated with CVaR measures (Model II).

5.2.1 Two-stage SCUC with Fixed Reserve Requirements

The objective of two-stage stochastic unit commitment is to minimize the total expected generation costs based on all scenarios. The objective function (5.1) include the startup cost, shutdown cost, regulation reserve costs on the first stage as well as the fuel costs and load-shedding loss penalty on the second stage. Although the reliability can be secured by enforcing fixed regulation reserve requirements on the first stage, the load-shedding loss possibly occurs in some scenarios, especially in the extreme scenarios. The cost of load loss thus is required to involve in the objection function as loss penalty, represented by $VOLL \sum_{\xi \in \Xi} prob^{\xi} \sum_{t \in T} \sum_{i \in N} \Delta_{it}^{\xi}$.

$$
\begin{aligned}
\min \quad & \sum_{g \in G} \sum_{t \in T} (SU_g v_{gt} + SD_g w_{gt} + C_g^U rc_{gt}^u + C_g^D rc_{gt}^d) \\
& + \sum_{\xi \in \Xi} prob^{\xi} \sum_{t \in T} \sum_{g \in G} [F_g(p_{gt}^{\xi}) + F_r(r_{gt}^{u\xi}) + F_r(r_{gt}^{d\xi})] + VOLL \sum_{\xi \in \Xi} prob^{\xi} \sum_{t \in T} \sum_{i \in N} \Delta_{it}^{\xi} \quad (5.1)
\end{aligned}
$$

Note that the fuel cost is the quadratic function of the dispatch level, p, *i.e.*, for generator g, $F_g(p) = a + bp + cp^2$, where a, b and c are usually positive coefficients.

In addition, the overall regulation cost consists of the unit fuel cost in the second stage as well as the regulation reserve cost occurring in the first stage. Since the system reserves a part of generation resources as regulation, which causes the regulation reserve costs. However, in the dispatch operations, only the real-time regulation dispatched is charged for the corresponding fuel

costs. Thus, the dispatched regulation cost function $F_r(r_{gt}^\xi)$ is considered as

$$F_r(r_{gt}^\xi) = F^o(r_{gt}^\xi) - C_g^U r_{gt}^\xi,$$

where $F^o(\cdot)$ is the overall regulation cost equivalent to the sum of regulation reserve cost and fuel cost on dispatched regulation, higher than the regular energy generation cost $F_g(p_{gt}^\xi)$. Here, we assume that the fuel cost of real-time regulation up(down) corresponds to the the quadratic function of the regulation level, $r^u(r^d)$, but with larger cost coefficients, represented by $F_r(r^u) = a' + b'r^u + c'(r^u)^2$. Meanwhile, the regulation down service $r_{gt}^{d\xi}$ is assumed to incur cost based on the same dispatched regulation cost function. Due to the nonlinear objective function, a piecewise linear approximation is again used to obtain very close solutions.

5.2.1.1 First-Stage Unit Commitment

In the first stage, unit commitment is scheduled according to the operation requirements for generating units such as minimum ON time, minimum OFF time, startup action and shutdown action. The regulation up and down reserves also are included to satisfy the forecasted reserve level in each period.

$$u_{gt} - u_{g(t-1)} \leq u_{g\tau} \qquad \forall g \in G,\ t \in T,\ \tau = t, \ldots, min\{t + L_g - 1\} \qquad (5.2)$$

$$u_{g(t-1)} - u_{gt} \leq 1 - u_{g\tau} \qquad \forall g \in G,\ t \in T,\ \tau = t, \ldots, min\{t + l_g - 1\} \qquad (5.3)$$

$$v_{gt} \geq u_{gt} - u_{g(t-1)} \qquad \forall g \in G,\ t \in T \qquad (5.4)$$

$$w_{gt} \geq -u_{gt} + u_{g(t-1)} \qquad \forall g \in G,\ t \in T \qquad (5.5)$$

$$\sum_{g \in G_i} rc_{gt}^u \geq R_{it}^u \qquad \forall i \in N,\ t \in T, \qquad (5.6)$$

$$\sum_{g \in G_i} rc_{gt}^d \geq R_{it}^d \qquad \forall i \in N,\ t \in T, \qquad (5.7)$$

$$u_{gt},\ v_{gt},\ w_{gt} \in \{0,1\}, \qquad \forall g \in G,\ t \in T, \tag{5.8}$$

$$rc^u_{gt}, rc^d_{gt} \geq 0, \qquad \forall g \in G,\ t \in T \tag{5.9}$$

where three binary variables, u_{gt}, v_{gt}, w_{gt}, are defined as commitment decision, startup action and shutdown action of unit g at period t respectively. L_g and l_g represent minimum-on time and minimum-down time, respectively.

5.2.1.2   Second-Stage Economic Dispatch

The second stage constraints contain the economic dispatch including generation limits (5.10) and ramping limits (5.11)-(5.12), real-time regulation up/down limits (5.13)-(5.14), regulation capacities (5.15)-(5.16) and power transmission (5.17)-(5.18). Since the regulation up/down takes up a part of generation capacities when the units are ON, the ramping up/down is considered to cover both generation and regulation at the same time. Any of generation changes or regulation changes can not exceed the ramp rate limit in successive periods. Meanwhile, constraints (5.13)-(5.14) ensure the real-time regulation up and down constrained by the regulation reserves determined from first stage. Additionally, constraints (5.17)-(5.18) show the traditional DC approximation of Kirchhoff's current law and Kirchhoff's voltage law applied into load balance, where the regulation up/down, renewable energy output and potential load-shedding loss are taken into account.

$$(P_g^{min} + rc^d_{gt})u_{gt} \leq p^\xi_{gt} \leq (P_g^{max} - rc^u_{gt})u_{gt}, \quad \forall\, g \in G,\ t \in T,\ \xi \in \Xi \tag{5.10}$$

$$p^\xi_{gt} - p^\xi_{gt-1} \geq -RD_g, \quad \forall\, g \in G,\ t \in T,\ \xi \in \Xi \tag{5.11}$$

$$p^\xi_{gt} - p^\xi_{gt-1} \leq RU_g, \quad \forall\, g \in G,\ t \in T,\ \xi \in \Xi \tag{5.12}$$

$$0 \leq r^{u\xi}_{gt} \leq rc^u_{gt}, \quad \forall\, g \in G, t \in T,\ \xi \in \Xi \tag{5.13}$$

$$0 \leq r^{d\xi}_{gt} \leq rc^d_{gt}, \quad \forall\, g \in G, t \in T,\ \xi \in \Xi \tag{5.14}$$

95

$$0 \leq rc_{gt}^u \leq P_g^{max} u_{gt}, \quad \forall g \in G, t \in T \tag{5.15}$$

$$0 \leq rc_{gt}^d \leq P_g^{max} u_{gt}, \quad \forall g \in G, t \in T \tag{5.16}$$

$$\sum_{(i,j)\in A_i^+} f_{ijt}^\xi - \sum_{(j,i)\in A_i^-} f_{jit}^\xi - \sum_{g\in G_i} (p_{gt}^\xi + r_{gt}^{u\xi} - r_{gt}^{d\xi}) - \Delta_{it}^\xi = W_{it}^\xi - D_{it}^\xi,$$
$$\forall i \in N, t \in T, \xi \in \Xi \tag{5.17}$$

$$(f_{ijt}^\xi - f_{jit}^\xi) - M_{ijt}^\xi (\beta_{it}^\xi - \beta_{jt}^\xi) = 0, \quad \forall (i,j) \in A, t \in T, \xi \in \Xi \tag{5.18}$$

$$-F_{ij}^{Cap} \leq f_{ijt}^\xi \leq F_{ij}^{Cap}, \quad \forall (i,j) \in A, t \in T, \xi \in \Xi \tag{5.19}$$

$$p_{gt}^\xi \geq 0, \quad \forall g \in G, t \in T, \xi \in \Xi \tag{5.20}$$

$$\Delta_{it}^\xi \geq 0, \quad \forall i \in N, t \in T, \xi \in \Xi \tag{5.21}$$

$$f_{ijt}^\xi \geq 0, \quad \forall (i,j) \in A, i \in N, t \in T, \xi \in \Xi. \tag{5.22}$$

5.2.2 Two-Stage SCUC With CVaR Constraints

To identify the effects of risk constraints on system reliability, rather than implementing fixed reserve requirements, Model I is modified to incorporate the risk constraints. The two-stage stochastic unit commitment with risk-constrained measure (Model II) does not enforce the fixed regulation reserve requirements on the first stage. However, it remains to be scheduled on the second stage, depending on the real-time regulation up/down in all scenarios.

Either fixed reserve requirements or CVaR risk measure is a strategy to maintain the system reliability. Their operations and effects are similar in nature. The Model II uses the same objective function as Model I, where the occurrence of potential load-shedding loss also cause penalty, $VOLL \times \Delta$. In this way, two models can be allowed to perform apple-to-apple comparison.

96

5.2.2.1 First-Stage Unit Commitment

The model II includes all common UC constraints (5.2)-(5.5) in the previous model, excluding the regulation reserve constraints (5.6) and (5.7). Although the day-ahead regulation reserve is not considered in the first stage, it's still able to be determined in the dispatch level as necessary. Without the consideration of regulation reserve scheduling, the first-stage problem with purely binary decisions is the traditional unit commitment problem.

5.2.2.2 Second-Stage Economic Dispatch

The second-stage problem is subject to the constraints involving generation limits (5.10) and ramping limits (5.11)-(5.12), regulation up/down limits (5.13)-(5.14), power transmission (5.17)-(5.19), as well as the CVaR constraints. The following CVaR constraints describe the system loss representation and the conditional loss control restricted by loss allowance, respectively.

$$\sum_{i\in I}\Delta_{it}^{\xi} \leq \eta_t + \zeta_t^{\xi}, \qquad\qquad \forall\, t \in T,\, \xi \in \Xi \qquad (5.23)$$

$$\eta_t + (1-\theta)^{-1}\sum_{\xi\in\Xi}\text{Prob}^{\xi}\zeta_t^{\xi} \leq \bar{\phi}, \qquad\qquad \forall\, t \in T \qquad (5.24)$$

$$\eta_t \geq 0,\ \zeta_t^{\xi} \geq 0, \qquad\qquad \forall\, t \in T,\, \xi \in \Xi \qquad (5.25)$$

To model the loss expectation exceeding $\text{VaR}_{\theta}[L(x,Y)]$, we define two continuous variables η_t and ζ_t^{ξ}, which represents the actual VaR in time t and the loss beyond VaR at time t of scenario ξ, respectively. The summation of loss at time t thus can be bounded by the summation of η_t and ζ_t^{ξ} for each scenario, shown in (5.23). Constraint (5.24) ensure the conditional expectation of losses on the left hand side can not exceed the given loss allowance $\bar{\phi}$. Then the Model II integrated with

CVaR constraints is proposed as follow,

$$
\min \quad \sum_{g \in G} \sum_{t \in T} (SU_{gt} v_{gt} + SD_{gt} w_{gt} + C_g^U rc_{gt}^u + C_g^D rc_{gt}^d)
$$

$$
+ \sum_{\xi \in \Xi} prob^\xi \sum_{t \in T} \sum_{g \in G} [F_g(p_{gt}^\xi) + F_r(r_{gt}^{u\xi}) + F_r(r_{gt}^{d\xi})] + VOLL \sum_{\xi \in \Xi} prob^\xi \sum_{t \in T} \sum_{i \in N} \Delta_{it}^\xi
$$

s.t.   (5.2)-(5.5), (5.10), (5.11)-(5.12), (5.13)-(5.14), (5.15)-(5.16),

(5.17)-(5.19), (5.23)-(5.25)

5.2.3   *Reformulation of Nonlinear SUC Model*

After building SUC-Reliability models, we note that two bilinear terms shown in these stochastic mixed integer programs, i.e. $rc_{gt}^u u_{gt}$ and $rc_{gt}^d u_{gt}$, which are constructed by a continuous variable and a binary variable. Due to the bilinear terms, they would increase the computation difficulty especially when solving SMIP is still time consuming. Thus, we apply a reformulation approach to the proposed models in order to eliminate these computational issues.

These two nonlinear terms appear in the current SUC models as in constraint (5.10). For simplicity, we intuitively split this constraint into two constraints, generation upper limit (5.26) and generation lower limit (5.27).

$$
P_{gt}^{max} u_{gt} - rc_{gt}^u u_{gt} - p_{gt}^\xi \geq 0, \quad \forall\, t,\, g,\, \xi \tag{5.26}
$$

$$
P_{gt}^{min} u_{gt} + rc_{gt}^d u_{gt} - p_{gt}^\xi \leq 0, \quad \forall\, t,\, g,\, \xi \tag{5.27}
$$

Firstly, we can transform them to bilinear constraints as shown in (5.26) and (5.27). Secondly, we replace the fractional variables by combination of binary variables. Thirdly, we linearize the bilinear term with exactly one binary variable and one continuous variable. Then we get a stochas-

tic MILP optimization problem. We refer this procedure to Discretization-Linearization procedure as discussed in [**?**]. The validity and accuracy to the original model is mainly controlled by the number of binary variables introduced to replace each fractional variable.

To linearize constraints (5.26) and (5.27), we introduce another new continuous variable φ to substitute the bilinear term $rc_{gt}^u u_{gt}$.

$$\varphi_{gt} = rc_{gt}^u u_{gt} \text{ and } \chi_{gt} = rc_{gt}^d u_{gt}, \tag{5.28}$$

Variable φ_{gt} means two possible values, i.e. rc_{gt}^u and 0, which is equivalently further replaced by two following constraints. If $u_{gt} \neq 0$, the φ_{gt} is equal to the value of rc_{gt}^u through setting the upper bound and the lower bound in (5.29) and (5.30). Otherwise, the φ_{gt} is equal to 0 because the unit is forced to be offline and no reserve can be provided.

$$0 \leq \varphi_{gt} \leq rc_{gt}^u, \quad \forall\, t,\, g \tag{5.29}$$

$$rc_{gt}^u - R(1 - u_{gt}) \leq \varphi_{gt} \leq R u_{gt}, \quad \forall\, t,\, g \tag{5.30}$$

Overall, the upper generation capacity on constraint (5.26) can further replaced by the following constraints so as to remove the bilinear terms.

$$P_{gt}^{max} u_{gt} - \varphi_{gt} - p_{gt}^{\xi} \geq 0, \quad \forall\, t,\, g,\, \xi$$

$$0 \leq \varphi_{gt} \leq rc_{gt}^u, \quad \forall\, t,\, g$$

$$rc_{gt}^u - R(1 - u_{gt}) \leq \varphi_{gt} \leq R u_{gt}, \quad \forall\, t,\, g$$

Similarly, with introducing a new continuous variable χ_{gt}, the lower generation capacity in (5.27)

is replaced by the following constraints.

$$P_{gt}^{min} u_{gt} + \chi_{gt} - p_{gt}^{\xi} \leq 0, \quad \forall\, t,\, g,\, \xi$$

$$0 \leq \chi_{gt} \leq rc_{gt}^{d}, \quad \forall\, t,\, g$$

$$rc_{gt}^{d} - R(1 - u_{gt}) \leq \chi_{gt} \leq Ru_{gt}, \quad \forall\, t,\, g$$

5.3 Solution Approach

The proposed Model I and Model II are formulated in the mixed integer programs, which become hard to solve as the uncertainties of wind output represented in a large number of scenarios. Some advanced solution approached have been developed to deal with these computational issues, e.g. Benders' Decomposition and sample average approximation. Particularly, Benders' decomposition has been successfully applied in solving in stochastic programs on power systems. Here this study uses a modified Benders Decomposition algorithm to solve these two models.

The Model I is naturally decomposed to the first-stage unit commitment in relaxed master problem and the second-stage economic dispatch in the subproblem based on one scenario. Therefore, the RMP is a mixed integer program while the SPs are linear programs. This decomposition strategy also can be implemented in Model II. However, due the coupling constraint shown in CVaR constraints, this coupling structure is not easy to decouple on decomposition algorithms if multiple Benders' cuts are generated from individual scenarios. We then consider the alternative decomposition strategy that all CVaR constraints are placed on **RMP**, and only the incumbent solutions $(\mathbf{u}, \mathbf{l})$ will allow to be passed on $\mathbf{SP}^{\xi}$. In this way, the decision variable **l** is involved in Benders cuts so that it is helpful to generate a stronger Benders' cut and thus restrict more solution space of **RMP** during the solution process. Meanwhile, solving the multiple uncoupled subproblems can benefit from the parallel computing resources to reduce computing times. The

decomposition of Model II is selected to illustrate the modified Benders decomposition algorithm.

$$[\textbf{RMP}]: \quad \min \quad \sum_{g \in G} \sum_{t \in T} (SU_{gt} v_{gt} + SD_{gt} w_{gt} + C_g^U rc_{gt}^u + C_g^D rc_{gt}^d) + \sum_{\xi \in \Xi} \text{Prob}^\xi \pi^\xi$$

$$\text{s.t.} \quad (5.2)\text{-}(5.5), \ (5.15)\text{-}(5.16), \ (5.23)\text{-}(5.25),$$

$$\mathbb{O}(u_{gt}, l_{it}^\xi, \pi^\xi) \geq 0, \ \forall \, \xi \in \Xi$$

$$\mathbb{F}(u_{gt}, l_{it}^\xi, \pi^\xi) \geq 0, \ \forall \, \xi \in \Xi$$

$$u_{gt}, \ v_{gt}, \ w_{gt} \in \{0,1\}, \forall g \in G, \ t \in T$$

where π^ξ is defined as an unrestricted variable to represent the minimum total fuel cost in a scenario; $\mathbb{O}(u_{gt}, l_{it}^\xi, \pi^\xi) \geq 0$ stands for the optimality cuts associated with the commitment variable u_{gt}, loss variable l_{it}^ξ and π^ξ, while $\mathbb{F}(u_{gt}, l_{it}^\xi) \geq 0$ denotes the feasibility cuts.

$$[\textbf{SP}^\xi]: \quad \min \quad \sum_{g \in G} \sum_{t \in T} [F_g(p_{gt}^\xi) + F_r(r_{gt}^{u\xi}) + F_r(r_{gt}^{d\xi})] + VOLL \sum_{\xi \in \Xi} prob^\xi \sum_{t \in T} \sum_{i \in N} \Delta_{it}^\xi$$

$$\text{s.t.} \quad (5.11)\text{-}(5.12), \ (5.13)\text{-}(5.14), \ (5.18)\text{-}(5.19), \ (5.20)\text{-}(5.22)$$

$$P_{gt}^{max} \hat{u}_{gt} - \varphi_{gt} - p_{gt}^\xi \geq 0, \quad \forall \, t, \, g, \, \xi \tag{5.31a}$$

$$0 \leq \varphi_{gt} \leq rc_{gt}^u, \quad \forall \, t, \, g \tag{5.31b}$$

$$rc_{gt}^u - R(1 - u_{gt}) \leq \varphi_{gt} \leq Ru_{gt}, \quad \forall \, t, \, g \tag{5.31c}$$

$$P_{gt}^{min} u_{gt} + \chi_{gt} - p_{gt}^\xi \leq 0, \quad \forall \, t, \, g, \, \xi \tag{5.31d}$$

$$0 \leq \chi_{gt} \leq rc_{gt}^d, \quad \forall \, t, \, g \tag{5.31e}$$

$$rc_{gt}^d - R(1 - u_{gt}) \leq \chi_{gt} \leq Ru_{gt}, \quad \forall \, t, \, g \tag{5.31f}$$

$$\sum_{(i,j) \in A_i^+} f_{ijt}^\xi - \sum_{(j,i) \in A_i^-} f_{jit}^\xi - \sum_{g \in G_i} (p_{gt}^\xi + r_{gt}^{u\xi} - r_{gt}^{d\xi})$$

$$= W_{it}^\xi + D_{it}^\xi - \hat{\Delta}_{it}^\xi, \ \forall \, i \in N, \, t \in T \tag{5.31g}$$

We implement the new Benders' Decomposition strategy with the help of CALLBACK function

in CPLEX. Figure 5.1 explicitly shows the solution flowchart of Benders' decomposition used to solve Model II by calling CALLBACK function. Compared to the classical Benders' Decomposition, the modified Benders' Decomposition algorithm has a significant difference in solution process that **RMP** is solved only once using the Branch-and-Bound-and-Cut algorithm. During the solving procedure, the feature of CALLBACK function holds the Benders' cuts generated from $\mathbf{SP}^\xi$ and only allow the violated cuts added to **RMP**. Meanwhile, the optimality cuts or feasibility cuts are generated at the branching nodes (in the branch-and-bound tree) where the lower bound is being updated and the upper bound is also updated after solving the $\mathbf{SP}^\xi$ for all scenarios. This **RMP** solving procedure is able to speed up the convergence, since it can handle the issue of iteratively solving **RMP** without improving the lower bound in the classical Bender's decomposition. Furthermore, in the couple with proposed decomposition strategy, **RMP** is maintained in a small size of active constraints and added with a limited number of stronger Benders' cuts.
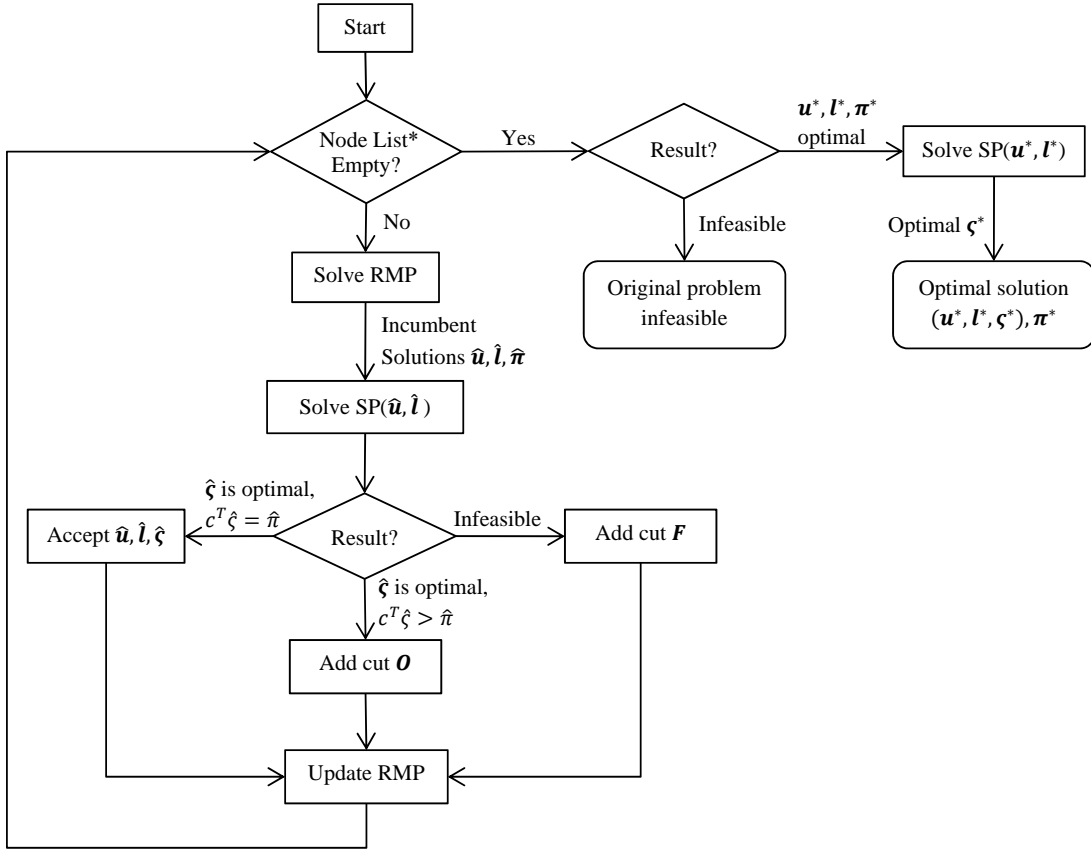
Figure 5.1: The solution flowchart of Benders' Decomposition with CALLBACK function

5.4 Computational Results

To show the results between two operation strategies, we perform the computational experiments on the proposed two models individually. The effects of fixed regulation reserve requirements and CVaR measure on the reliability of power generation system are investigated, respectively. Initially, a 7-bus system is selected to test both models in a normal state, where the system includes 4 generators, 1 wind farm, and 10 transmission lines with given capacities. Then, both models are used to solve an enhanced 118-bus system by modified Benders' decomposition approach. All

models are coded in C++ while solved by CPLEX 12.5. All experiments are implemented on a PC Dell OPTIPLEX 980 with Intel Core i7 vPro at 2.80 GHz and 4 GB memory in a Windows 7 operating system.

5.4.1   Seven-Bus System

In most cases, the power system operates in a normal state, in which the generation equipments and transmission facilities are under good maintenance and no outages would happen. In this experiment, the load and renewable energy outputs are assumed to volatile significantly in a few successive time periods. Two models are tested in the IEEE 7-bus system based on a day ahead 100-scenario case, sharing the same generators' parameters, transmission lines, wind energy outputs and forecasted demands. The detailed information for buses and generators is shown in Table 5.1 and 5.2, respectively. The penalty cost of load-shedding loss is introduced at the rate of $\$100/MWh$ to prevent the occurrence of load shedding. In Model II, the confidence level θ is set to 99% and the loss allowance $\bar{\phi}$ is set to $5MW$. Through solving above two cases with 24 periods and 100 scenarios, the computation times are 239 seconds and 176 seconds for Model 1 and Model 2, respectively.

Table 5.1: Bus Parameters

ID	Type	Gen ID	Gen. Cap. (MW)	Regulation Requirement. (MW)
B1	Wind	R1	100	-
B2	Coal	G1	90	20
B2	Coal	G2	90	-
B3	-	-	-	-
B4	Gas	G3	200	20
B5	-	-	-	-
B6	Coal	G4	90	20
B7	-	-	-	-

[a] The symbol, '-', represents no generation unit available at a
corresponding bus

Table 5.2: Generator Parameters and Costs

	G1	G2	G3	G4
Min-ON (h)	2	1	2	4
Min-OFF (h)	2	2	2	1
Ramp-Up (MW/h)	60	30	60	60
Ramp-Down (MW/h)	60	30	60	60
Pmin (MW)	10	5	9	7
Pmax (MW)	110	50	90	70
Startup ($)	50	500	800	30
Shutdown ($)	50	500	800	20
Fuel Cost a ($)	6.78	6.78	31.67	10.15
Fuel Cost b ($/MWh$)	12.888	12.888	26.244	17.820
Fuel Cost c ($/MWh^2$)	0.0109	0.0109	0.0697	0.0128

The computational results for objective values and optimal unit commitment schedules are reported in Table 5.3. The objective values for each model are given in the second column, the maximum loss penalties are reported in the third column and the unit commitment schedules are reported in the fifth column. From Table 5.3, the commitment hours of G1 and G2 have no difference between two models. However, compared to Model II, generator 3 and 4 appears longer commitment periods in Model I. Although Model II has a longer unit commitment period in G3, the commitment time period of G4 is greatly reduced and turned off at hour 17. We observe that the objective value of Model II which only uses CVaR measure is less than that of Model I which applies fixed reserve requirements, with 5.3% of cost reduction. Given on the same operation conditions and hourly loads, the unserved energy penalty of Model II is lower than that of Model I, which means the

system can have higher load satisfaction with less load-shedding. Through individually comparing each scenario, it can be found that the maximum losses for Model II are greatly lower than Model II under a scenario, shown in the fourth column. Here, the big cost saving has two following main reasons resulting from the first-stage commitment schedules.

Table 5.3: Results of 7-Bus System in Normal State

Model	Obj. Val.	Loss Penalty	Max. Loss	Unit ID	Hour (1-24)
I	$74429	$1193	24	G1	1 1 1 1 1 1 1 1 1 1 1 1 1 1 1 1 1 1 1 1 1 1 1 1
				G2	1 1 1 1 1 1 1 1 1 1 1 1 1 1 1 1 1 1 1 1 1 1 1 1
				G3	0 0 0 0 0 0 1 0 0 0 0 0 0 0 0 1 1 1 1 1 0 0 0 0
				G4	1 1 1 1 1 1 1 1 1 1 1 1 1 1 1 1 1 1 1 1 1 1 1 1
II	$70488	$9.7	3	G1	1 1 1 1 1 1 1 1 1 1 1 1 1 1 1 1 1 1 1 1 1 1 1 1
				G2	1 1 1 1 1 1 1 1 1 1 1 1 1 1 1 1 1 1 1 1 1 1 1 1
				G3	0 0 0 1 0 0 1 0 0 0 0 0 0 0 0 1 1 1 1 1 1 0 0
				G4	1 1 1 1 1 1 1 1 1 1 1 1 1 1 1 1 1 0 0 0 0 0 0 0

The regulation reserve is the major component of first-stage cost, especially on the Model I. Through the fixed reserve requirements, the regulation up/down reserve must satisfy the given reserve requirements for each hour, even during the off-peak periods. Meanwhile, the regulation up reserve is necessarily increased to meet the peak load in certain hours. It's unavoidable to generate high reserve costs to offer the regulation service. Overall, compared to Model I , Model II has low hourly regulation reserve on the whole system, which is shown in Figure 5.2. Since the regulation reserve levels in Model II are only determined from the needs of real-time regulation based on each scenario. During on-peak hours, e.g. Hour 18 to Hour 21, the system tends to reserve more regulation resources to meet peak load changes. During off-peak hours, the regulation

reserves are reduced or not scheduled, and therefore the reserve costs can be cut off significantly. Additionally, by comparing the regulation up reserves on each unit from two models (in Figure 5.3 and 5.4), it can be observed that only online generators are scheduled with regulation reserve in Model II, which makes generating resource usage more flexible, like G3. This means the unused generating resources can be assigned for another tasks within same time periods.
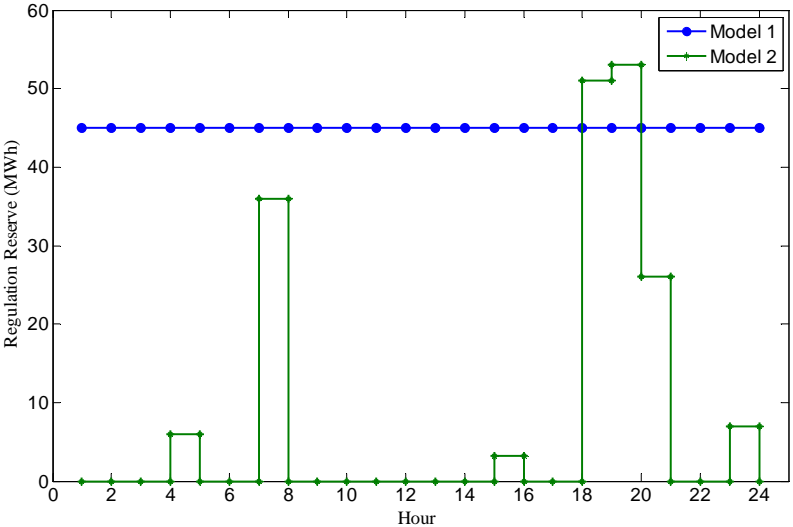
Figure 5.2: Total regulation reserve levels for two models

The unserved energy cost is another component that causes the high generation costs. On the expected loss of load, the result shows that Model I has 11.93 MW of unserved energy while Model II is 0.097 MW. After the unserved energy penalty weighted by the scenario probabilities, Model I has higher unserved energy costs than Model II. Although both models have the situation that the loss of load happen in an extreme scenario, Model II is able to limit the total loss expectation through CVaR constraints so that the the load loss penalty can be further minimized.
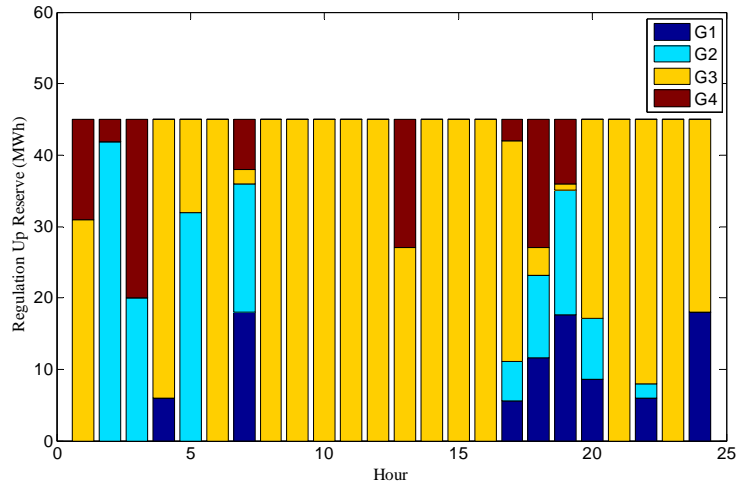
Figure 5.3: Regulation reserve levels for Model I
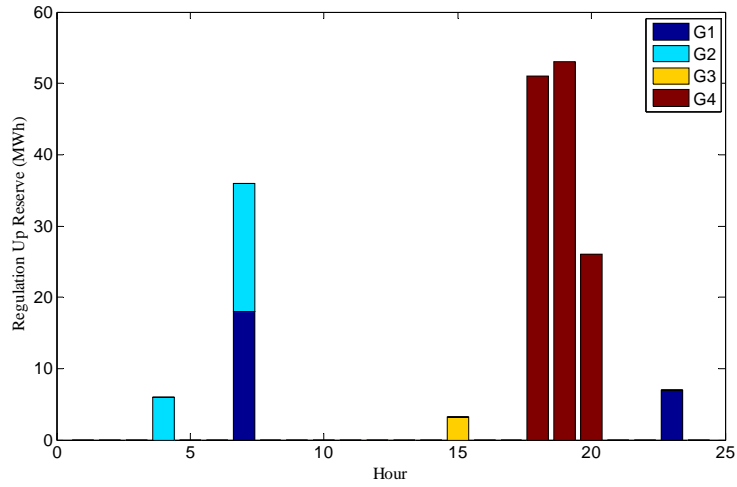
Figure 5.4: Regulation reserve levels for Model II

5.4.2 Enhanced 118-Bus System

The IEEE 118-bus system is modified as real case study and applied to study the effects of two different strategies on regulation reserve, operations and unserved energy. The modified 118-bus

system includes 118 buses, 54 generators, 186 transmission lines with 120 MW of flow capacities, and 4 wind farms which are able to provide at least 4% of total power generation per hour. This case involves 24 hours and 25 scenarios and assumes the penalty of loss load to be $100/MWh. In Model II, the confidence level θ is set to 99% and the loss allowance $\bar{\phi}$ is released to $70MW$, approximately 1.2% of peak load. The computation times for Model 1 and Model 2 are 771 seconds and 718 seconds, respectively.

The total costs of Model 1 is $1,698,430$, and the total costs of Model 2 is lowered to $1,667,960$ with 1.8% cost reduction. Using CVaR constraints instead of fixed reserve, the total online units can be reduced during peak hours, i.e. 10 AM to 8 PM, shown in Figure 5.5. To satisfy the same electricity demands, this reduced online unit numbers indicate that the efficiency of generating resources is improved without retaining some units that serve for fixed reserve requirements. More units thus can be released and assigned for another energy or ancillary service.
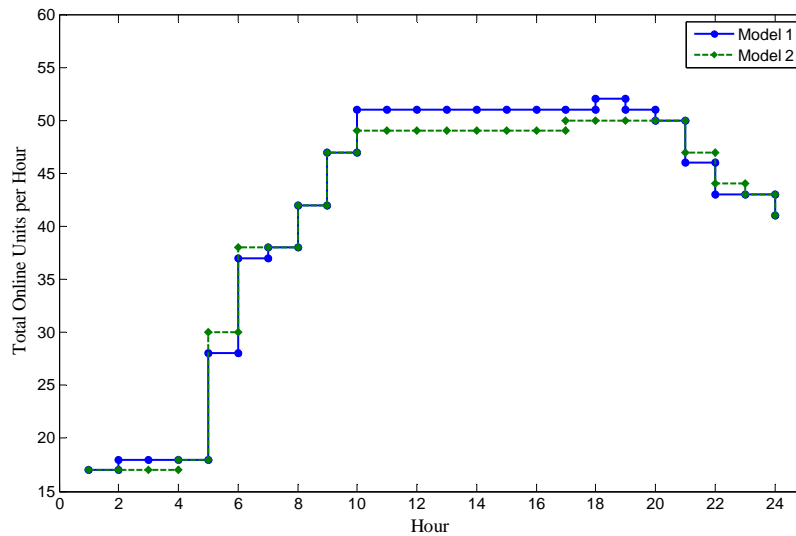
Figure 5.5: Total online units for 118-bus system

The system regulation reserve levels for 118-bus system are shown in Figure 5.6. The regulation

reserve requirement on Model 1 is set to 300 MW, which is equal to the maximum generation capacity in the system. As compared to the reserve levels of Model 1, the reserve levels of Model 2 are much lower and the maximum regulation up reserve is controlled within 100 MWh. The expected losses on Model 1 and Model 2 are 21.52 MW and 21.76 MW, respectively. These results clearly indicate that SUC model with CVaR constraints is able to reduce reserve commitments without increasing load-shedding losses.
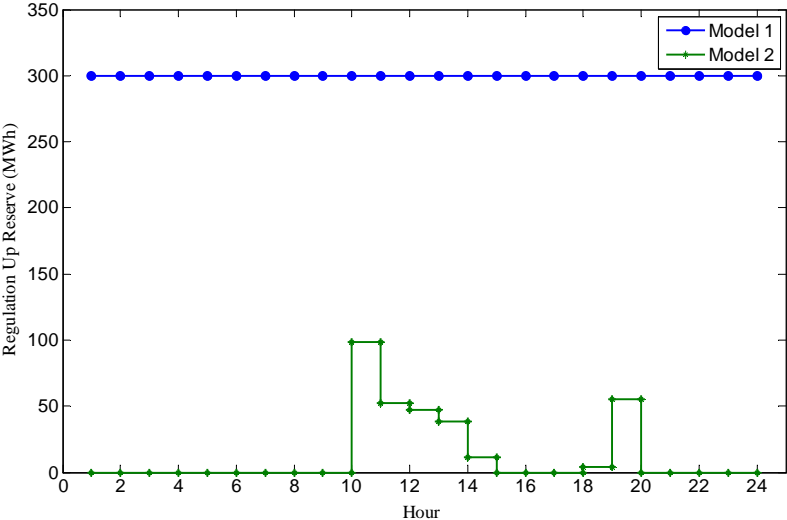
Figure 5.6: Total regulation reserve levels for 118-bus system

With the help of regulation service, the generation scheduling through either fixed reserve requirements or CVaR measure is able to offer the protection of system's reliability. When the power system operates in a normal status, the CVaR measure is superior to the fixed reserve requirements on the total generation costs as well as the expected unserved energy.

CHAPTER 6: CONCLUSIONS

To optimize an integrated energy system effectively, this dissertation discusses three main frameworks to solve for energy expansion planning and power system management. Considering impacts from uncertainties, this dissertation applies risk-constrained stochastic integer programming to improve the efficiency, reliability economic of integrated energy system. In additions, an enhanced Bender's Decomposition algorithm is proposed to solve for large-size SUC models incorporated with reliability constraints.

In Chapter 3, a capacity expansion planning strategy is proposed for combined natural gas system and power system under stochastic environment. The expansion investment decisions and long-term operation decisions are formulated by stochastic integer programming to achieve optimal planning. The stochastic expansion planning on an integrated system is verified that it is able to reduce the impacts of the uncertainties of one system on the other without forecast error accumulation. The co-optimization method can achieve lower facility expansion sizes and operational costs than individual-system optimization. As renewable energy system is expanded, the overall system requires a larger expansion size of gas system, particularly in LNG storage system and pipeline transportation, to handle increasingly uncertain energy outputs. This planning strategy can provide useful insights for decision makers to establish a more reasonable and reliable energy expansion plan.

In Chapter 4, a two-stage SUC model considering non-generation resources and risk control is developed. The optimization results indicate that the SUCR-DR-ES model yields the optimal UC schedule with the lowest total expected costs among four proposed models. When the same uncertainties occur, the models with non-generation resources appear more stable and flexible to handle supply-demand changes, compared to the basic model (SUCR). With growing renewable

energy penetration, the combination of demand response and energy storage provides a promising opportunity to improve efficiency and reliability of power systems.

Additionally, the reliability parameter analysis has been conducted regarding confidence level and load-shedding allowance based on the percentage change rates of total cost. Conservative decisions (higher confidence level or lower loss allowance) usually leads to high cost increment. It's also found that the confidence level dominates the cost increase, but loss allowance is a relatively more significant factor leading to the magnitude of total cost increment percentage change rate. Besides, the cost sensitivity range of individual model is located with the reliability parameter changes. The results also demonstrate that how the specific range of reliability parameters can affect the optimal costs given non-generation resources. As for a large-scale system like 118-Bus system, the individual non-generation resources become less beneficial to the system cost reduction. However, considering the optimal cost and risk resilience, the model with both non-generation resources still has the strongest ability to save generation costs and maintain the power system reliability.

In Chapter 5, the operation strategies based on ancillary services are compared between explicit reserve requirements and CVaR measures to improving system reliability and reducing generation cost. Two stochastic unit commitment models integrated with individual strategies, reserve requirements and CVaR measures, are proposed for the co-optimization of energy and ancillary services. The results have demonstrated that the strategy of CVaR measures outperforms the traditional strategy of prefixed reserve requirements in normal state. The operation strategy using CVaR measures is able to significantly reduce the regulation reserve levels, in addition to guarantee the load-shedding loss expectation not exceeding the pre-specified loss allowance at a certain confidence level. The risks of load-shedding loss becomes controllable. Accordingly, the reliability of the system can secured by day-ahead scheduling and more generation resources can be released for energy and ancillary markets.

The classic Bender's Decomposition approach is modified with new decomposition strategies for SUC models. Through solving large cases, the developed decomposition approach outperforms the classic Bender's Decomposition with common decomposition strategies. It successfully shortens computation times and improves large problem computation performance on SUCR-DR-ES model and SUCR-CVaR model, as scenario increases.

The future research could be directed to study the computation effectiveness of developed decomposition approach on SEP model. Because of stochastic mixed integer programs on two-layer systems, another decomposition strategy may be needed and tailored to increase convergence speed. As the secondary supplement, energy storage system can be considered in expansion planning to support the growing renewable energy integration. Meanwhile, risk control on expansion project is taken into account. Then the capacity expansion planning model can become more comprehensive and appropriate for policy making and project implementation.

APPENDIX A: NOMENCLATURE

Table A.1: Abbreviations

UC	Unit Commitment
SCUC	Security-Constrained Unit Commitment
SCRA	Security-Constrained Reliability Assessment
SUC	stochastic Unit Commiment
DR	Demand Response
ES	Energy Storage
ISO	Independent System Operator
RTO	Regional Transmission Organization
BD	Benders' Decomposition
LR	Lagrangian Relaxation
RMP	Relaxed Master Problem
SP	Subproblem
LB	Lower Bound
UB	Upper Bound
DAM	Day-Ahead Market
RTM	Real-Time Market
RTC	Real-Time Commitment
RTD	Real-Time Dispatch
LMP	Locational Marginal Price
RAA	Reserve Adequacy Assessment

Table A.2: SEP: Sets and Indices

N_G	Set of nodes in the gas network
N_E	Set of nodes in the electricity network
N_{LNG}	Set of LNG terminals, $N_{LNG} \subseteq N_G$
N_{REW}	Set of renewable energy farms, $N_{REW} \subseteq N_E$
N_{GEN}^G	Set of gas-fired power plants, $N_{GEN}^G \subseteq N_E$
N_{GEN}^C	Set of coal-fired power plants, $N_{GEN}^C \subseteq N_E$
A_G	Set of pipelines in the gas network
A_{Gi}^+	Set of outgoing arcs from i in the gas network
A_{Gi}^-	Set of incoming arcs to i in the gas network
A_E	Set of electric lines in the electricity network
Ξ	Set of all possible scenarios
K	Set of all possible expansion levels
i, j	Indices of nodes
t	Indices of time
k	Indices of expansion levels
ξ	Indices of scenarios

Table A.3: SEP: Decision Variables

α_{ij}^k	Binary variable to denote whether a GP_{ij}^k expansion is made for gas pipeline $(i,j) \in A_G$
β_i^k	Binary variable to denote whether a NP_i^k expansion is made for LNG terminal $i \in N_{LNG}$
x_{ij}	Binary variable to denote whether a EF_{ij}^k expansion is made for electric line $(i,j) \in A_E$
y_i^k	Binary variable to denote whether a EG_i^k expansion is made for power plant $i \in N_{GEN}^G$
ϕ_i^k	Binary variable to denote whether a RP_i^k expansion is made for renewable source $i \in N_{REW}$
$f_{ijt}^{G\xi}$	Gas flow of arc $(i,j) \in A_G$
z_{it}^{ξ}	Gas supply from LNG terminal at node $i \in N_{LNG}$
s_{it}^{ξ}	Total NG supply to node $i \in N_G$
$d_{it}^{P\xi}$	Gas delivered to power plant $i \in N_{GEN}^G$
$d_{it}^{P'\xi}$	Gas consumption by power plant $i \in N_{GEN}^G$
r_{it}^{ξ}	Gas holding amount at power plant $i \in N_{GEN}^G$ at time t
$p_{it}^{G\xi}$	Electricity generated from a gas-fired power plant $i \in N_{GEN}^G$
$p_{it}^{C\xi}$	Electricity generated from a coal-fired power plant $i \in N_{GEN}^C$
w_{it}^{ξ}	Renewable generation at node $i \in N_{REW}$
$f_{ijt}^{E\xi}$	Electricity flow at electric line $(i,j) \in A_E$

Table A.4: SEP: Parameters

GP_{ij}^k	The kth expansion size of gas pipeline $(i,j) \in A_G$
NP_i^k	The kth expansion size of LNG tank at node $i \in N_{LNG}$
ECA_{ij}^k	Expansion costs of the expansion of size GP_{ij}^k on arc $(i,j) \in A_G$
ECL_i^k	Expansion costs of size NP_i^k of LNG tank at node $i \in N_{LNG}$
EF_{ij}^k	The kth expansion size of electric line $(i,j) \in A_E$
EG_i^k	The kth expansion size of gas-fired power plant at node $i \in N_{GEN}^G$
RP_i^k	The kth expansion size of renewable farm at node $i \in N_E$
ECE_{ij}^k	Expansion costs of the expansion of size EF_{ij}^k on arc $(i,j) \in A_E$
ECP_i^k	Expansion costs of size EG_i^k of gas-fired power plant at node $i \in N_{GEN}^G$
ECN_i^k	Expansion costs of size RP_i^k of renewable farm at node $i \in N_E$
TC_{gq}	Transportation cost of gas pipeline $(i,j) \in A_G$ per unit
FP_{it}^{ξ}	Fuel price for generator $i \in N_{GEN}^G$ at time t
GH_{it}	NG holding cost at $i \in N_{GEN}^G$ at time t
CP_{it}	Coal-fired generation costs of generator $i \in N_{GEN}^C$ at time t
TL_{ij}	Transmission loss rate on arc $(i,j) \in A_G$
$D_{it}^{0\xi}$	NG demand at $i \in N_G$ at time t (not for power plants)
SL_i	LNG supply of node $i \in N_{LNG}$
SF_i	NG self-supply of node $i \in N_G$
$\underline{U}_{ij}$	Current capacity of gas pipeline $(i,j) \in A_G$
$\underline{V}_i$	Current capacity of LNG terminal $i \in N_{LNG}$
RL_t	Renewable energy expansion requirements at time t
ORE_{it}^{ξ}	Renewable energy output based on existing generators at node $i \in N_{Rew}$
NRE_{it}^{ξ}	Renewable energy output based on potential generators at node $i \in N_{Rew}$
D_i^{Cap}	NG storage capacity in power plant $i \in N_{GEN}^G$
μ_i	Efficiency of a power plant $i \in N_{GEN}^G$
$\underline{G}_i^{Gmax}$	Current NG-fired generation capacity at node $i \in N_{GEN}^G$
$\underline{G}_i^{Cmax}$	Current coal-fired generation capacity at node $i \in N_{GEN}^C$
EC_i	Emission coefficient of power plant, EC_i^G for NG and EC_i^C for coal
ψ_t	Emission allowance at time t
F_{ij}^{Emax}	Capacity of electrical line $(i,j) \in A_E$
$D_{it}^{E\xi}$	Electricity demand at $i \in N_E$ at time t

Table A.5: SUCR: Sets and Indices

A	Set of transmission lines
G	Set of all generators
G_i	Set of electrical power generators at bus i
N	Set of locations (buses)
T	Length of planning horizon
Ξ	Set of all possible scenarios
g	Indices of generators
i, j	Indices of buses
t	Time period
ξ	Indices of scenarios

Table A.6: SUCR: Parameters

SU_{gt}	start-up cost of unit g in period t
SD_{gt}	shut-down cost of unit g in period t
$Prob^{\xi}$	probability of scenario ξ
L_g	minimum ON time of unit g
l_g	minimum OFF time of unit g
P_g^{max}	maximum power generation of unit g
P_g^{min}	minimum power generation of unit g
RU_g	ramping up limit of unit g
RD_g	ramping down limit of unit g
RS_{it}	spinning reserve requirement at bus i in period t
S_g^{max}	maximum spinning reserve of unit g
R_{it}^{ξ}	renewable energy at bus i in period t of scenario ξ
D_{it}	forecasted demand at bus i in period t
E_{it}^{ξ}	price elasticity at bus i in period t of scenario ξ
ρ_i	storage efficiency at bus i
B_{ijt}	susceptance in branch $i-j$ in period t
θ	confidence level
β_{it}^{ξ}	voltage angle at bus i
$\bar{\phi}$	maximum load-shedding loss allowance
α, γ	price velocity indicators
κ_i	maximum storage capacity at bus i

Table A.7: SUCR: Decision Variables

u_{gt}	commitment decision of unit g at period t
v_{gt}	startup action of unit g at period t
w_{gt}	shutdown action of unit g at period t
p_{gt}^{ξ}	power generation of unit g in period t of scenario ξ
s_{gt}^{ξ}	spinning reserve of unit g in period t of scenario ξ
f_{ijt}^{ξ}	power transmission from bus i to bus j in period t of scenario ξ
q_{it}^{ξ}	electricity price at bus i in period t of scenario ξ
r_{it}^{ξ}	remaining power at bus i in period t of scenario ξ
v_{it}^{ξ}	power saving at bus i in period t of scenario ξ
x_{it}^{ξ}	renewable energy dispatch amount at bus i in period t of scenario ξ
y_{it}^{ξ}	shifted demand at bus i in period t of scenario ξ
η_t	value-at-risk at period t (VaR)
ζ_t^{ξ}	the loss exceeding VaR in period t of scenario ξ

APPENDIX B: RENEWABLE ENERGY SCENARIO GENERATION

Here, we introduce a simple method for scenario generation in C++. Scenario generation is initially to generate sequences of random numbers following a specific distribution like normal distribution or exponential distribution, and then randomly select a proportion of scenarios to construct a scenario set.

Since the wind energy output in Chapter 3-5 is assumed to follow a normal distribution, which is described by the probability density function:

$$p(x|\mu,\sigma) = \frac{1}{\sigma\sqrt{2\pi}} \cdot e^{-\frac{(x-\mu)^2}{2\sigma^2}} \tag{B.1}$$

The distribution parameters thus are input including mean (μ) and stand deviation (σ). The procedure of random number generation has two steps:

- a generator produces sequences of uniformly distributed numbers;

- a distribution transforms above numbers into sequences of numbers with a specific distribution.

Let $x \sim N(0,100)$, the C++ codes for scalable scenario generation are shown as follow.

```
typedef std::tr1::ranlux64_base_01            ENG;
typedef std::tr1::normal_distribution<double> DISTA;
typedef std::tr1::variate_generator<ENG,DISTA> GENA;


double x;
ENG eng;
    eng.seed((unsigned int)time(NULL));


for(i=0;i<numscn;i++)
        for(k=0;k<numbus;k++)
```

```
DISTA  dist(0,10);
GENA   gen(eng,dist);
x = 0; dist.reset();
x = gen();


if (k==0)
        for(j=0;j<numhr;j++)
                wind[j][k]= mean[j]+x;
else
        for(j=0;j<numhr;j++)
                wind[j][k] = 0;


dist.reset();
    end
end
```

Given the mean of wind energy output for each hour, we generate a hundred of scenarios and randomly select 10 scenarios, shown in Table B.1.

Table B.1: Ten Scenarios of Wind Energy Outputs

Mean	S1	S2	S3	S4	S5	S6	S7	S8	S9	S10
45.0	48.4	59.1	49.3	43.4	46.5	34.1	43.5	41.6	52.4	42.1
51.0	54.4	65.1	55.3	49.4	52.5	40.1	49.5	47.6	58.4	48.1
58.0	61.4	72.1	62.3	56.4	59.5	47.1	56.5	54.6	65.4	55.1
36.0	39.4	50.1	40.3	34.4	37.5	25.1	34.5	32.6	43.4	33.1
39.0	42.4	53.1	43.3	37.4	40.5	28.1	37.5	35.6	46.4	36.1
34.0	37.4	48.1	38.3	32.4	35.5	23.1	32.5	30.6	41.4	31.1
43.0	46.4	57.1	47.3	41.4	44.5	32.1	41.5	39.6	50.4	40.1
41.0	44.4	55.1	45.3	39.4	42.5	30.1	39.5	37.6	48.4	38.1
33.0	36.4	47.1	37.3	31.4	34.5	22.1	31.5	29.6	40.4	30.1
31.0	34.4	45.1	35.3	29.4	32.5	20.1	29.5	27.6	38.4	28.1
28.0	31.4	42.1	32.3	26.4	29.5	17.1	26.5	24.6	35.4	25.1
28.0	31.4	42.1	32.3	26.4	29.5	17.1	26.5	24.6	35.4	25.1
30.0	33.4	44.1	34.3	28.4	31.5	19.1	28.5	26.6	37.4	27.1
31.0	34.4	45.1	35.3	29.4	32.5	20.1	29.5	27.6	38.4	28.1
33.0	36.4	47.1	37.3	31.4	34.5	22.1	31.5	29.6	40.4	30.1
24.0	27.4	38.1	28.3	22.4	25.5	13.1	22.5	20.6	31.4	21.1
20.0	23.4	34.1	24.3	18.4	21.5	9.1	18.5	16.6	27.4	17.1
31.0	34.4	45.1	35.3	29.4	32.5	20.1	29.5	27.6	38.4	28.1
33.0	36.4	47.1	37.3	31.4	34.5	22.1	31.5	29.6	40.4	30.1
38.0	41.4	52.1	42.3	36.4	39.5	27.1	36.5	34.6	45.4	35.1
41.0	44.4	55.1	45.3	39.4	42.5	30.1	39.5	37.6	48.4	38.1
43.0	46.4	57.1	47.3	41.4	44.5	32.1	41.5	39.6	50.4	40.1
44.0	47.4	58.1	48.3	42.4	45.5	33.1	42.5	40.6	51.4	41.1
41.0	44.4	55.1	45.3	39.4	42.5	30.1	39.5	37.6	48.4	38.1

LIST OF REFERENCES

[1] Alexander, G.J., Baptista, A.M.: A comparison of VAR and CVaR constraints on portfolio selection with the mean-variance model. Management Science **50**(9), 1261–1273 (2004)

[2] Angelidis, G.: Integrated day-ahead market. Technical description, California ISO (2012)

[3] Arroyo, J.M., Galiana, F.D.: Energy and reserve pricing in security and network-constrained electricity markets. IEEE Transactions on Power Systems **20**(2), 634–643 (2005)

[4] Atamtürk, A.: Sequence independent lifting for mixed-integer programming. Operations research **52**(3), 487–490 (2004)

[5] Barth, R., Brand, H., Meibom, P., Weber, C.: A stochastic unit-commitment model for the evaluation of the impacts of integration of large amounts of intermittent wind power. In: Probabilistic Methods Applied to Power Systems, 2006. PMAPS 2006. International Conference on, pp. 1–8 (2006)

[6] Benders, J.: Partitioning procedures for solving mixed-variables programming problems. Computational Management Science **2**(1), 3–19 (2005)

[7] Bouffard, F., Galiana, F.D., Conejo, A.J.: Market-clearing with stochastic security-part i: formulation. IEEE Transactions on Power Systems **20**(4), 1818–1826 (2005)

[8] CAISO: Draft final proposal for participation of non-generator resources in california iso ancillary service markets. Tech. rep., California ISO (2010)

[9] Castillo, E., Garca-Bertrand, R.M.R.: Decomposition techniques in mathematical programming. Springer (2006)

[10] Cerisola, S., Baíllo, A., Fernández-López, J.M., Ramos, A., Gollmer, R.: Stochastic power generation unit commitment in electricity markets: A novel formulation and a comparison of solution methods. Operations Research **57**(1), 31–46 (2009)

[11] Chakraborty, S., T.Senjyu, Toyama, H., Saber, A., Funabashi, T.: Determination methodology for optimising the energy storage size for power system. IET Generation, Transmission and Distribution **3**(11), 987–999 (2009)

[12] Conejo, A.J., Castillo, E., Mínguez, R., García-Bertrand, R.: Decomposition Techniques in Mathematical Programming - Engineering and Science Applications. Springer-Verlag, Heidelberg (2006)

[13] Constantinescu, E.M., Zavala, V.M., Rocklin, M., Lee, S., Anitescu, M.: A computational framework for uncertainty quantification and stochastic optimization in unit commitment with wind power generation. IEEE Transactions on Power Systems **26**(1), 431–441 (2011)

[14] Daneshi, H., Srivastava, A.: Security-constrained unit commitment with wind generation and compressed air energy storage. IET Generation, Transmission and Distribution **6**(2), 167–175 (2012)

[15] Dicorato, M., Forte, G., Trovato, M., Caruso, E.: Risk-constrained profit maximization in day-ahead electricity market. IEEE Transactions on Power Systems **24**(3), 1107–1114 (2009)

[16] Dietrich, K., Latorre, J., Olmos, L., Ramos, A.: Demand response in an isolated system with high wind integration. IEEE Transactions on Power Systems **27**(1), 20–29 (2012)

[17] DOE/EIA: Annual energy outlook 2014 with projections to 2040. Tech. rep., U.S. Energy Information Administration (2014)

[18] Ellison, J.F., Tesfatsion, L.S., Loose, V.W., Byrne, R.H.: A survey of operating reserve markets in us iso/rto-managed electric energy regions. Tech. rep., Sandia National Laboratories (2012)

[19] Fischetti, M., Lodi, A.: Local branching. Mathematical Programming **98**(1-3), 23–47 (2003)

[20] Fu, Y., Shahidehpour, M., Li, Z.: Security-constrained unit commitment with ac constraints. IEEE Transactions on Power Systems **20**(2), 1001–1013 (2005)

[21] Fu, Y., Shahidehpour, M., Li, Z.: Ac contingency dispatch based on security-constrained unit commitment. Power Systems, IEEE Transactions on **21**(2), 897–908 (2006)

[22] Gu, Z., Nemhauser, G.L., Savelsbergh, M.W.: Lifted flow cover inequalities for mixed 0-1 integer programs. Mathematical Programming **85**(3), 439–467 (1999)

[23] Gu, Z., Nemhauser, G.L., Savelsbergh, M.W.: Sequence independent lifting in mixed integer programming. Journal of Combinatorial Optimization **4**(1), 109–129 (2000)

[24] Hedman, K.W., Ferris, M.C., O'Neill, R.P., Fisher, E.B., Oren, S.S.: Co-optimization of generation unit commitment and transmission switching with n-1 reliability. IEEE Transactions on Power Systems **25**(2), 1052–1063 (2010)

[25] Hobbs, B.F., Rothkopf, M.H., O'Neil, R.P., Chao, H.: The Next Generation of Electric Power Unit Commitment Models. Kluwer Academic Publishers, Norwell, MA, USA (2001)

[26] Huang, Y., Rahil, A., Zheng, Q.P.: A quasi exact solution approach for scheduling enhanced coal bed methane production through CO_2 injection. In: Optimization in Science and Engineering, pp. 247–261. Springer New York (2014)

[27] Huang, Y., Rebennack, S., Zheng, Q.P.: Techno-economic analysis and optimization models for carbon capture and storage: a survey. Energy Systems **4**(4), 315–353 (2013)

[28] Huang, Y., Zheng, Q.P., Fan, N., Aminian, K.: Optimal scheduling for enhanced coal bed methane production through CO_2 injection. Applied Energy **113**, 1475–1483 (2014)

[29] Huang, Y., Zheng, Q.P., Wang, J.: Two-stage stochastic unit commitment model including non-generation resources with conditional value-at-risk constraints. Electric Power Systems Research **116**(0), 427–438 (2014)

[30] ISO New England Inc.: ISO New England Manual for Market Operations Manual M-11, 47 edn. (2013)

[31] Johnson, S.: Nyiso day-ahead market overview. In: FERC Technical Conference on Unit Commitment Software. Washington DC. FERC, pp. 1–29 (2010)

[32] Jonghe, C.D., Delarue, E., Belmans, R., D'haeseleer, W.: Determining optimal electricity technology mix with high level of wind power penetration. Applied Energy **88**(6), 2231 – 2238 (2011)

[33] Kirschen, D.S., Strbac, G., Cumperayot, P., de Paiva Mendes, D.: Factoring the elasticity of demand in electricity prices. IEEE Transactions on Power Systems **15**(2), 612–617 (2000)

[34] Kowli, A., Meyn, S.: Supporting wind generation deployment with demand response. In: Power and Energy Society General Meeting, 2011 IEEE, pp. 1–8 (2011)

[35] Liu, X.: Optimization of a combined heat and power system with wind turbines. International Journal of Electrical Power & Energy Systems **43**(1), 1421–1426 (2012)

[36] Louveaux, Q., Wolsey, L.A.: Lifting, superadditivity, mixed integer rounding and single node flow sets revisited. Quarterly Journal of the Belgian, French and Italian Operations Research Societies **1**(3), 173–207 (2003)

[37] Madaeni, S., Sioshansi, R.: The impacts of stochastic programming and demand response on wind integration. Energy Systems **4**(2), 109–124 (2013). DOI 10.1007/s12667-012-0068-7

[38] Marchand, H., Wolsey, L.A.: The 0-1 knapsack problem with a single continuous variable. Mathematical Programming **85**(1), 15–33 (1999)

[39] Matos, M.A., Bessa, R.J.: Setting the operating reserve using probabilistic wind power forecasts. IEEE Transactions on Power Systems **26**(2), 594–603 (2011)

[40] Meibom, P., Barth, R., Hasche, B., Brand, H., Weber, C., O'Malley, M.: Stochastic optimization model to study the operational impacts of high wind penetrations in ireland. IEEE Transactions on Power Systems **26**(3), 1367–1379 (2011)

[41] Mohammadi, S., Soleymani, S., Mozafari, B.: Scenario-based stochastic operation management of microgrid including wind, photovoltaic, micro-turbine, fuel cell and energy storage devices. International Journal of Electrical Power & Energy Systems **54**, 525–535 (2014)

[42] Ni, E., Luh, P.B., Rourke, S.: Optimal integrated generation bidding and scheduling with risk management under a deregulated power market. IEEE Transactions on Power Systems **19**(1), 600–609 (2004)

[43] Ntaimo, L., Tanner, M.W.: Computations with disjunctive cuts for two-stage stochastic mixed 0-1 integer programs. Journal of Global Optimization **41**(3), 365–384 (2008)

[44] Oren, S.S., Sioshansi, R.: Joint energy and reserves auction with opportunity cost payment for reserves. In: Bulk Power System Dynamics and Control VI. Cortina D'Ampezzo, Italy (2003)

[45] Ozturk, U.A., Mazumdar, M., Norman, B.A.: A solution to the stochastic unit commitment problem using chance constrained programming. IEEE Transactions on Power Systems **19**(3), 1589–1598 (2004)

[46] Papavasiliou, A., Oren, S.S.: A comparative study of stochastic unit commitment and security-constrained unit commitment using high performance computing. In: Control Conference (ECC), 2013 European, pp. 2507–2512 (2013)

[47] Papavasiliou, A., Oren, S.S., O'Neill, R.P.: Reserve requirements for wind power integration: A scenario-based stochastic programming framework. IEEE Transactions on Power Systems **26**(4), 2197–2206 (2011)

[48] Partovi, F., Nikzad, M., Mozafari, B., Ranjbar, A.M.: A stochastic security approach to energy and spinning reserve scheduling considering demand response program. Energy **36**(5), 3130 – 3137 (2011)

[49] Pozo, D., Contreras, J.: A chance-constrained unit commitment with an security criterion and significant wind generation. IEEE Transactions on Power Systems **28**(3), 2842–2851 (2013)

[50] Rei, W., Cordeau, J.F., Gendreau, M., Soriano, P.: Accelerating benders decomposition by local branching. INFORMS Journal on Computing **21**(2), 333–345 (2009)

[51] Richard, J.P.P.: Lifting techniques for mixed integer programming. Wiley Encyclopedia of Operations Research and Management Science (2010)

[52] Richard, J.P.P., de Farias, I.R., Nemhauser, G.L.: Lifted inequalities for 0-1 mixed integer programming: Basic theory and algorithms. Lecture notes in computer science pp. 161–175 (2002)

[53] Rockafellar, R.T., Uryasev, S.: Optimization of conditional value-at-risk. Journal of Risk **2**, 21–42 (2000)

[54] Rong, A., Lahdelma, R., Luh, P.B.: Lagrangian relaxation based algorithm for trigeneration planning with storages. European Journal of Operational Research **188**(1), 240–257 (2008)

[55] Ruiz, P., Philbrick, C., Zak, E., Cheung, K., Sauer, P.: Uncertainty management in the unit commitment problem. IEEE Transactions on Power Systems **24**(2), 642–651 (2009)

[56] Ruiz, P.A., Philbrick, C.R., Sauer, P.W.: Wind power day-ahead uncertainty management through stochastic unit commitment policies. In: Power Systems Conference and Exposition, pp. 1–9 (2009)

[57] Sarykalin, S., Serraino, G., Uryasev, S.: Value-at-risk vs. conditional value-at-risk in risk management and optimization. Tutorials in Operations Research.INFORMS, Hanover, MD pp. 270–294 (2008)

[58] Senjyu, T., Miyagi, T., Yousuf, S.A., Urasaki, N., Funabashi, T.: A technique for unit commitment with energy storage system. Electrical Power and Energy Systems **29**(1), 91–98 (2007)

[59] Shahidehopour, M., Fu, Y.: Benders decomposition: applying benders decomposition to power systems. Power and Energy Magazine, IEEE **3**(2), 20–21 (2005)

[60] Shahidehpour, M., Yamin, H., Li, Z.: Market Operations in Electric Power Systems. John Wiley and Sons (2002)

[61] Shebalov, S., Klabjan, D.: Sequence independent lifting for mixed integer programs with variable upper bounds. Mathematical Programming **105**(2-3), 523–561 (2006)

[62] Sherali, H.D., Fraticelli, B.M.P.: A modification of benders' decomposition algorithm for discrete subproblems: An approach for stochastic programs with integer recourse. Journal of Global Optimization **22**(1-4), 319–342 (2002)

[63] Sherali, H.D., Smith, J.C.: Two-stage stochastic hierarchical multiple risk problems: models and algorithms. Mathematical Programming **120**(2), 403–427 (2009)

[64] Sherali, H.D., Zhu, X.: On solving discrete two-stage stochastic programs having mixed-integer first- and second-stage variables. Mathematical Programming **108**(2-3), 597–616 (2006)

[65] Shiina, T., Birge, J.R.: Stochastic unit commitment problem. International Transactions in Operational Research **11**, 19–32 (2004)

[66] Siahkali, H., Vakilian, M.: Stochastic unit commitment of wind farms integrated in power system. Electric Power Systems Research **80**(9), 1006–1017 (2010)

[67] Sigrist, L., Lobato, E., Rouco, L.: Energy storage systems providing primary reserve and peak shaving in small isolated power systems: An economic assessment. International Journal of Electrical Power & Energy Systems **53**, 675–683 (2013)

[68] Sioshansi, R.: Evaluating the impacts of real-time pricing on the cost and value of wind generation. Power Systems, IEEE Transactions on **25**(2), 741 –748 (2010)

[69] Takriti, S., Birge, J.R., Long, E.: A stochastic model for the unit commitment problem. IEEE Transactions on Power Systems **11**(3), 1497–1508 (1996)

[70] Takriti, S., Krasenbrink, B., Wu, L.S.Y.: Incorporating fuel constraints and electricity spot prices into the stochastic unit commitment problem. Operations Research **48**(2), 268–280 (2000)

[71] Tan, Y.T., Kirschen, D.S.: Co-optimization of energy and reserve in electricity markets with demand-side participation in reserve services. In: Power Systems Conference and Exposition, 2006., pp. 1182–1189. IEEE PES (2006)

[72] Tuohy, A., Meibom, P., Denny, E., O'Malley, M.: Unit commitment for systems with significant wind penetration. IEEE Transactions on Power Systems **24**(2), 592 –601 (2009)

[73] Uryasev, S.: Conditional value-at-risk: Optimization algorithms and applications. In: Computational Intelligence for Financial Engineering, pp. 49–57. IEEE (2000)

[74] U.S. EPA: Sources of greenhouse gas emissions: Electricity. http://www.epa.gov/climatechange/ghgemissions/sources/electricity.html (2014)

[75] Vrakopoulou, M., Margellos, K., Lygeros, J., Andersson, G.: A probabilistic framework for reserve scheduling and $rmN - 1$ security assessment of systems with high wind power penetration. IEEE Transactions on Power Systems **28**(4), 3885–3896 (2013)

[76] Wang, J., Botterud, A., Conzelmann, G., Vladimiro Miranda Cláudio Monteiro, G.S.: Impact impact of wind power of wind power forecasting on unit commitment and dispatch. In: 8th Int. Wind Integration Workshop. Bremen, Germany (2009)

[77] Wang, J., Kennedy, S., Kirtley, J.: A new wholesale bidding mechanism for enhanced demand response in smart grids. In: Innovative Smart Grid Technologies (ISGT), 2010, pp. 1–8 (2010). DOI 10.1109/ISGT.2010.5434766

[78] Wang, J., Kennedy, S.W., Kirtley, J.L.: Optimization of forward electricity markets considering wind generation and demand response. IEEE Transactions on Smart Grid **5**(3), 1254–1261 (2014)

[79] Wang, J., Shahidehpour, M., Li, Z.: Security-constrained unit commitment with volatile wind power generation. IEEE Transactions on Power Systems **23**(3), 1319–1327 (2008)

[80] Wang, J., Shahidehpour, M., Li, Z.: Contingency-constrained reserve requirements in joint energy and ancillary services auction. IEEE Transactions on Power Systems **24**(3), 1457–1468 (2009)

[81] Wang, J., Wang, J., Liu, C., Ruiz, J.P.: Stochastic unit commitment with sub-hourly dispatch constraints. Applied Energy **105**, 418–422 (2013)

[82] Wang, Q., Guan, Y., Wang, J.: A chance-constrained two-stage stochastic program for unit commitment with uncertain wind power output. IEEE Transactions on Power Systems **27**(1), 206–215 (2012)

[83] Wang, Q., Wang, J., Guan, Y.: Stochastic unit commitment with uncertain demand response. Power Systems, IEEE Transactions on **28**(1), 562–563 (2013)

[84] Wu, L., Shahidehpour, M., Li, T.: Cost of reliability analysis based on stochastic unit commitment. IEEE Transactions on Power Systems **23**(3), 1364–1374 (2008)

[85] Wu, Z., Zhou, S., Li, J., Zhang, X.P.: Real-time scheduling of residential appliances via conditional risk-at-value. IEEE Transactions on Smart Grid **5**(3), 1282–1291 (2014)

[86] Xu, M., Zhuan, X.: Identifying the optimum wind capacity for a power system with interconnection lines. International Journal of Electrical Power & Energy Systems **51**, 82–88 (2013)

[87] Yu, H., Chung, C.Y., Wong, K.P., Zhang, J.H.: A chance constrained transmission network expansion planning method with consideration of load and wind farm uncertainties. IEEE Transactions on Power Systems **24**(3), 1568–1576 (2009)

[88] Zeng, B., Richard, J.P.P.: Sequence independent lifting for 0-1 knapsack problems with disjoint cardinality constraints. School of Industrial Engineering, Purdue University, West Lafayette, IN (2006)

[89] Zeng, B., Richard, J.P.P.: A framework to derive multidimensional superadditive lifting functions and its applications, pp. 210–224. Springer (2007)

[90] Zhao, C., Wang, J., Watson, J.P., Guan, Y.: Multi-stage robust unit commitment considering wind and demand response uncertainties. IEEE Transactions on Power Systems **28**(3), 2708–2717 (2013)

[91] Zhao, L., Zeng, B.: Robust unit commitment problem with demand response and wind energy. In: IEEE Power and Energy Society General Meeting, pp. 1–8 (2012)

[92] Zheng, Q., Wang, J., Pardalos, P., Guan, Y.: A decomposition approach to the two-stage stochastic unit commitment problem. Annals of Operations Research pp. 1–24 (2012)

[93] Zheng, Q.P., Pardalos, P.M.: Stochastic and risk management models and solution algorithm for natural gas transmission network expansion and lng terminal location planning. Journal of Optimization Theory and Applications **147**, 337–357 (2010)

[94] Zheng, Q.P., Rebennack, S., Pardalos, P.M., Pereira, M.V.F., Iliadis, N.A.: Handbook of CO_2 in Power Systems. Energy Systems. Springer (2012)

[95] Zheng, Q.P., Shen, S., Shi, Y.: Loss-Constrained Minimum Cost Flow under Arc Failure Uncertainty with Applications in Risk-Aware Kidney Exchange, (2014). Accepted

[96] Zheng, T.: Real-time energy and reserve co-optimization (2011). URL `http://www.iso-ne.com/support/training/courses/wem301/`

[97] Zheng, T., Litvinov, E.: Contingency-based zonal reserve modeling and pricing in a co-optimized energy and reserve market. IEEE Transactions on Power Systems **23**(2), 277–286 (2008)